

МІНІСТЕРСТВО ОСВІТИ ТА НАУКИ УКРАЇНИ  
НАЦІОНАЛЬНИЙ ТЕХНІЧНИЙ УНІВЕРСИТЕТ  
«ХАРКІВСЬКИЙ ПОЛІТЕХНІЧНИЙ ІНСТИТУТ»

Ministry of Education & Science of Ukraine  
National Technical University  
«Kharkiv Polytechnic Institute»

**РІЗАННЯ  
ТА  
ІНСТРУМЕНТИ  
В ТЕХНОЛОГІЧНИХ СИСТЕМАХ**

---

**CUTTING & TOOLS  
IN TECHNOLOGICAL SYSTEM**

**Міжнародний науково-технічний збірник  
International Scientific-Technical Collection**

*Заснований у 1966 р. М. Ф. Семко  
Found by M. F. Semko in 1966*

**ВИПУСК № 94  
Edition № 94**

Харків НТУ «ХПІ» – 2021 – Kharkiv NTU «KhPI»

ББК 34.63  
УДК 621.91

Державне видання  
Свідоцтво Державного комітету телебачення і радіомовлення України  
КВ № 7840 від 8 вересня 2003 року  
Друкується за рішенням Вченої Ради НТУ "ХПІ",  
протокол №7 від 02 липня 2021 р.

Редакційна колегія:

*Головний редактор* Грабченко А.І., *заступники головного редактора* Беліков С.Б., Ковальов В.Д., Федорович В.О., Трищ Р.М., *відповідальний редактор* Островерх Є.В., *члени редакційної колегії, рецензенти*: Антонюк В.С., Басова Є.В., Волкогон В.М., Доброскок В.Л., Добротворський С.С., Залого В.О., Іванов В.О., Іванова М.С., Кальченко В.В., Криворучко Д.В., Лавриненко В.І., Павленко І.В., Пермяков О.А., Піжов І.М., Пупань Л.І., Ступницький В.В., Тонконогий В.М., Усов А.В., Хавін Г.Л. (Україна), Міко Балаш, Кундрак Янош, Тамаш Петер, Фельо Чаба, (Угорщина), Хатала Міхал, Каганова Дагмар, Манкова Ільдико, Хорнакова Наталія (Словаччина), Маркопулус Ангелос, Мамаліс Атанасіос (Греція), Гуйда Доменіко (Італія), Дашич Предраг (Сербія), Мір'яніч Драголюб (Боснія і Герцоговина), Марусіч Влатко (Хорватія), Цішак Олаф, Трояновска Юстіна (Польща), Еммер Томас (Німеччина), Едл Мілан (Чехія), Турманідзе Рауль (Грузія).

У збірнику представлені наукові статті, в яких розглядаються актуальні питання в області механічної обробки різних сучасних матеріалів із застосуванням високопродуктивних технологій, нових методик, вимірювальних приладів для контролю якості оброблених поверхонь і високоефективних різальних інструментів. Розглядаються аспекти оптимізації та математичного моделювання на різних етапах технологічного процесу.

Для інженерів і наукових співробітників, що працюють в області технології машинобудування, різання матеріалів, проектування різальних інструментів в технологічних системах.

*Науковий збірник «Різання та інструменти в технологічних системах» включений в Перелік фахових видань України категорії «Б», наказ МОН України від 17.03.2020 р., №409*

**Р34 Резание и инструменты в технологических системах:** Междунар. науч.- техн. сб. – Харьков: НТУ «ХПИ», 2021. – Вып. 94. – 152 с.

**Адреса редакційної колегії:** вул. Кирпичова, 2, Харків, 61002, Національний технічний університет «Харківський політехнічний інститут», кафедра «Інтегровані технології машинобудування» ім. М.Ф. Семка, тел. +38 (057) 706-41-43.

**ББК 34.63**

Матеріали відтворені з авторських оригіналів  
НТУ «ХПІ», 2021

M. Balanou, E. I. Papazoglou, A. P. Markopoulos, Athens, Greece,  
P. Karmiris-Obratański, Cracow, Poland

## **EXPERIMENTAL INVESTIGATION OF SURFACE TOPOGRAPHY OF AL7075-T6 ALLOY MACHINED BY EDM**

**Abstract.** *Electrical discharge machining is one of the most important non-conventional machining processes for removing material from electrically conductive materials by the use of controlled electric discharges. EDM is a non-contact machining process, therefore, is free from mechanical stresses. This paper investigates the machining Al7075-T6 alloy by EDM using a copper electrode. Al7075-T6 alloy was selected, because of its growing use in a lot of engineering applications. The effect of electrical parameters, peak current and pulse-on time, on the surface integrity, was studied. Area surface roughness parameters (arithmetical mean height,  $S_a$ , and maximum height,  $S_z$ ) were measured on all samples and 3D surface characterization has been carried out with confocal laser scanning microscopy. The experimental results showed that the surface roughness is mainly affected by the pulse-on time.*

**Keywords:** *Electrical discharge machining; Aluminum alloys; Surface topography; Surface roughness; Peak current; Pulse-on time.*

### **Introduction**

Electrical discharge machining (EDM) is one of the most important non-conventional manufacturing processes and is used for machining with high precision and accuracy electrically conductive materials which are difficult to machine by conventional machining processes. EDM finds extensive use in many engineering applications like machining surgical components, dies and mold-making, and in automobile and aerospace industries [1], [2].

EDM is a thermo-electric process and characterized by an erosion effect produced when electrical discharges occurred between two conductive electrodes. In this process, when a voltage difference is applied between the electrode and the workpiece, which are separated by a dielectric fluid, causes the formation of an electric discharge. The electric discharge generates high temperatures (6000 – 12000 °C) and leads to melting of the material at the point of discharge. [3]. The melted material is removed from the tool electrode and the workpiece, and as a result a small crater is created on both surfaces. The molten material which had not been efficiently flushed away by the dielectric fluid is re-solidified in the crater, forming a white layer.

The literature shows that a lot of works have been carried out for the machining of hard materials such as tool steels, tungsten and ceramics. However, lately, soft materials like aluminum alloys have been machined by EDM as well. Aluminum alloys have been widely used in a lot of industries like marine,

aerospace, automotive and electrical equipment. Above all aluminum alloys, the 7xxx series (also called aluminum– zinc alloy) is the strongest wrought aluminum alloys series with a better response to age hardening, obtaining better mechanical properties [4].

The studies in the EDM machining of aluminum 7xxx alloys have been focused on machining performance parameters such as material removal rate (MRR), tool wear rate (TWR) and the machined surface quality (SQ). Gatto et al. [5] studied the machinability of Al2219-T6, Al7050-T6 and Al7075-T6 with EDM. Surface roughness, dimensional and accuracy of the workpieces and the wear mechanism of the electrodes were evaluated. Kasman and Tosun [6] conducted experiments for AA7075 aluminum alloy under different process parameters peak current, pulse-on time, pulse-off time, gap voltage and using copper and graphite electrode. Taguchi method was used to design the experiment. Routara et al. [7] analyzed MRR, TWR and SR on T6-Al 7075 alloy using Cu tool in steady and rotary conditions. For conducting experiments, spark gap, pulse-off time and peak current was selected as machining parameters. Furthermore, a few of works have been carried out on machining Al alloy 7075 as a base matrix alloy in composite materials by EDM. Some examples of AMCs machined by EDM are Al7075-B4C [8] and Al7075/SiC/Mg [9].

The present study investigates the machining of aluminum alloy Al7075-T6 with EDM by using a copper electrode. Al7075-T6 is a high strength engineering alloy, which is used as structural material in marine, automotive and aviation applications, while it is suitable for use in injection moulds applications. The effect of peak current and pulse-on time on the Surface Roughness (SR) was studied. The surface characteristics were also evaluated by confocal laser scanning microscopy.

## **Experimental procedure**

Experiments were conducted on a die-sinking EDM machine (ANGIETRON EMT 1.10). Aluminum alloy Al7075-T6 was machined by EDM using a rectangular copper electrode with dimensions of 38×23 mm. The chemical composition, density and hardness of Al7075-T6 are shown in Table 1. A hydrocarbon mineral oil was used as a dielectric fluid. The selected input parameters are given in Table 2. Peak current and pulse-on time were used to investigate the effect of surface roughness. The selected input parameters are given in Table 2. In all experiments, straight polarity was used, with 100 and 30 V as the open and close circuit voltage, respectively. Moreover, the dielectric fluid flushing pressure was constant for all the experiments, while the duty cycle was automatically adjusted by the machine, for optimized machining efficiency. The duty cycle ( $\eta$ ) is calculated by using Equation (1):

$$\eta = \frac{\bar{I}_p}{I_p} \quad (1)$$

with  $\bar{I}_p$  the ammeter indication of the mean current intensity in A, and  $I_p$  the pulse current in A.

Table 1 – Chemical composition, density and hardness of Al-7075 T6 (wt.%)

Zn	Si	Fe	Ti	Cu	Mn	Mg	Cr	Other	Density (g/mm <sup>3</sup> )	Hardness (HV)
5.1-6.1	0.40	0.50	0.20	1.2-2.0	0.30	2.1-2.9	0.18-0.28	0.65	0.00281	175

Table 2 – Input parameters

Parameters	
Peak Current ( $I_p$ )	15, 18, 21 and 24 A
Pulse-on duration ( $T_{on}$ )	100, 200, 300 and 500 $\mu$ s
Open-circuit voltage	100 V
Close-circuit voltage	30 V
Polarity	Straight
Dielectric Fluid	Hydrocarbon mineral oil

SR of the machined surface is measured on random surface area by TOPO 01P contact profilometer by using the ISO 25178-2 to analyze the collected data. The cut-off length was set at 2.5mm with a cutting length of 8 mm. In this present study, the following surface roughness parameters have been taken:

- $S_a$  is the arithmetical mean of the difference in height within a definition area (A) and calculated using Equation (2)

$$S_a = \frac{1}{A} \iint_A |z(x, y)| dx dy \quad (2)$$

- $S_z$  is the sum of the largest peak height value and the largest pit depth value within the defined area.

The confocal laser scanning microscopy (CLSM) was used to study the machined surface characteristics. To measure the slot dimensions, a VHX-6000 ultra-deep-field microscope (KEYENCE, Mechelen, Belgium) was used, which is based on Focus Variation Microscopy (FVM), equipped with a 20-2000x objective. After the experiments were conducted, 3D surfaces was generated. The results of surface roughness parameters are shown in Table 3.

Table 3 – Experimental results

<b>I<sub>p</sub> (A)</b>	<b>T<sub>on</sub> (μs)</b>	<b>S<sub>a</sub> (μm)</b>	<b>S<sub>z</sub> (μm)</b>
15	100	9.83	68.8
18	100	9.03	68.55
21	100	8.5	83.83
24	100	9.97	78.7
15	200	11.69	103.1
18	200	13.19	98.03
21	200	14.11	109.41
24	200	15.33	134.57
15	300	14.54	114.89
18	300	16.88	118.75
21	300	17.76	130.85
24	300	17.97	150.3
15	500	18.21	147.75
18	500	19.88	128.55
21	500	17.27	143.27
24	500	20.09	162.77

## **Results and Discussion**

### *Surface Roughness*

SR is one of the most major performance measures in EDM and is influenced by the machining parameters. The machined surface obtained by EDM is the result of the amount of energy released during the process which causes material removal. The discharge energy is affected by the machining parameters. Therefore, peak current and pulse-on time are the major factors that affect the surface roughness. Surface roughness increases with an increase in peak current and pulse-on time, due to the increase in thermal energy which transferred to the machined surface [10], [11]. This can be explained by the fact that, as pulse-on time gets higher, the plasma column expands beyond the point of electrical discharge, leading to a larger diameter crater, on the other hand, the peak current influences the depth of the crater [1]. Thus, the amount of the molten material is increased. If this molten material is not flushed away by the dielectric fluid, it will re-solidify on the machined surface and form a white layer. The surface roughness is also influenced by the white layer formation [11].

In Figure 1 the main effect plots and the interaction plots for the  $S_a$  parameters are presented. In general, from the main effect plot it can be observed that the peak current does not have a significant effect on  $S_a$ . On the other hand, an increase in pulse-on time results in an increase in  $S_a$ . Particularly,  $S_a$  increased up to 50.8% as the pulse-on time increased from 100 to 500  $\mu$ s. The interaction plot confirms those results. It is observed that as the  $T_{on}$  is increased,  $S_a$  is getting higher values in re spect of peak current.

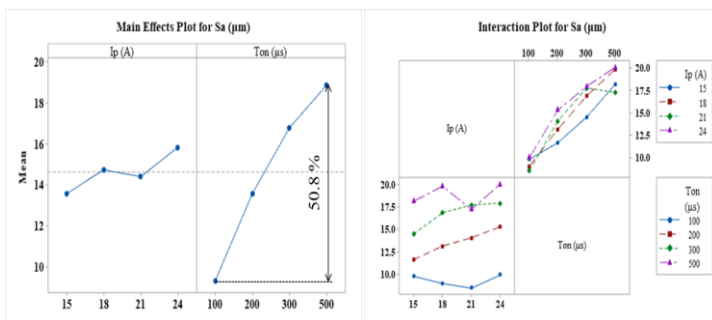


Figure 1 – Main effect plot and interaction plot for  $S_a$

The main effect plots and the interaction plots for the  $S_z$  parameters are illustrated in Figure 2. The peak current plot in the main effect diagram shows reduce in  $S_z$  up to 18A, followed by an increase of  $S_z$  as the peak current gets higher at 24A. At the same time, as the pulse-on time increased an increase up to 57.9% in the  $S_z$  take place. From the interaction plot it can be concluded that as the  $T_{on}$  is increased,  $S_z$  is increased in respect of peak current.

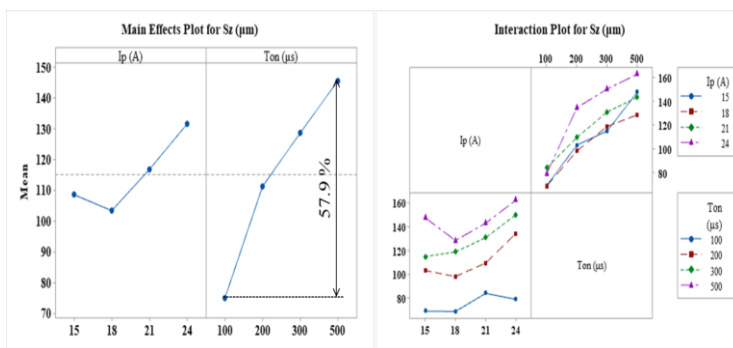


Figure 2 – Main effect and interaction plot for  $S_z$

### *Surface Topography*

As has been stated above, the topography of the machined surface is due to the enormous amount of heat generated by the discharges. After the EDM, the condition of the surface is changed due to erosion and vaporization of the material from both the electrodes followed by re-solidification. The machined surface is characterized by the presence of a distribution of overlapping craters with irregular flow marks of molten metal and debris particles. The size of the craters produced affected by the machining parameters and consequently peak current and pulse-on time influence the surface topography.

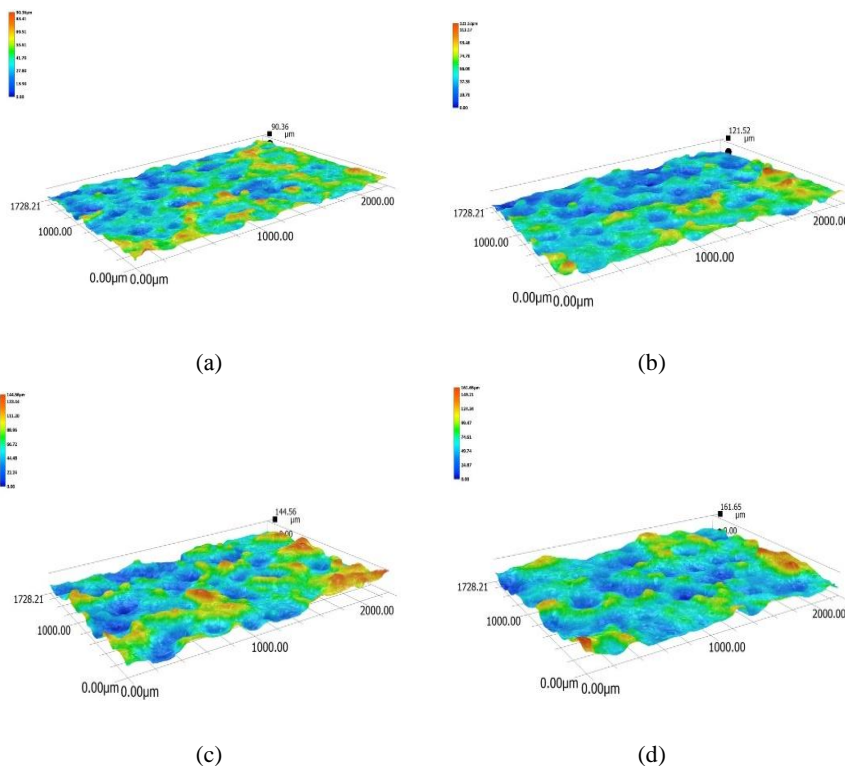


Figure 3 – Surface topography of the machined surface for (a)  $I_p= 18$  A and  $T_{on}= 100$  μs, (b)  $I_p= 15$  A and  $T_{on}= 200$  μs, (c)  $I_p= 21$  A and  $T_{on}= 100$  μs and (d)  $I_p= 24$  A and  $T_{on}= 500$  μs

The 3-D image in Figs. 3 presents the variation of the machined surface for different machining parameters from the analysis of CLSM. The machined surface is covered with a distribution of craters and as well as solidified crater boundaries. As discharge energy increased, the sizes of the craters are changing and become more distinct. The images showed that the height difference between the base of the crater and the white layer has been increased. Thus, surface roughness and surface height inhomogeneity increased as the machining parameters changing. These results are agreed with the surface roughness measurements. The  $S_a$  and  $S_z$  take higher values under more intense conditions. This can be confirmed and by the 3-D images, the machined surface becomes rougher as the peak current and pulse-on time get higher values.

## Conclusion

This paper presented an experimental study on the surface integrity of Al7075-T6 alloy, machined EDM. The studied machining parameters were the pulse current ( $I_p$ ) and the pulse-on time ( $T_{on}$ ). The surface topography was studied through roughness measurements ( $S_a$  and  $S_z$ ) and confocal laser scanning microscopy. From the experimental results, the conclusions are summarized as follows:

- The  $S_a$  is strongly affected by the pulse-on time. The mean value of  $S_a$  increased up to 50.8 % as the pulse-on time increased from 100 to 500  $\mu$ s.
- The  $S_z$  significantly increased for an increase in pulse-on current from 100 to 500  $\mu$ s.
- From the CLSM the morphology of the machined was observed. . The size of the craters produced affected by the machining parameters and become more distinct when the thermal is increased.

**References:** 1. *Muhammad Pervej Jahan, Ed.*, Electrical Discharge Machining (EDM): Types, Technologies and Applications. New York: Nova Science Publishers, 2015. 2. *M. Niamat, S. Sarfraz, E. Shehab, S. O. Ismail, and Q. S. Khalid*, "Experimental Characterization of Electrical Discharge Machining of Aluminum 6061 T6 Alloy using Different Dielectrics," *Arab. J. Sci. Eng.*, vol. 44, no. 9, pp. 8043–8052, 2019, doi: 10.1007/s13369-019-03987-4. 3. *K. H. Ho and S. T. Newman*, "State of the art electrical discharge machining (EDM)," *Int. J. Mach. Tools Manuf.*, vol. 43, no. 13, pp. 1287–1300, 2003, doi: 10.1016/S0890-6955(03)00162-7. 4. *K. Dehghani, A. Nekahi, and M. A. M. Mirzaie*, "Optimizing the bake hardening behavior of Al7075 using response surface methodology," *Mater. Des.*, vol. 31, no. 4, pp. 1768–1775, 2010, doi: 10.1016/j.matdes.2009.11.014. 5. *A. Gatto, E. Bassoli, and L. Iuliano*, "Performance Optimization in Machining of Aluminium Alloys for Moulds Production: HSM and EDM," *Alum. Alloy. Theory Appl.*, 2011, doi: 10.5772/14847. 6. *Kasman and N. Tosun*, "Investigation of surface roughness in machining of aluminum alloy with EDM," no. May, pp. 101–104, 2015. 7. *B. C. Routara, D. Das, M. P. Satpathy, B. K. Nanda, A. K. Sahoo, and S. S. Singh*, "Investigation on machining characteristics of T6-Al7075 during EDM with Cu tool in steady and rotary mode," *Mater. Today Proc.*, vol. 26, pp. 2143–2150, 2019, doi: 10.1016/j.matpr.2020.02.462. 8. *S. Gopalakannan, T. Senthilvelan, and S. Ranganathan*, "Modeling and optimization of EDM process parameters on machining of Al7075-B4C MMC using RSM," *Procedia Eng.*, vol. 38, pp. 685–690,

2012, doi: 10.1016/j.proeng.2012.06.086. **9.** P. Malhotra, R. K. Tyagi, N. K. Singh, and B. S. Sikarwar, "Experimental investigation and effects of process parameters on EDM of Al7075/SiC composite reinforced with magnesium particles," *Mater. Today Proc.*, vol. 21, pp. 1496–1501, 2020, doi: 10.1016/j.matpr.2019.11.069. **10.** S. Kar, S. Chakraborty, V. Dey, and S. K. Ghosh, "Optimization of Surface Roughness Parameters of Al-6351 Alloy in EDC Process: A Taguchi Coupled Fuzzy Logic Approach," *J. Inst. Eng. Ser. C*, vol. 98, no. 5, pp. 607–618, 2017, doi: 10.1007/s40032-016-0297-y. **11.** H. T. Lee and T. Y. Tai, "Relationship between EDM parameters and surface crack formation," *J. Mater. Process. Technol.*, vol. 142, no. 3, pp. 676–683, 2003, doi: 10.1016/S0924-0136(03)00688-5.

Марія Балану, Емануїл Л. Папазоглу, Ангелос П. Маркопулос, Афіни, Греція,  
Панагіотіс Карміріс-Обратанські, Краків, Польща

## **ЕКСПЕРИМЕНТАЛЬНЕ ДОСЛІДЖЕННЯ РЕЛЬЄФУ ПОВЕРХНІ СПЛАВУ AL7075-T6, ОБРОБЛЕНОГО ЕЛЕКТРОЕРОЗІЙНИМ МЕТОДОМ**

**Анотація.** *Електроерозійна обробка (ЕЕО) є одним з найбільш важливих нетрадиційних виробничих процесів і використовується для обробки з високою точністю електропровідних матеріалів, які важко обробляти звичайними процесами обробки. ЕЕО знаходить широке застосування в багатьох інженерних додатках, таких як обробка хірургічних компонентів, штампів та виготовлення прес-форм, а також в автомобільній і аерокосмічній промисловості. Останнім часом за допомогою електроерозійної обробки обробляються також м'які матеріали, такі як алюмінієві сплави, які широко використовуються в багатьох галузях промисловості, таких як морське, аерокосмічне, автомобільне та електричне обладнання. З усіх алюмінієвих сплавів серія 7xxx (яка також має назву алюмінієво-цинковий сплав) є найміцнішою серією алюмінієвих сплавів які підлягають деформації з кращими показниками на старіння і політисеними механічними властивостями. У цій статті досліджується обробка алюмінієвого сплаву Al7075-T6 за допомогою ЕЕО з використанням мідного електрода. Al7075-T6 - це високоміцний сплав, який використовується в якості конструкційного матеріалу в морських, автомобільних і авіаційних виробництвах, а також підходить для використання в ливарних формах. Було вивчено вплив пікового струму і тривалості імпульсу на шорсткість поверхні (SR). Характеристики поверхні також оцінювали за допомогою конфокальної лазерної сканувальної мікроскопії. Загалом, можна помітити, що піковий струм не має значного впливу на Sa. З іншого боку, збільшення часу включення призводить до збільшення Sa. Зокрема, Sa збільшився до 50,8% при збільшенні часу імпульсу від 100 до 500 мкс. Оброблена поверхня характеризується наявністю розподілу кратерів, які перекриваються, з нерівномірними слідами течії розплавленого металу і частинок відходів. Розмір утворених кратерів залежить від параметрів обробки і, отже, піковий струм і час імпульсу впливають на топографію поверхні.*

**Ключові слова:** *електроерозійна обробка; алюмінієві сплави; топографія поверхні; шорсткість поверхні; піковий струм; тривалість імпульсу.*

P. Veres, Miskolc, Hungary

## THE IMPORTANTS OF CLUSTERING IN LOGISTIC SYSTEMS

**Abstract.** *Nowadays, the development of higher efficient processes and procedures is the key for success in industrial environment. The companies have machines, production lines, software and hardware tools with high level principles of efficient working. Example: the Industry 4.0 concept use the machines and methods of the near past, upgrade them, and gave them new purpose, as a more efficient tool. Some of the bases of those tools are not as efficient as which many would think, like in group generating or in other word clustering. Clustering is a very hard process, and it is in almost every decision making in every company's lives. It is important to sometimes examine its significance and flaws. This paper presents the clustering briefly and shows its errors through an example.*

**Keywords:** *Industry 4.0; clustering, heuristics; decision-making; routing.*

### 1. INTRODUCTION

Nowadays, everything is about working efficiently [1]. Globalization was the first step for giant logistic networks to emerge across the world [2]. Most of the times it is cheaper to produce or buy components or full products from the other side of the planet. Lots of multination companies realises this, and made connections. Our world is and was so interconnected, that if an error or a failure occured somewhere, it was hard to find, and even harder to fix. Our sensore technology, tracking devices and mobil computers help to eliminate the long seaching, but in most case they cant help in the recovery. This is where old and new technologies combines. The Industry 4.0 concept uses the existing technolgies and connects them into a system, that can do more then individually [3]. It creates new inforamtion from exist data and information. One of the most used princeple of the Industry 4.0 concept is machine decision making without human interaction in a situation, which has not yet occured for either the machine or a human. This makes the machine, the production or the whole system smart. This is a smart factory, and it contains some sort of Artificial Intelligence[4]. There are multiple IT companies, that want to create the most advanced AI, but in our situation, in the assembly or production industry, a basic algorithm that able to „learn“ with minimal computing power is enough [5]. One of this minimalistic AI is clustering algorithms, that can create groups based on measured or calculated parameters.

In almost every part of a any logistic system there are some clustering task. It used in route planning, package and unit load planing, location determination, warehouse allocation, high bay storage service, order and delivery management, and so more. It is a very important subtask, which is neglected by many manager

and engineer, because they said it is so „basic“, it's implemented in everything perfectly. But most of these algorithms of the early ERP-s, are not capable of handling efficiently the increased databases[6].

In this paper I would like to show the importance of clustering with small examples, and show how much a clustering error affects an optimization process.

## **2. CLUSTERING ALGORITHMS IN GENERALEAL AND LOGISTICS**

Clustering is a NP-Hard problem in mathematics, which translates to: it has no exact mathematical method to solve the problem. Therefore there are numerous clustering algorithms which try to produce a reasonable good solution in a short time. There are commonly used algorithms, such as: the most used K-mean and other K algorithms, nearest neighbor, Cobweb, CURE, Fuzzy cluster, BIRCH, DBSCAN, Human intuition, and so on [7]. Most of them must follow the same rules of their data tables and parameters. If two or more parameters share some convergence, that makes the progress faster or more reliable, but this is not necessary for the clustering algorithms. There are two important conditions for reliable usage of these algorithms:

- Every individual object needs to have values in every parameter that we want to involve into the clustering process,
- If the parameters are not share the same unit of measure, it needs to be weighted.

There are exceptions in both conditions: Some advanced algorithms have AI to fill out blank parameters, if there are correlations in the dataset (big dataset is necessary); and if there are few parameters to consider some clustering process can be done with great success without weighting [8].

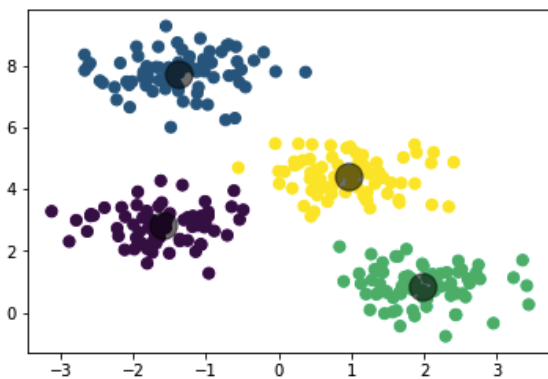


Figure1 – K-mean used in 2D clustering [9]

One of the most important and spectacular use of the algorithms in logistics is in route planning with multiple vehicles. In this situation to get a good solution, first you have to determine which vehicle visits which point and then optimise the route separately in the groups. Most of the clustering algorithms today use this method, which gives us a fairly good result but there is a chance, that it won't be the optimal solution. To get the optimal solution with a greater chance the two optimization process (clustering and route planning) have to work parallel, because both have influence over on the other. This is where Heuristics can help. Heuristic algorithms handles all parameters at once, where grouping is just another parameter. Besides that, no other parameter has to change, and if it's not necessary, it doesn't need weighting the parameters. However, an evaluation function, like the fitness function in evolutionary algorithms, is necessary for this method. In my personal studies I use both methods and I recommend using them in this division:

- Use the Clustering algorithms, if there are just a few parameters (under 10) and only need mild weighting.
- Use Heuristics, if there are big databases, with high number of parameters.

### **3. CLUSTERING EXAMPLE IN MULTI-VEHICLE ROUTING**

The multi-vehicle routing problem is a combination of at least two problem, but most of the time there are four basic logistics problem, which plays a role in the difficulty [10]:

- routing problem
- clustering problem
- capacity problem
- location determination problem

In this paper the first two has already been explained. The capacity problem is a real life problem of transporting. because, the capacity of the vehicles and the locations are predetermined, and can't be violated. The capacity acts like a limit, that can determine the quantity of the vehicles, storages, docks, etc. in a company. The location determination problem creates „floating objects“, until the optimization problem routes them and gives them their own parameters. It can be a parking slot or a charging station for our vehicles. Also it can be a prospective warehouse in the future or any object, that will be part of the route, but the optimization process should decide where it needs to be. These are the four fundamental problems of the multi-vehicle routing problem. In the next example besides, the location determination problem, all other has a role.

In the example there are 20 objects in a circle in the map giving the same volume and weight of wares. In the middle of the circle, there will be the company that collects the wares. We like to get the least amount of driven length, with the data in Table 1. This is a highly specific data, because we know what need to come

out. With this setup, there will be 3 routes, and the perfect solution should look like a radiation warning sign, which can be seen in figure 2. The solution is created by a Heuristical method called Evolutionary algorithm, and the total length of the route, that the 3 vehicles have to take is 965,85. It has no dimensions, because we don't define it in the coordinates.

Table 1 – Coordinates and basic data of the artificial problem

#	X	Y	Weight	Volume
Center	0	0		
1	-60,079	52,82534	2	2
2	-79,3423	-10,2371	2	2
3	-44,7031	-66,3448	2	2
4	20,30587	-77,38	2	2
5	71,51973	-35,8459	2	2
6	74,14548	30,04077	2	2
7	26,39927	75,51873	2	2
8	-39,2817	69,69179	2	2
9	-78,276	16,51858	2	2
10	-64,0922	-47,8768	2	2
11	-6,36629	-79,7463	2	2
12	55,68468	-57,4388	2	2
13	79,90534	3,89068	2	2
14	49,84098	62,57697	2	2
15	-14,0837	78,75056	2	2
16	-68,4403	41,42365	2	2
17	-76,3009	-24,0451	2	2
18	-32,3252	-73,1784	2	2
19	33,61117	-72,5968	2	2
20	76,71326	-22,6953	2	2
SUM			40	40

	Max Weight	Max Volume
<b>Routes: 3</b>	<b>27</b>	<b>15</b>

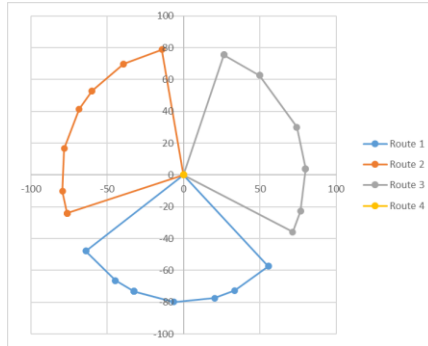


Figure 2 – Perfect solution of artificial routing problem

To get the perfect solution, there were advanced programming, fine tuning and multiple re-runs of the optimization method. This is not acceptable in an industrial environment. Most of the time the result was a semi-perfect circle or 1-2 object in the wrong group as shown in figure 3-5.

Figure 3 shows a routing optimization problem, where the solution is 1216,85. It is 26% higher than the optimal.

In figure 4, there are a mild clustering solution with a value 1072,49. It is 9% higher than, the optimal.

In figure 5 we can see a mild clustering and route optimization error, where the solution is 1238,53, which is 28% higher, than the perfect score.

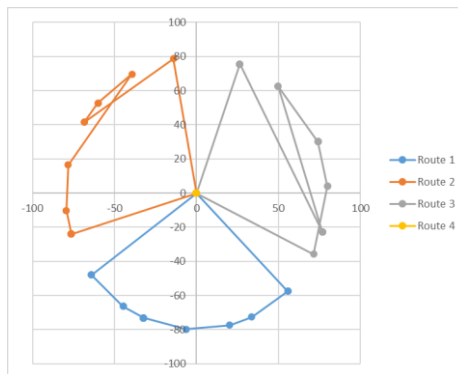


Figure 3 – Problem with routing optimization in the solution of artificial routing problem

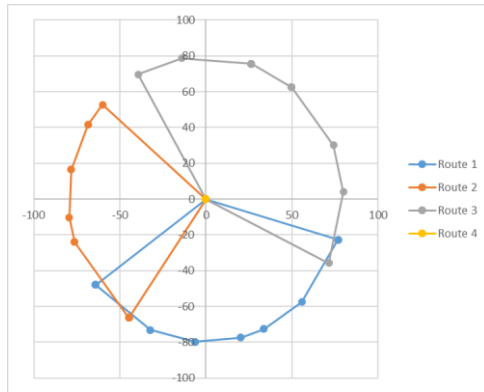


Figure 4 – Problem with clustering in the solution of artificial routing problem

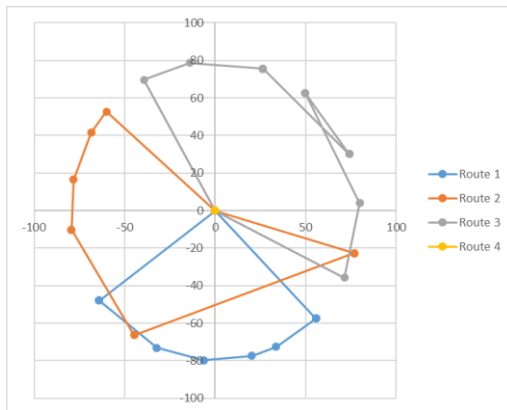


Figure 5 – Problem with routing and clustering optimization in the solution of artificial routing problem

#### 4. SUMMARY

Clustering algorithms and other methods to create groups and gather more information of a database is necessary in the industry today to be as efficient as the competitors. If you can get information or save money with little or no efforts, that is a win for everybody. Nowadays a few percent increase or decrease in efficiency can mean that a company can turn in profit or not. The example shows us that a

little error in clustering and/or a connecting problem can decrease efficiency with more than 10%, which is a huge loss. This is a very important reason to look after which tools, we use in our calculations, software, and databases.

## **ACKNOWLEDGEMENT**

The research was financially supported by the Higher Education Excellence Program (FIKP) of the Ministry of Human Capacities in the framework of the “Optimization of natural resources Research on the efficiency improvement procedures and methods of logistics systems based on modern technologies” research topic in logistics system design of the University of Miskolc.

**References:** 1. *Bányai, T.*: Introductory Chapter: Industry 4.0 and Its Impact on Logistics – A Retrospective Review, *INDUSTRY 4.0 – IMPACT ON INTELLIGENT LOGISTICS AND MANUFACTURING*, pp. 1–9, 2020; <https://doi.org/10.5772/2Fintechopen.89387>; 2. *Dobos, P., Tamás, P., Illés, B., Balogh, R.*: Application possibilities of the Big Data concept in Industry 4.0, *IOP CONFERENCE SERIES: MATERIALS SCIENCE AND ENGINEERING* 448: 1 Paper: 012011, 2018; 3. *Illés, B., Tamás, P., Dobos, P., Skapinyecz, R.*: New challenges for quality assurance of manufacturing processes in industry 4.0, *Solid State Phenomena*. Vol. 261. Trans Tech Publications Ltd, 2017; <https://doi.org/10.4028/www.scientific.net/SSP.261.481>; 4. *Borodavko, B., Illés, B., Banyai, Á.* Role of artificial intelligence in supply chain, *ACADEMIC JOURNAL OF MANUFACTURING ENGINEERING* 19: 1 pp. 75–79, 2021; 5. *Timothy, R.*: Google's DeepMind AI discovers physics, *NEW SCIENTIST*, Volume 232, Issue 3100, p. 25, 2016; [https://doi.org/10.1016/S0262-4079\(16\)32121-2](https://doi.org/10.1016/S0262-4079(16)32121-2); 6. *Saraswati J., Brian F., Rafiq A.*: Lean OR ERP – A Decision Support System to Satisfy Business Objectives, *PROCEDIA CIRP* Volume 70, pp. 422–427, 2018; <https://doi.org/10.1016/j.procir.2018.02.048>; 7. *Bryar A.H., Tarik A. R., Seyedali M.*: Performance evaluation results of evolutionary clustering algorithm star for clustering heterogeneous datasets, *DATA IN BRIEF* Volume 36, 2021, p. 107044, 2021; 8. *Zun-yang L., Feng D., YingX.X.H.*: Background dominant colors extraction method based on color image quick fuzzy c-means clustering algorithm, *DEFENCE TECHNOLOGY* 2020; <https://doi.org/10.1016/j.dt.2020.10.002>; 9. *Muthukrishnan:* Mathematics behind K-Mean Clustering algorithm *ARTIFICIAL INTELLIGENCE DATA SCIENCE*, 2018; 10. *Tamás P., Illés B., Banyai T., Banyainé T. Á., Umetaliev A., Skapinyecz R.*: Intensifying Cross-border Logistics Collaboration Opportunities Using a Virtual Logistics Center, *JOURNAL OF ENGINEERING RESEARCH AND REPORTS* 13, Paper :3, 2020.

Петер Вереш, Мішкольц, Угорщина

## **ВАЖЛИВІСТЬ КЛАСТЕРИЗАЦІЇ У ЛОГІСТИЧНИХ СИСТЕМАХ**

**Анотація.** Концепція Індустрії 4.0 використовує існуючі технології і об'єднує їх в систему, яка може робити більше, ніж індивідуально. Вона створює нову інформацію з існуючих даних. Одним з найбільш часто використовуваних принципів концепції Індустрії 4.0 є прийняття

рішень машиною без втручання людини в ситуації, яка ще не відбулася ні для машини, ні для людини. Це робить машину, виробництво або всю систему розумними. Це розумна фабрика, і в ній є свого роду штучний інтелект (ШІ). Є кілька ІТ-компаній, які хочуть створити найбільш просунутий ШІ, але в даній ситуації, в сфері збирання або виробництва, досить простого алгоритму, який може «вчитися» з мінімальною обчислювальною потужністю. Один з цих мінімалістичний  $P$  - алгоритми кластеризації, які можуть створювати групи на основі вимірних або розрахованих параметрів. Кластеризація - це  $NP$ -важке завдання в математиці, яка зводиться до того, що у неї немає спеціального математичного методу для її вирішення. Тому існує безліч алгоритмів кластеризації, які намагаються в короткі терміни дати розумне гарне рішення. Одним з найбільш важливих і специфічних способів використання алгоритмів в логістиці є планування маршруту з декількома транспортними засобами. У цій ситуації, щоб отримати гарне рішення, спочатку визначається, який транспортний засіб відвідує яку точку, а потім оптимізується маршрут окремо по групах. Більшість алгоритмів кластеризації сьогодні використовують цей метод, який дає досить хороший результат, але є шанс, що він не буде оптимальним рішенням. Щоб отримати оптимальне рішення з більшою ймовірністю, два процеси оптимізації (кластеризація і планування маршруту) повинні працювати паралельно, тому що обидва мають вплив один на одного. Тут може допомогти евристика. Евристичні алгоритми обробляють всі параметри відразу, а угруповання - це просто ще один параметр. Крім того, ніякі інші параметри не повинні змінюватися, і, якщо в цьому немає необхідності, не потрібно зважувати параметри. Однак для цього методу необхідна функція оцінки, така як функція пристосованості в еволюційних алгоритмах. В даний час збільшення або зменшення ефективності на кілька відсотків може означати, що компанія може отримувати прибуток чи ні. Невелика помилка в кластеризації і / або проблема з підключенням можуть знизити ефективність більш ніж на 10%, що є величезною втратою. Це дуже важлива причина, щоб визначити, які інструменти повинні використовуватися в наших розрахунках, програмному забезпеченні і базах даних.

**Ключові слова:** Індустрія 4.0; кластеризація; евристика; прийняття рішень; маршрутизація.

S. Dyadya, Ye. Kozlova, A. Germashev, V. Logominov,  
Zaporizhzhia, Ukraine

## **SIMULATION OF THE MACHINED SURFACE AFTER END MILLING WITH SELF-OSCILLATIONS**

**Abstract.** *Thin-walled parts are widely used in the aviation industry. It is mainly carried out with end mills and is accompanied by self-oscillation during rough milling. They negatively affect the quality of the machined surface. Therefore, it is important to model it taking into account the dynamics of the milling process to predict the accuracy. In the early works of the authors, the mechanism of the profile forming of the machined surface was determined. In this case, the identity of the shape of the cutting surface and the oscillogram of part's oscillations during milling is taken as a basis. The first wave of self-oscillations takes part in the shaping of the machined surface during cut-up milling with self-oscillation, and during cut-down milling - the last wave. The change in the distances of the cut depressions to the position of the elastic equilibrium of the part is periodically repeated from the maximum value to the minimum. Based on this, when modeling the waviness pitch of the machined surface after cut-up milling, it is necessary to know the feed rate and how many cuts were made by the tool from the largest to the smallest depression. When modeling the machined surface after cut-down milling, you need to know the length of the cutting surface. It is calculated based on cutting speed and cutting time. The formula for determining the waviness pitch after cut-down milling is derived taking into account the tool feed. The waviness height of the machined surface after cut-up and cut-down milling is determined as the difference between the largest and smallest depressions. To determine the size of the pitch and the height of the waviness, formulas are derived for converting electrical and time values of oscillograms into linear ones. These formulas also allow you to determine areas of the oscillogram with oscillations of the part during cutting and the resulting surface areas on the profilogram. The methods for modeling machined surfaces were tested after cut-up and cut-down milling with self-oscillation. In this case, the pitch and height of the waviness on the profilograms were compared with those calculated from the results of measurements of the oscillograms. Based on their analysis, refined formulas for calculating the waviness height have been derived. The error between the measurements of the waviness pitch and height and the calculated values is within 6%.*

**Keywords:** *milling; self-oscillation; waviness; pitch; height; cutting surface; modeling.*

### **1. INTRODUCTION**

The issues of processing accuracy and productivity, regardless of the level of technology development, always remain relevant. This also applies to end milling of thin-walled parts, which are widely used in the products of the aviation industry. Their rough processing falls on the third high-speed zone [1], where self-oscillations act, the intensity of which affects the shape of the machined surface.

The data obtained during the experiments on the mechanisms of formation of the machined surface during end milling with self-oscillations [2–8] make it possible to develop a methodology for its modeling.

End milling machined surfaces are formed by depressions remaining from the cutting surface when the part is moved. The depression depth ( $\Delta$ ) is determined by the distance to the elastic equilibrium position of the part (Fig. 1).

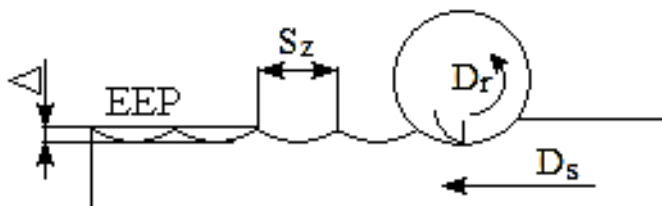


Figure 1 – Diagram for determining the depression depth after end milling

The elastic equilibrium position (EEP) is the position of the part's surface when no driving force is acting on it. If these distances are equal, the machined surface does not have the waviness. This is typical for milling in the first and second high-speed oscillation zones. In the third high-speed zone, the distance of depressions to the EEP periodically changes from the maximum value to the minimum, forming waviness on the machined surface.

The modeling is based on the identity of the cutting surface shape and the oscillogram of the part oscillations during cutting [3]. Therefore, when constructing a model of the machined surface, the data are used, which are determined from the basic fragments of the oscillogram (BFO) [6], taking into account the peculiarities of the cutting processes during cut-up and cut-down milling. With cut-up milling, the workpiece moves to the tool and the forming area is at the beginning of the cutting surface [3, 7]. During cut-down milling, the workpiece moves in the direction of the tool rotation and the forming area is at the end of the cutting surface [2, 4, 8].

## 2. MATERIALS AND METHODS

To simulate the machined surface obtained in the third high-speed oscillation zone after cut-up milling, it is necessary to know the feed per tooth -  $S_z$  and the number of the mill cuts -  $N$ , at which the deviation from the EEP of the first self-oscillation wave changes from the maximum value -  $\Delta_{max}$  to the minimum -  $\Delta_{min}$  (Fig. 2).

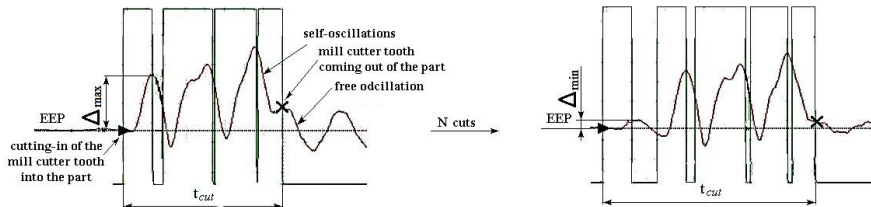


Figure 2 – Change in deviation from EEP of the first wave of self-oscillations during cut-up milling, determined by BFO

The waviness pitch on the machined surface -  $S_w$  is determined by the formula:

$$S_w = S_z N \quad (1)$$

The waviness height -  $W_z$  is determined as the difference between the maximum and the minimum values of the deviation from the EEP of the first wave of self-oscillations, within the analyzed cuts:

$$W_z = \Delta_{\max} - \Delta_{\min} \quad (2)$$

When modeling the machined surface after cut-down milling, it is necessary to take into account the peculiarity that the cutting time -  $t_{cut}$  at each subsequent cut, in the range of variation of the deviation from the EEP of the last self-oscillation wave from the maximum value to the minimum, increases (Fig. 3) [2, 4, 8].

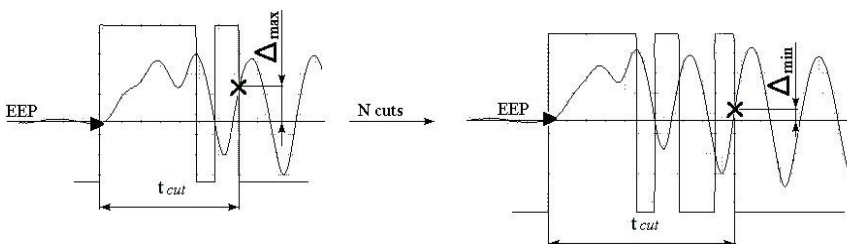


Figure 3 – Change in cutting time and deviation from EEP of the last wave of self-oscillations during cut-down milling

In this case, the length of the cutting surface also increases -  $L_{cut}$ , which is calculated by the formula:

$$L_{cut} = \frac{\pi D_{mill} n}{60} t_{cut} \quad , \quad (3)$$

where  $D_{mill}$  – cutter diameter, mm;  
 $n$  – cutter rotation frequency, rpm;  
 $t_{cut}$  – cutting time, s.

With cut-down milling, as well as with cut-up milling, each subsequent plunge of the tool into the part occurs after its movement by the amount of feed per tooth -  $S_z$ . But because each subsequent cutting surface is longer than the previous one, the remaining depression from the next cut is in front of the previous one. This order of formation of depressions is periodically repeated. As a result, a wavy profile is formed on the machined surface.

To theoretically determine the waviness pitch during cut-down milling, the following method was used. Since the length of the cutting surface during cut-down milling with self-oscillation periodically changes from the minimum value to the maximum value, the minimum cutting time was chosen as the reference point, according to which, based on formula (3), the minimum cutting surface length is calculated. When the tool leaves it, a depression is cut out, which is the most distant from the EEP. From the minimum length of the cutting surface, the position of the depressions of subsequent cuts is determined to the most distant and closest to the EEP, which will be one of the peaks of the waviness. Next, the position of the next cutting surface with the minimum length is determined, from which the abovementioned constructions are performed, and the next peak is located. The distance between the peaks is equal to the waviness pitch -  $S_w$  (Fig. 4).

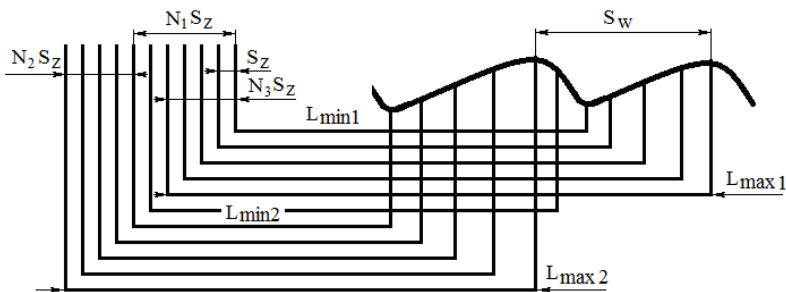


Figure 4 – Diagram for determining the waviness pitch on the machined surface after cut-down milling

The waviness pitch –  $S_w$ , as the distance between adjacent protrusions on the machined surface, calculated by the formula:

$$S_w = L_{\max 1} - L_{\max 2} + S_z \cdot (N_1 + N_2 - N_3), \quad (4)$$

where  $L_{\max 1}$  and  $L_{\max 2}$  – maximum lengths of cutting surfaces at maximum times of profiling, mm;

$S_z$  – feed per tooth, mm;

$N_1$  – the number of cuts by the cutter tooth between the minimum lengths of the cutting surfaces;

$N_2$  – the number of cuts with the cutter tooth from the minimum length of the cutting surface to the maximum in the area where the current wave is formed;

$N_3$  – the number of cuts with the cutter tooth from the minimum length of the cutting surface to the maximum in the area where the previous wave was formed.

The waviness height during cut-down milling, as well as with cut-up milling, is calculated by the formula (2).

To evaluate the proposed method for modeling machined surfaces after end milling, a comparison of the geometric parameters of waviness, determined from the profilograms after milling, and calculated from the parameters of the basic fragments of the oscillograms was carried out. This is possible with the help of analog-to-digital converters and an inductive proximeter XS1M18AB120 when recording oscillograms. Its calibration allows converting electrical and time signals into linear ones. In this case, on the profilograms, the pitch -  $S_w$  and height -  $W_z$  of the waviness of the machined surface are calculated by the formulas:

$$S_w = t \cdot v, \quad (5)$$

where  $t$  – time of the signal recording between two adjacent protrusions on the profilogram, s;

$v$  – signal recording speed, determined by the feed of the machine table, mm / s.

$$W_z = k \cdot V, \quad (6)$$

where  $k$  – calibration value for the XS1M18AB120 inductive proximeter used when recording the profilogram, mm / V;

$V$  – the greatest deviation of the recorded signal from the EEP, V.

### **3. EXPERIMENTS AND RESULTS DISCUSSION**

The studies were carried out in the third high-speed oscillation zone on an experimental stand [6] with a special single-tooth cutter with cutting modes: spindle speed  $n_{sp} = 280$  rpm; feed per tooth  $S_z = 0.1$  mm; axial depth  $a_p = 3.4$  mm; radial depth  $a_e = 0.5$  mm, with free cut-up and cut-down milling.

After milling, profilograms were recorded, fragments of which are shown in Fig. 5.

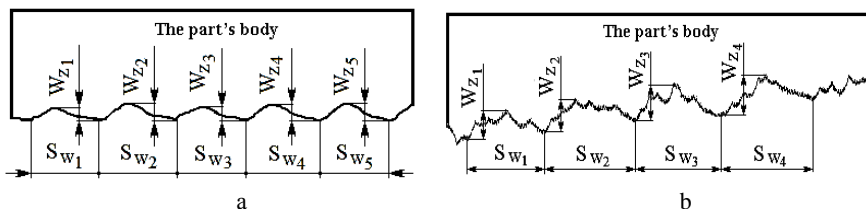


Figure 5 – Fragments of profilograms after cut-up (a) and cut-down (b) milling

The unique ability to digitize the signal allows using the formula (5) on the oscillogram to find the base fragments corresponding to the formation of the surface recorded on the profilogram.

On the basis of this and according to the methods described above, models of the machined surfaces were built after cut-up and cut-down milling (Fig. 6).

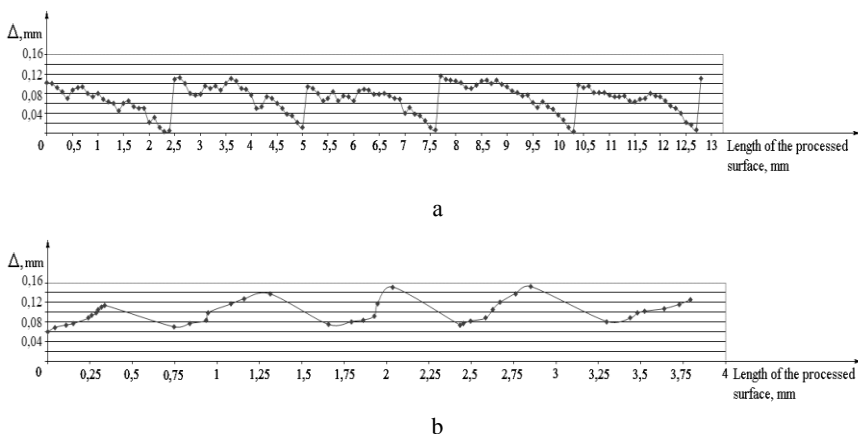


Figure 6 – Models of machined surfaces after cut-up (a) and cut-down (b) milling

It should be noted that due to the radius of the tip of the indicator clock in the device for recording profilograms [6], the most distant depressions on the machined surface are not recorded. Therefore, instead of formula (2), when determining the waviness height -  $W_{zi}$  more than 0.07 mm using oscillograms, formula (7) is used, and with waviness height up to 0.07 mm - formula (8):

$$W_{zi} = -4,6334 \cdot \Delta_i^2 + 2,1319 \cdot \Delta_i - 0,0746, \quad (7)$$

$$W_{zi} = -17,387 \cdot \Delta_i^2 + 2,9825 \cdot \Delta_i - 0,071. \quad (8)$$

where  $\Delta_i$  – the difference between the max and min deviation of the wave (the first one for cut-up milling and the last one for cut-down milling) of self-oscillations from the EEP on the oscillogram within the change period, mm.

Table 1 and 2 show the values of the pitch and the height of the waviness of the machined surface after cut-up milling. Table 3 and 4 - after the cut-down milling.

Table 1 – The waviness pitch of the machined surface, determined from profilograms and calculated by the formula (1)

Section number on the profilogram (Fig. 5, a)	1	2	3	4	5
The waviness pitch, $S_w$ on the profilogram, mm	2.54	2.65	2.57	2.65	2.49
Number of cuts with a cutter tooth, $N_s$	25	26	26	27	24
Feed per tooth, $S_z$ , mm	0.1				
The waviness pitch $S_w$ , calculated by the formula (1), mm	2.5	2.6	2.6	2.7	2.4
Error, %	1.57	1.89	1.15	1.85	3.61

Table 2 – The waviness height, measured on the profilogram and calculated by the formula (6)

Section number on the profilogram (рис. 5, a)	1	2	3	4	5
The waviness height on the profilogram, $W_{zi}$ , mm	0.083	0.091	0.083	0.107	0.082
The difference between the max and min deviation of the first wave of self-oscillations from the EEP, $\Delta_i$ mm	0.092	0.103	0.091	0.112	0.094
The waviness height $W_{zi}$ , calculated by formula (6), mm	0.082	0.095	0.081	0.106	0.084
Error, %	1.2	4.21	2.4	0.93	2.38

Table 3 – The waviness pitch, measured on the profilogram and calculated by the formula (4)

Section number on the profilogram (рис. 5, b)	1	2	3	4
The waviness pitch on the profilogram $S_{wi}$ , mm	0.768	0.902	0.809	0.92
The waviness pitch $S_{wi}$ , calculated by formula (4), mm	0.75	0.91	0.77	0.87
Error, %	2.34	0.88	4.82	5.43

Table 4 – The waviness height, determined from the profilogram and calculated by the formula (7)

Section number on the profilogram (рис. 5, b)	1	2	3	4
The waviness height $W_{zi}$ , measured on profilogram, mm	0.040	0.048	0.052	0.055
The difference between the max and min deviation of the last wave of self-oscillations from the EEP, $\Delta_i$ mm	0.054	0.067	0.075	0.078
The waviness height $W_{zi}$ , calculated by formula (7), mm	0.039	0.051	0.055	0.056
Error, %	2.5	5.9	5.45	1.78

The errors of the models of the machined surfaces, built according to the shape-generating parameters of the oscillograms, after the cut-up and cut-down milling, in comparison with the profilograms, do not exceed 6%.

#### 4. CONCLUSIONS

Methods for constructing the profile of the machined surface after cut-down and cut-up milling with self-oscillations are proposed. It is based on the identity of the shape of the cutting surface and the oscillogram of the part's oscillations. Based on this, the shaping parameters from the oscillograms are used to build a model of the machined surface. The calculated values of the pitch and height of the waviness on it are close to those measured on the profilograms. Building a model of a machined surface based on BFO data allows one to predict the effect of cutting conditions and tool geometry on it.

**References:** 1. Vnukov Yu.N, Dyadya S.I, Kozlova Ye.B, Logominov V.A, Chernovol N.N. Self-oscillations when milling thin-walled elements of workpiece s. Zaporizhzhia: ZNTU; 2017. 208 p.

2. *Svinin V.M.* Milling with modulated cutting speed. ed. A.I. Promtova. Irkutsk: Publishing house Ir: TTU; 2007. 304 p. 3. *Shapoval Yu.V, Zaloga V.O.* Improving the efficiency of machining parts by control the dynamics of the turning process with high spindle speeds. BULLETIN OF ZhSTU; 2017. 2 (80). pp. 175-184. DOI: [https://doi.org/10.26642/tu-2017-2\(80\)-175-184](https://doi.org/10.26642/tu-2017-2(80)-175-184) pp. 175-184. 4. *Tashliisky N.I.* Primary source of energy for excitation of self-oscillations when cutting metals. Bulletin of mechanical engineering. 1960. 2. pp. 10–20. 5. *Mazur N.P, Vnukov Yu.N, Grabchenko A.I. and others.* Osnovy teorii rezaniya materialov, NTU KhPI, Kharkiv. 2003. 534 p. 6. *Zharkov I.G.* Vibrations during processing with a blade tool. Mechanical Engineering, 1986. 184 p. 7. *Dyadya S.I.* Investigation of the formation of the machined surface of a thin-walled element of the workpiece during end cylindrical milling with self-oscillations. Modern Technologies in Machinery. 2017;12: pp. 5–18. 8. *Hung C.Y, Junz J.J.* Wang Effects of cutting conditions on dynamic cutting factor and process damping in milling. Internation jornal of Machine Tools and Manufacture. 51, 2011. pp. 320–330.

Сергій Дядя, Олена Козлова, Антон Гермашев, Віктор Логомінов,  
Запоріжжя, Україна

## МОДЕЛЮВАННЯ ОБРОБЛЕНОЇ ПОВЕРХНІ ПІСЛЯ КІНЦЕВОГО ФРЕЗЕРУВАННЯ З АВТОКОЛИВАННЯМИ

**Анотація.** *В авіаційній промисловості широко поширена обробка тонкостінних деталей. Переважно вона виконується кінцевими фрезами і при чорновому фрезеруванні супроводжується автоколиваннями. Вони негативно впливають на якість обробленої поверхні. Тому важливим є її моделювання з урахуванням динаміки процесу фрезерування для прогнозування точності. У ранніх роботах авторів визначено механізм формування профілю обробленої поверхні. При цьому за основу взята ідентичність форми поверхні різання і осцилограми коливань деталі при фрезеруванні. У формоутворенні обробленої поверхні при зустрічному фрезеруванні з автоколиваннями бере участь перша хвиля автоколивань, при попутному фрезеруванні - остання хвиля. Зміна відстаней вирізаних западин до положення пружної рівноваги деталі періодично повторюється від найбільшого значення до найменшого. На підставі цього, при моделюванні кроку хвилястості обробленої поверхні після зустрічного фрезерування, необхідно знати величину подачі і кількість різів, що зроблено інструментом від найбільшої до найменшої западини. При моделюванні обробленої поверхні після попутного фрезерування треба знати довжину поверхні різання. Вона розраховується на підставі швидкості різання і часу формування поверхні різання. Формула для визначення кроку хвилястості після попутного фрезерування отримана з урахуванням подачі інструменту. Висота хвилястості обробленої поверхні після зустрічного і попутного фрезерування визначається як різниця між найбільшою і найменшою западинами. Для визначення розмірів кроку і висоти хвилястості отримано формули по перетворенню електричних і часових величин осцилограм в лінійні. Ці формули також дозволяють визначати ділянки осцилограми з коливаннями деталі при різанні і отримані при цьому ділянки поверхні на профілограмі. Методики моделювання оброблених поверхонь перевірялися після зустрічного і попутного фрезерування з автоколиваннями. При цьому порівнювалися крок і висота хвилястості на профілограмі і розраховані за результатами вимірювань осцилограм. На підставі їх аналізу виведені уточнені формули для розрахунку висоти хвилястості. Похибка між результатами вимірювань кроку і висоти хвилястості і розрахованими значеннями знаходиться в межах 6%.*

**Ключові слова:** *фрезерування; автоколивання; хвилястість; крок; висота; поверхня різання; моделювання.*

S. Oliinyk, Kramatorsk, Ukraine, L. Kalafatova, Pokrovsk, Ukraine

## **TECHNOLOGICAL FIXTURES FOR MACHINING LARGE-SIZED THIN-WALLED SHELLS OF COMPLEX PROFILE**

**Abstract.** *The paper analyzes the structure of technological fixtures for the positioning and fixing of large-sized thin-walled pyroceram shells as a factor affecting the dynamic characteristics of the grinding system. The solution to the problem of ensuring the dynamic stability of the «mandrel-workpiece» subsystem is necessary to increase the efficiency of shell machining in present conditions. Studying the vibrations frequency spectrum of the technological system during grinding has made it possible to determine their sources. The magnitude and frequency of vibrations depend on the mandrel structure - the clamping fixture. The study results are the requirements for a new mandrel structure, considering the dynamic stability of the technological system.*

**Keywords:** *thin-walled shell; pyroceram; diamond grinding; technological system; structure of fixture - mandrel; vibrations; natural vibration frequency.*

### **1. INTRODUCTION**

Thin-walled shells are a component of rocket and aviation technology. Products have a complex profile (paraboloid of rotation), large dimensions with the following parameters: diameter of 200-500 mm, length of 1000-2000 mm, wall thickness of 5-6 mm, and are made of fragile, difficult to machine material (pyroceram, ceramics). Finished parts must meet the requirements for mechanical strength, heat resistance, radio-technical properties, which is ensured by the accuracy of the detail's profile and its thickness, as well as the characteristics of the surface layer (structure, stresses, waviness, roughness). Deviations from the accuracy of the wall thickness of the finished product should be in the range of  $\pm 0.02$  mm, the roughness of the machined surface should not exceed the parameter  $R_a = 0.08 \dots 0.04 \mu\text{m}$  [1]. Shell workpieces are produced by centrifugal casting. The workpiece is characterized by significant unevenness in wall thickness. This is due to the properties of the material and the instability of the technological molding process parameters [1]. Machining of shells can be performed both using universal and special machines with horizontal and vertical workpiece installation schemes, as well as using modern machines with parallel structures. The latter allows you to change the machining scheme and apply innovative ways to ensure the accuracy of the product surface while reducing the complexity of machining [2].

The technological process of shell machining consists of several stages, during which a significant allowance is removed. The main stages of processing are preliminary and final operations of diamond grinding of the inner contour with basing on the outer contour of the workpiece, grinding of the outer contour with

basing on the machined inner surface. At the last stage of machining the outer contour, it is necessary to fulfill the requirements for the accuracy of the wall thickness, waviness, and roughness of the formed surface. However, due to the problems with the dynamic instability of the technological system elements (workpiece, mandrel, tool), these requirements are not met. Therefore, for the final shaping of the product, the operations of finishing with diamond bars of its inner and outer contours are performed. This is a time-consuming manual operation, which reduces the efficiency of the entire technological process. Therefore, the problem of increasing the dynamic stability of the technological system of grinding shells is relevant.

## **2. ANALYSIS OF THE CAUSES OF THE DYNAMIC INSTABILITY OF THE TECHNOLOGICAL SYSTEM DURING DIAMOND GRINDING OF PYROCERAM SHELLS**

For thin-walled shells, the following relationship is characteristic:  $h/R_o = 1/20$ , where  $h$  is the wall thickness of the product,  $R_o$  is the minimum curvature radius of its middle surface. According to this parameter, the considered shells can be classified as thin walled. Such products are difficult to install and secure in machining operations. The thin wall of the workpiece lacks static rigidity and dynamic stability when it is subjected to clamping and cutting forces. The result of the analysis of vibrations in the technological system during grinding, presented in studies [1, 3], showed that their level is influenced by beating and deformation of the grinding wheel. The beating of the grinding wheel creates a source of vibration excitation with a frequency that depends on the speed of the wheel rotation. At a wheel speed  $v = 42$  m/s (the wheel speed when machining the outer contour), the frequency of the driving force is 67 Hz. Measurements using a round measuring device showed that during machining, three waves are formed on the working surface of the grinding wheel. This creates sources of oscillation excitation with a frequency of 201 Hz [1, 3], which provokes the occurrence of forced vibrations in the technological system during machining. Their level is influenced by both the parameters of the cutting process (the value of the cutting force and the direction of its components relative to the elements of the technological system), and the parameters of the technological system elements, including the structure of the mandrel - fixture.

The amplitude of forced vibrations depends on the condition of the grinding wheel surface, its wear, geometry of the machined section of the workpiece profile, which can provoke the dynamic instability of such workpieces during grinding and be accompanied by the appearance of parametric vibrations of the shell wall. The amplitude and frequency of such vibrations depend on the geometry of the shell, the way of its fastening in the fixture, the properties of the construction material,

the speed and direction of movement of the local moving load during cutting. Certain ratios of external force (cutting force) oscillation frequencies, the speed of its movement on the surface of the workpiece and natural frequencies of the shell cause unstable parametric vibrations in the system. The most dangerous in terms of the appearance of vibrations in the system is the presence of low (up to 1000 Hz) natural frequencies of the shell.

During machining, the shell is positioned and fixed in a fixture, i.e. a mandrel. In this case, even at the finishing stage of machining the outer surface, the basic inner surface of the workpiece, obtained after its final grinding, has a significant error - up to 0.2 mm [1]. Such conditions of basing and fixation determine the values of natural frequencies of the «mandrel-workpiece» subsystem vibrations and influence the level of forced and self-excited vibrations. Therefore, the level of vibrations in the technological system largely depends on the mandrel structure.

In the present work the analysis of mandrel structures for positioning and fixing thin-walled shells during grinding is carried out. The results of the analysis will make it possible to develop the necessary requirements for such fixtures, based on ensuring the accuracy and quality of machining.

### **3. STUDY OF DYNAMIC CHARACTERISTICS OF THE TECHNOLOGICAL SYSTEM UNDER PRODUCTION CONDITIONS**

The paper deals with diamond grinding of the outer contour of a thin-walled pyroceram shell. Overall dimensions of the finished product are as follows: outer diameter is 350 mm, length is up to 1000 mm, wall thickness is 7-8 mm. In production conditions a modernized universal lathe with an aggregate grinding head is used. The workpiece 2 is placed horizontally on a two-supporting mandrel 1 with cylindrical and conic supports (fig.1). The workpiece nose rests on the support 3, which ensures its longitudinal fixation on the mandrel during machining. The support 3 has an elongated design due to the positioning of the aggregate grinding head on the lathe slide.

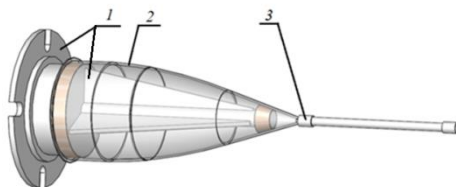


Figure 1 – Scheme of installation of the workpiece during machining in production conditions

It is difficult to ensure the necessary accuracy of the workpiece positioning in machining operations. This is due to the low accuracy of the base surfaces of the workpiece, errors in the shape and location of its inner surface relative to the outer surface. These errors appear at the preliminary machining of the inner contour and are transferred with a certain degree of refinement to the final machining of the inner surface. The workpiece is based on the tapered and cylindrical surfaces (see Fig. 1) during the grinding operation of the outer contour. Positioning error of tapered surface causes a basic positioning error along the workpiece axis up to 1,13 mm [1]. The error of the cylindrical base surface creates a clearance when basing the workpiece on the mandrel. The study of the positioning error in production conditions has shown that the value of this clearance is 0.1-0.4 mm [1]. This leads to the rotation of the workpiece during machining under the influence of cutting force and vibrations.

To determine the influence of the state of the technological system elements on its dynamic characteristics, we have measured the frequency spectrum of vibrations arising in the process of grinding. The parameters of the frequency spectrum were measured using a vibrometer 795M107B. The vibrometer sensor was installed on the mandrel of the grinding head. The frequency spectrum of the technological system vibrations for the parabolic section of the shell, which is located at a distance of 300 mm along the axis from the workpiece base, is shown in Fig. 2. The main values of technological system vibrations are marked at the frequency spectrum along the axis OX in the range from 0 to 1000 Hz, the acceleration of vibrations ( $\text{mm/s}^2$ ) are shown along the axis OY.

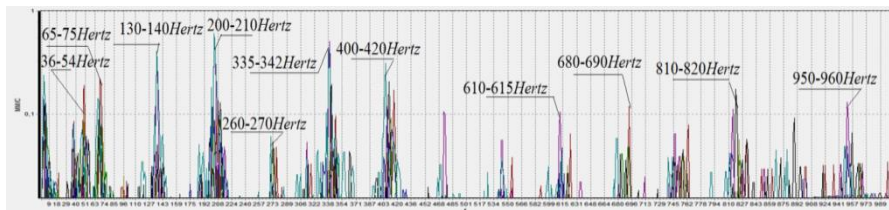


Figure 2 – Frequency spectrum of the technological system vibrations during finishing the outer contour of the workpiece

Table 1 presents the results of the frequency spectrum analysis. For the analysis we have used the measurement results (see Fig. 2) and studies of the dynamic characteristics of a similar technological system, carried out in the research [1, 3].

Table 1 – Analysis of the frequency spectrum of the technological system vibrations

Frequency range, Hz	Source (cause) of the harmonic
Less than 20	Non-synchronous spectrum components (environmental noise; low-frequency spectrum of vibrations of other elements of the technological system)
36-54	Subharmonics resulting from the grinding wheel rotation; natural frequencies of the «spindle assembly – mandrel - workpiece» subsystem
65-75	Frequencies corresponding to the operating frequency of the grinding wheel and the lowest natural frequency of the shell
130-140	Superharmonics, which occurs during the grinding wheel rotation
200-210	Superharmonics, which appears due to changes in the shape of the grinding wheel
260-270	Natural frequencies of the shell workpiece vibration
335-342; 400-420	Natural frequencies of the «spindle - mandrel» subsystem and superharmonics from the grinding wheel rotation caused by its imbalance
610-615; 680-690; 950-960	Natural frequencies of the «mandrel - workpiece» subsystem
810-820	Natural frequencies of the «spindle assembly - grinding wheel»

#### **4. FINITE ELEMENT ANALYSIS OF THE DYNAMIC CHARACTERISTICS OF THE «MANDREL - WORKPIECE» SUBSYSTEM FOR DIFFERENT MANDREL DESIGNS**

To assess the impact of the fixture design on the level of vibrations in the technological system when grinding thin-walled shells of a complex profile, an analysis of its dynamic characteristics depending on the type of mandrels used in production and proposed by modern researchers has been conducted.

The theoretical study of the dynamic behavior of the technological system is performed in the Solid Works Simulation software package by the finite element method. Three-dimensional models of mandrels with a workpiece mounted on them have been developed. For the «mandrel - workpiece» subsystem deformations from the local load (cutting force) in its action area has been calculated to determine the subsystem rigidity. Also the spectrum of natural frequencies and vibration modes for the «mandrel - workpiece» subsystem, arising under the influence of the local load (cutting force) have been calculated to determine the dynamic behavior of the subsystem.

Fig. 3 shows the frequency spectrum of vibrations of the «mandrel - workpiece» subsystem and the frequency waveforms when grinding in production conditions (Variant I) obtained by calculation. The workpiece basing has been carried out on the mandrel according to Fig. 1. The calculated model is made for the real conditions: there is a clearance of 0.1 mm on the cylindrical support. The calculated values of vibration frequencies have been compared with the spectrum of vibration frequencies measured in production conditions (Fig. 3, a), and with the frequency of the vibration source.

The shapes of vibration frequencies (Fig. 3, b, c, d) allow us to determine the nature of possible vibrations. Red color shows the greatest deformation of the product relative to the resting state, blue - the absence of deformation, green - intermediate variant of the deformation value. The graphs of the frequency spectrum (see Fig. 3, a) show the frequency in Hz on the axis OX, and the product deformation, mm, on the axis OY.

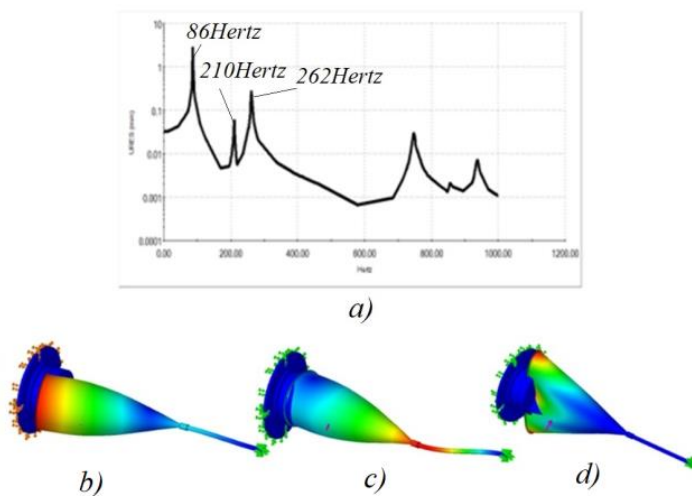


Figure 3 – Calculated frequency spectrum of vibrations of the «mandrel-workpiece» subsystem and the frequency forms for production conditions (Variant I)

The forced vibrations of the «mandrel - workpiece» subsystem and the parametric vibration of the shell are mostly influenced by the frequencies up to 1000 Hz, i.e. the first three natural frequencies (see Fig. 3, a).

To confirm the assumption that the low frequency spectrum is related to the presence of a clearance between the mandrel and the workpiece, the frequency

spectrum of vibrations for the virtual mandrel of similar design, but without the clearance (Fig. 4, a, b), as well as the version of the spectrum for the conditions of exclusion of the support 3 (Fig. 4, c, d; Variant II) have been calculated.

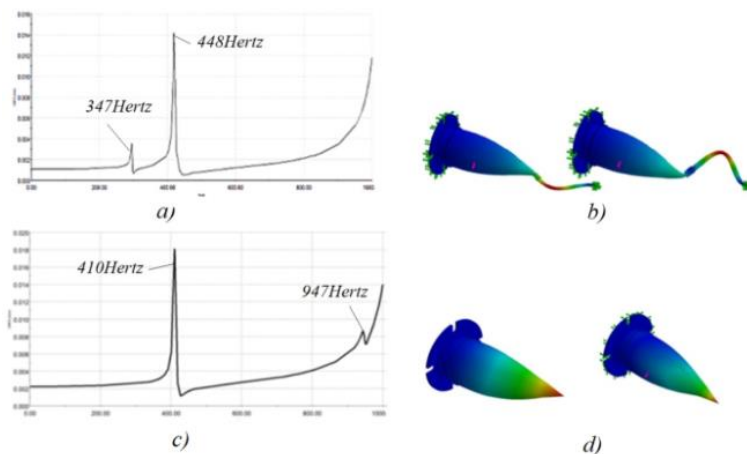


Figure 4 – Calculated frequency spectrum of vibrations and the frequency forms of the «mandrel-workpiece» subsystem (Variant II)

For the models of Variant I and Variant II, the static calculation of the workpiece deformations under the influence of the cutting force is performed. For all variants of the workpiece positioning, the characteristic value of the cutting force, which is 400 N, has been taken for the selected machining conditions [3]. Grinding area is located on the parabolic section of the workpiece at the distance of 300 mm from its' base. The static calculation shows that the workpiece surface displacements under the cutting force in the grinding area is, respectively, 0.12 mm (Variant I), which is close to the measurement results according to [1], and 0.024 mm (Variant II).

The calculated natural frequency of the mandrel is 284 Hz, the measured frequency is 305 Hz. The mandrel 1 (see Fig. 1) has a rather rigid structure. The first natural frequency of the «mandrel-workpiece» subsystem (Variant I) is 86 Hz due to the bending forms of the subsystem vibrations and is a result of the presence of a clearance on the cylindrical support. The first three frequencies have the greatest influence on the vibration amplitude (Variant I). The frequency of 210 Hz (see Fig. 3, a) is close to the frequency of the driving force of 201 Hz. The frequency of 262 Hz has the form of the shell vibrations and their value, close to

the bending vibrations of the «mandrel-workpiece» subsystem, is sufficient to cause parametric vibrations (see Fig. 3, d).

The computer model of the «mandrel-workpiece» subsystem (Variant II) has shown that low forms of natural frequencies of the shell vibrations do not occur (see Fig. 4). The lowest frequency in the presence of the support 3 is associated with its bending vibrations (see Fig. 4, a, b). In the absence of the support 3 the low frequency is determined by the presence of bending vibrations of the «mandrel-workpiece» subsystem at the frequency of 410 Hz. For all cases of Variant II, the lowest frequencies are remote from the influence of exciting frequencies from the side of the grinding wheel.

In the present paper we have also analyzed the mandrel structures proposed by other researchers [5-9] for fixing the shells of similar type during the grinding operations.

The mandrel structure [5], shown in Fig. 5, has two main supports 3 - cylindrical and 4 - conical, two additional supports 5 to increase the rigidity of the shell wall and stop 6. It has been assumed that when basing a workpiece on such a mandrel, a clearance may occur due to the low accuracy of dimensions and the shape of the base surface between the cylindrical support 3 and the workpiece 1.

The static calculation has shown that deformation of shell surface under the cutting force in the grinding area is as follows: 0.014 mm in the absence of the clearance on the cylindrical support (Variant III); from 0.018 to 1.4 mm in the presence of clearances, depending on the point of force application (Variant IV).

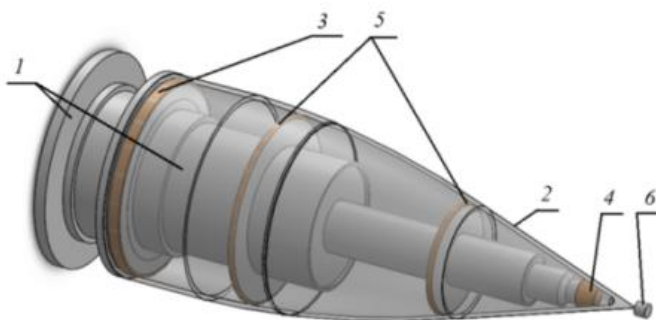


Figure 5 – Structural diagram of the «mandrel workpiece» subsystem for the mandrel structure according to [5]

The results of calculations by the finite element method in Solid Works Simulation have shown that the natural frequency of the mandrel structure [5] is 195 Hz. The mandrel structure [5] is less rigid than the mandrel shown in Fig. 1.

Also, for this mandrel the following has been established by calculating the dynamic characteristics of the system (Fig. 6).

For the «mandrel-workpiece» subsystem according to Variant III (Fig. 6, a), the first natural frequency of vibrations is 331 Hz, which removes the subsystem from the influence of excitatory vibrations, but natural vibrations of the shell, which provoke the parametric vibrations of its wall, still have a rather (below 1000 Hz) small value - 872 Hz. The presence of the clearance lowers the first frequency to 36 Hz, which will cause forced vibrations when grinding the workpiece. Low natural frequencies of vibrations of the shell wall - 244 Hz, can cause the appearance of its parametric vibrations.

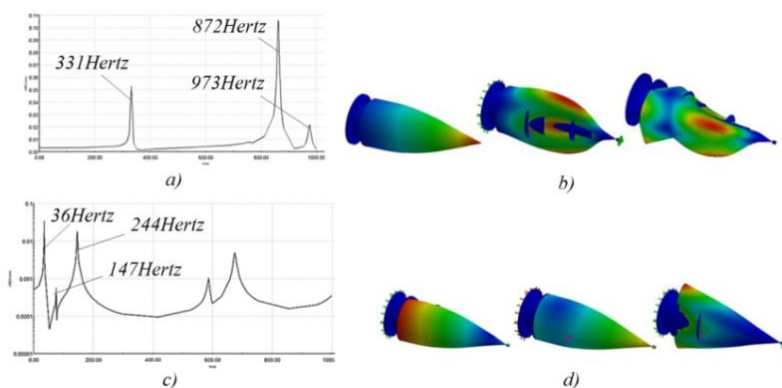


Figure 6 – Calculated frequency spectrum and vibration modes of the «mandrel-workpiece» subsystem for the mandrel structure according to [5]

The disadvantage of the mandrel [5] is that due to the low accuracy of dimensions and the shape of the inner surface of the shell, i.e. errors in the thickness of a given profile, it is difficult to adjust the fixing unit (cylindrical support) to the size during external grinding operations. As a result, the shell wall is not completely fixed. Additional fixation points increase the stiffness of the product on the limited surface, but the adjustments of these supports to the size of the inner surface have low accuracy.

*The design of the mandrel [6],* shown in Fig. 7, assumes that in the mandrel 1 there is a rubber chamber 5 between the fixation points (cylindrical support 3 and conical support 4). The chamber is filled with water 6 under pressure, which leads to its gradual expansion and uniform arrangement of the chamber along the inner surface of the workpiece 2, which ensures a uniform support of the shell wall during grinding.

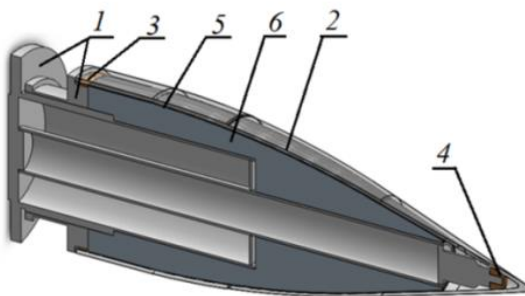


Figure 7 – Structural diagram of the «mandrel – workpiece» subsystem for the mandrel structure according to [6]

The installation and the mechanism of fixing the shell on the cylindrical mandrel has not changed in comparison with Variants III and IV. At the support 3, a clearance is possible. Two computer models have been created: with the clearance (Variant V) and without the clearance (Variant VI). The results of the static calculation (Fig. 8) show that the deformation of the workpiece surface under the influence of the cutting force in the grinding area is 0,004 mm both for Variant V and Variant VI.

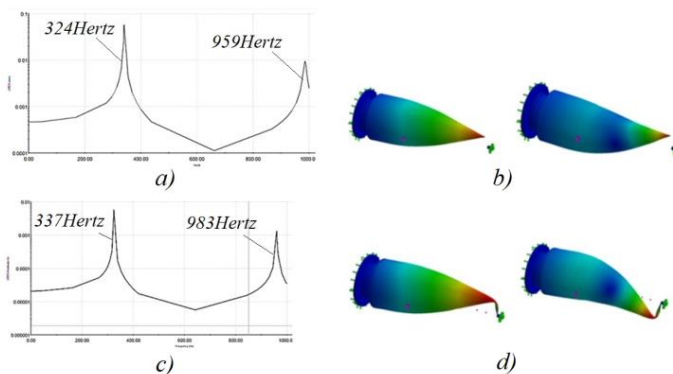


Figure 8 – Calculated frequency spectrum and frequency waveforms of the «mandrel-workpiece» subsystem for the mandrel structure [6]

The structure of the mandrel [6] significantly reduces the deformation of the shell wall, increases the lowest natural frequency, which eliminates the influence of vibrations of the exciting force. At low frequencies (up to 1000 Hz), there are no

forms of the shell vibrations, which may lead to the parametric vibrations. The frequency spectra of vibrations for Variant V and Variant VI are similar. However, the vibration amplitude in the presence of a clearance increases by a factor of almost 10 when approaching the resonance frequencies. The disadvantages of this mandrel structure are the necessity to provide its hermeticity, the laboriousness of the workpiece installation on the mandrel and the complexity of manufacturing the rubber chamber.

The mandrel structure [7], shown in Fig. 9, implies a multilayer temporary liner 6, which consists of 3 to 5 sheets of elastomer bonded with adhesive to each other. The liner is placed on the adhesive along the inner surface of the shell. The rubber chambers 5 are filled with air, creating the cavity pressure of 1 to 4 bar [7]. According to the patent [7], the fixture has a reconfigurable structure and can be applied to similar shell structures, which differ in size.

The structure of the fixture (see Fig. 9) has been adapted to the shells considered above when building the model. The authors of the fixture [7] assume machining the shell using machines with a vertical axis of the workpiece installation. This does not change the essence of the study since the influence of the mandrel on the dynamic behavior of the technological system is preserved. In the study [2], the advantages of machining such products using machines with the vertical axis and with parallel kinematics have been considered.

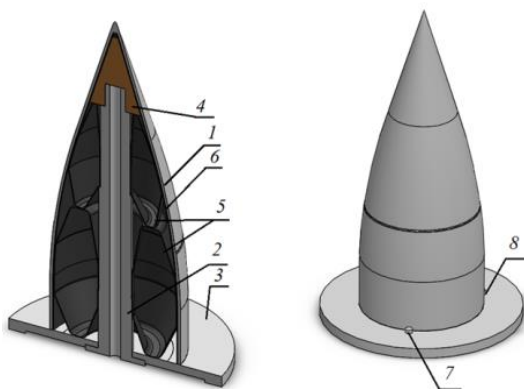


Figure 9 – Structural diagram of the «mandrel-workpiece» subsystem for the mandrel structure according to [7]:

- 1 - workpiece; 2 - mandrel; 3 - base; 4 - conical support; 5 - chamber;  
6 – liner; 7 - support; 8 – clamp

The results of the static calculation (Fig. 10) showed that the workpiece surface displacement under the influence of the cutting force in the grinding area is

0,024 mm when working with a pressure of 2 bar (200000 N/m<sup>2</sup>) and 0,022 mm with the pressure of 4 bar (400000 N/m<sup>2</sup>) (Variant VII).

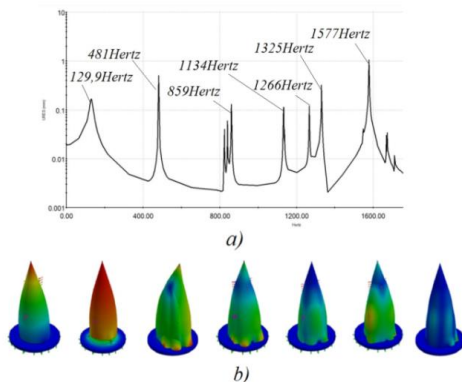


Figure 10 – Calculated frequency spectrum and the frequency waveforms of the «mandrel-workpiece» subsystem for the mandrel structure [7]

The frequency analysis for the variant of setting the workpiece according to the model (see Fig. 10, a) has been performed at the frequency of vibrations up to 1600 Hz to compare the obtained calculation results with the measurement results given in [7]. The results of measuring the frequency characteristics of the shell showed a decrease of apparent vibration peaks at frequencies from 573 to 1000 Hz and decrease of vibration amplitude at all other frequencies. The vibration amplitudes are reduced by 2.5 times at frequencies up to 500 Hz and by 2.67 times at frequencies from 500 to 1000 Hz. Calculations showed the similarity of the obtained frequency spectrum, including complete similarity in terms of the first frequency of the subsystem: 129.24 Hz in [7] and 129.9 Hz, according to Fig.10, a.

The workpiece is placed on the base 3 (see Fig. 9) on supports 7 and pressed to them by clamps 8, which, however, does not provide shell rigidity on the mandrel, leads to a decrease of the first natural frequency of the «mandrel-workpiece» subsystem, creates undesirable force effects on the surface of the workpiece from the clamp and does not allow machining the workpiece along the full contour.

Table 2 presents the calculation results of the dynamic characteristics of the «mandrel-workpiece» subsystem for the considered variants of the clamping fixture designs. The deformation of the workpiece surface from the static load is an indirect indicator of the reduced rigidity of the «mandrel-workpiece» subsystem in the machining area. The value of the first natural frequency is an indicator of the possibility of forced vibrations. The natural frequency of vibrations according to

the shape of the shell is an indirect indicator of the possibility of parametric vibrations of the shell wall.

Table 2 – Calculation results of the dynamic characteristics

Mandrel structure variants	Static load strain, mm	First natural frequency of the «mandrel-workpiece» subsystem, Hz	Natural frequency of the shell (up to 1000 Hz), Hz
Variant I	0,12	86	262
Variant II	0,024	410	-
Variant III	0,018	331	872
Variant IV	1,4	36	244
Variant V	0,004	324	-
Variant VI	0,004	337	-
Variant VII	0,022	129,9	859

According to the results presented in Table 2, it can be concluded that the mandrel structures according to Variants II, V, VI provide a stable flow of the cutting process. However, the operation of mandrels according to Variants V and VI is difficult because of the complexity of their structure.

## 5. SUMMARY

The complex, non-technological shape of the shell affects the peculiarities of positioning its workpiece in the machine and machining. The research has shown that when designing the mandrel, which will provide dynamic stability of the technological system and the required accuracy of machining, it is necessary to ensure the presence of two supports to fix the profile of the workpiece shell over the entire contact surface without a clearance; basing on the end surface; the presence of the positioning scheme allowing to process the full workpiece profile.

Among the examined mandrel structures, Variant II meets these requirements. The wall deformation is within the operational tolerance, and natural frequencies of the «mandrel-workpiece» technological subsystem are not influenced by exciting vibrations. Such conditions are not fully satisfied for the existing structures, so there is a need to develop a new progressive mandrel structure, the use of which will provide the required level of characteristics of the technological system of grinding thin-walled shells.

**References:** 1. *Pokolenko D. V.* (2014) Pidvyshchennia efektyvnosti obrobky antenykh obtichnykiv iz sytaliv za rakhunok udoskonalennia tekhnolohii almaznoho shlifuvannia [Increase of the efficiency of processing the antenna domes made of cetalss due to upgrading of diamond grinding technology]. Extended abstract of candidate's thesis. Donetsk (in Ukraine). 2. *Oliinyk, S.Yu. & Kalafatova, L.P.* (2020). Analiz skhemy obrobky skladnoprofilnykh obolonok obertannia [Analysis of the machining scheme of complex-profiles shells of rotation]. *Rizannia ta instrumenty v tekhnolohichnykh systemakh - Cutting & Tools in Technological System*, no 92, pp.122-135. Retrieved from <http://rits.khpi.edu.ua/article/view/2078-7405.2020.92.13>. 3. *Oliinyk S.Yu.* (2014) Zabezpechennia

yakosti obrobky tonkostinnykh sytalovykh obolonok shliakhom pokrashchennia dynamichnykh kharakterystyk tekhnolohichnoi systemy shlifuvannia [Ensuring quality of processing the thin-walled shells made of cetalss by improving the dynamic characteristics of the technological system of grinding]. Extended abstract of candidate's thesis. Krasnoarmiisk (in Ukraine). **4. Suzdal'cev E. I., Hamicaev A. S. & Haritonov D. V.** (2003). Ustrojstvo dlya mekhanicheskoi obrabotki krupnogabaritnykh slozhnoprofil'nykh keramicheskikh izdelij [Device for machining of large-sized complex-shaped ceramic products]. Patent RF. No 2258596. **5. Suzdal'cev E. I., Haritonov D. V. & Suslova M. A.** (2007). Ustrojstvo dlya mekhanicheskoi obrabotki krupnogabaritnykh slozhnoprofil'nykh keramicheskikh izdelij [Device for machining of large-sized complex-shaped ceramic products]. Patent RF. No 2313438. **6. Zumin Geng** (2010). Adaptive design of fixture for thin-walled shellacylindrical components. Patent US. No 2010/0164187.

Світлана Олійник, Краматорськ, Україна,  
Людмила Калафатова, Покровськ, Україна

## **ТЕХНОЛОГІЧНА ОСНАТКА ДЛЯ ОБРОБКИ ВЕЛИКОГАБАРИТНИХ ТОНКОСТІННИХ ОБОЛОНОК СКЛАДНОГО ПРОФІЛЮ**

**Анотація.** Для забезпечення точності обробки та якості поверхні тонкостінних великогабаритних оболонок з ситалу на операціях алмазного шліфування необхідно підвищувати динамічну стійкість технологічної системи. На динамічну стійкість технологічної системи впливають як характеристики процесу різання, так і динамічні характеристики її елементів. Заготовка – тонкостінна оболонка є нетехнологічним елементом. Стінці заготовки не вистачає статичної жорсткості та динамічної стійкості під впливом на неї сил закріплення у пристосуванні та різання. Рівень коливань стінки оболонки під час обробки залежить від геометрії заготовки, режиму різання та конструкції технологічної оснастки – затискної оправки, яка впливає на власні коливання стінки заготовки. Складність забезпечення точності установки заготовки на операціях механічної обробки пов'язана з низькою точністю її базових поверхонь, похибками форми і розташування внутрішньої поверхні заготовки щодо зовнішньої. Дослідження частотного спектра коливань технологічної системи під час шліфування у виробничих умовах дозволило визначити джерела їх виникнення. Було виявлено, що нижча власна частота коливань підсистеми «оправка-заготовка» в діапазоні від 50 до 200 Гц негативно впливає на вимушені коливання в технологічній системі. Власна нижча частота оболонки (до 1000 Гц) впливає на появу та рівень параметричних коливань її стінки. За допомогою методів комп'ютерного моделювання виконано оцінку впливу існуючих та віртуальних, з необхідними ознаками, конструкцій пристосувань - оправок на рівень вібрацій у системі. Всього було оцінено чотири конструкції оправок та сім варіантів їх реалізації на операції зовнішнього шліфування тонкостінної оболонки. Дослідження показали, що в конструкції оправки, яка забезпечить динамічну стійкість технологічної системи і задану точність обробки, необхідно забезпечити: наявність двох опор для фіксації профілю заготовки оболонки по всій контактній поверхні без зазорів; базування по торцевій поверхні; наявність схеми установки заготовки, яка дозволить виконати обробку її повного профілю. Існуючі конструкції оправок повністю не задовольняють переліченим вимогам, тому є необхідність у розробці нової прогресивної конструкції оправки.

**Ключові слова:** тонкостінна оболонка; ситал; алмазне шліфування; технологічна система; конструкція пристосування – оправки; вібрації; власна частота коливань.

A. Mitsyk, V. Fedorovich, A. Grabchenko, Kharkiv, Ukraine

## **INTERACTION OF THE ABRASIVE MEDIUM WITH THE TREATED SURFACE AND THE PROCESS OF METAL REMOVAL DURING VIBRATION TREATMENT IN THE PRESENCE OF A CHEMICALLY ACTIVE SOLUTION**

**Abstract.** *Interaction of working medium granules with the processed surface of the part is considered. It is noted that the processing methods are characterized by the dynamic interaction of the abrasive medium with the processed surface. It is indicated that during vibration treatment there is an impact contact of the abrasive granule with the surface of the part, which leads to the formation of characteristic traces during the formation of the surface relief. The types of impact of abrasive grains of working medium granules on the surface of the processed part are identified. It is indicated that the effect of abrasive grains depends on the geometric parameters of the tops of the grains and the working contour of the granule as a whole. The alternation of the operation of abrasive grains in the connection with the nature of the motion of the granule over the surface of the part is shown. The interaction of surfaces of bodies during vibration treatment is considered. The distinctive features of the vibration treatment method from other analogs are indicated. The conditions for the formation of the surface layer of the part during vibration processing are given. The analysis of the mechanical-physicochemical model of the micro-cutting process in the presence of a chemically active solution is carried out and a comparison of the intensity of technologies for vibration treatment of steel parts is given.*

**Keywords:** *abrasive medium; types of medium action; surface layer; mechanical-physicochemical model; metal removal; chemically active solution; vibration treatment technologies.*

**Introduction.** Processes of treatment in abrasive media are characterized by a wide range of mechanical-physicochemical phenomena caused by various technological schemes of interaction between the medium and the treated surface, the variety of characteristics of processing media, technological chemically active solutions, and parameters of processing modes [1].

The interaction of the medium with the surface to be treated is accompanied by plastic deformation and micro-cutting, friction, thermal phenomena, chemical interaction, the manifestation of the action of electromagnetic and electric fields, and adhesion processes.

The peculiarities of the interaction of the abrasive medium and the processed parts make it possible to assess the technological capabilities of the applied processing method and its regularities. In the study of the processing of parts in abrasive media, a significant influence is given to the contact interaction of the processing medium with the processed surface, that is, to local contact and their integral manifestation in the form of deformation processes and micro-cutting, to the properties of materials contacting during processing [2].

**Interaction of medium granules with the processed surface.** Despite the variety of processing methods in abrasive media, there is sufficient generality in the assessment of the mechanism of interaction of medium granules with the processed surface. Most of the processing methods under consideration are characterized by the dynamic interaction of the abrasive medium with the processed surface, in which there is an impact contact of the medium granule with the surface of the part (jet-abrasive, turbulence processing, tumbling, etc.), the formation of characteristic traces of processing and the formation of the surface.

So, for example, during vibration processing, the analysis of the phenomena in the zone of the working medium granules collision with the processed surface shows that during vibration action there is an impact contact of the abrasive granule with the surface of the part. In this case, the abrasive grains of granules in contact with the processed surface carry out micro-cutting, plastic and elastic flow around the material, and the formation of many traces of processing [3].

Considering a single granule moving relative to the processed surface, it can be noted that its profile consists of grains that carry out micro-cutting, plastic and elastic repression, and grains that are not involved in the operation.

**Types of action of abrasive grains on the processed surface.** The nature of the action of abrasive grains on the metal depends on the geometric parameters of their tops and the working contour of the granule as a whole. Depending on the orientation of the cutting edges of the abrasive grains relative to the forming granules, there are three main types of action of the abrasive grain on the surface to be processed: cutting; plastic repression; friction. In this case, each abrasive grain in the process of treatment over time can first produce only friction, then plastic repression; and, finally, carry out cutting, and vice versa.

This alternation of operation performed by the abrasive grains of the granule is associated with the nature of its movement over the surface of the processed part. High-speed filming of the process has shown that granules can leave on the contact surface complex traces of processing, which differ in depth and location on the surface. The depth of the track changes in the direction of movement of the granule and is determined by the speed of its movement, the force and frequency of penetration during the contact time, and other factors.

**Interaction of surfaces of bodies during vibration treatment.** During vibration treatment, the surfaces of two bodies interact, that is, the working surfaces of an individual granule and the processed part. The nature of mechanical and physical-mechanical processes is determined by: physical and mechanical properties of cutting grains, their sizes, shape, quantity and location on the surface of the granules; characteristics of the processed material; its physical and

mechanical properties, process parameters, depending on the technological mode of processing.

The vibration treatment process depends on the nature of the local contact of the "working grains" of the abrasive granule with a thin surface layer of the processed part. In the contact of parts with a mass of abrasive granules oscillating and moving along their surface, mutual intensive destruction of the surfaces of the contacting solids occurs, that is, the mutual running-in process occurs.

The nature of the dynamic loads in the contact zones of the working medium granules and parts distinguishes the vibration treatment method from other known methods [4]. The distinctive features include the following:

- grains of abrasive granules are loaded more evenly, and the depth of penetration of each of them is stable;
- the alternation of deforming and cutting grains is ensured due to the discontinuity of their interaction with the surface of the part;
- the presence of oscillations ensures a decrease in friction forces on the contact surfaces of the "granule-part" system;
- the abrasive granule, due to its small size, is reliably impregnated with a chemically active solution and ensures its supply to the zone of mutual contact of the abrasive granule with the processed surface;
- provides a decrease in micro-cutting forces and contact temperature.

**Conditions for the formation of the surface layer of the part after vibration treatment.** Most of the listed distinctive features are due to the self-regulation process characteristic for vibration processing, which allows a moving granule with grains embedded in the metal surface to occupy an optimal position, uniformly apply elementary traces to the surface, displaced relative to each other. This creates conditions for the formation of a more uniform surface layer, eliminates the possibility of coarse traces of destruction. It is noted that a complex spectrum of stresses arises at the points of actual contact of the bodies, micro-cutting, elastic-plastic deformation with a significant increase in the dislocation density and the formation of active dislocation-vacancy centers occur.

Due to specific patterns of vibration processing, the noted effects are distributed fairly evenly over the entire surface of the part. In general, micro- and sub-micro-relief is formed as a result of the presence of smooth areas with oxide films, rough areas formed during the destruction of the film and adhered to the surface of the smallest metal particles, as well as transition areas from smooth to rough.

It should also be noted the peculiarity of the course of the process in time. It is observed that the destruction of the material begins only after a certain period, during which preparatory processes occur, namely the formation of traces of

processing, surface hardening, the initiation of micro-cracks, etc. The duration of this period depends on the physical and mechanical properties of the material and processing conditions.

In connection with the presence of the effects of multiple elastic-plastic deformation and re-deformation of sections of the processed surface, along with the process of direct fracture, the process of high-cycle plastic deformation and fracture is manifested. The processes of micro-cutting, elastic-plastic deformation, activation of the surface layer of the metal, the formation and destruction of secondary structures, poly-deformational destruction are repeated with the frequency of collision of the medium granules with the processed surface.

**Mechanical-physicochemical model of the micro-cutting process in the presence of a chemically active solution and comparison of the intensity of vibration treatment technologies for steel parts.** The analysis makes it possible to construct a mechanical-physicochemical model of the process of destruction of the processed surface, that is, the process of micro-cutting the material of a part, which ensures the metal removal in the presence of a chemically active solution. This model relates the parameters of metal removal and surface micro-roughness with factors affecting them and includes the following:

- shock mechanical contact, on which there is elastic, plastic, elastic-plastic deformation and destruction of the surface layer with the removal of metal particles;
- the formation of a loosened layer of active metal;
- interaction of the active metal layer with the environment, that is characterized by the formation of weakened secondary structures;
- destruction of secondary structures by subsequent impacts of medium granules;
- the formation of a specific sub-micro-relief, which is a layer of finely divided particles.

Fig. 1 shows a comparison of technological processes of vibration treatment of steel parts to high classes of surface cleanliness.

The technological process of vibration treatment of parts of carbon steels [5], as shown by curve *1* of the graph, consists of five transitions, for which the processing modes and the used abrasive material are indicated.

For example, for technological process *1*, the first transition is performed under the conditions of 25KЧ25, BT1, 1,5A3, where 25 is the size of the granules of the working medium, KЧ is the grain material, 25 is the granularity of the

granules, BT1 is the hardness of the bond, 1.5 is the vibration frequency of the vibrating machine reservoir, thousand counts / min., A3 – vibration amplitude, mm (Ukrainian standard).

In this case, obtaining a micro-roughness of  $R_a = 0.32 \dots 0.16 \mu\text{m}$  with an initial  $R_a = 20 \dots 10 \mu\text{m}$  is achieved in 12 ... 16 hours of processing in the medium of abrasive granules of a certain granularity for each transition. The reservoir is flushed with a soap and soda solution. The final finishing of the processed surfaces is carried out with felt wads, caricatured with polishing paste.

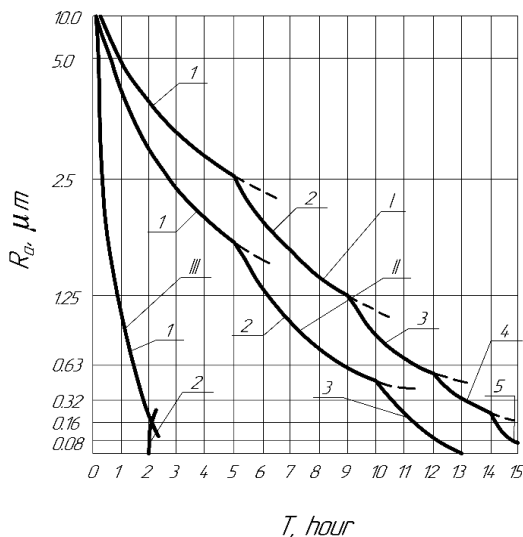


Figure 1 – Comparison of technological processes of vibration processing of parts of carbon steel: *I* – technological process of NIITM, 1, 2, 3, 4, 5 – technological transitions; *II* – ENIMS technology; *III* – technology of V. Dahl EUNU

Technology [6] offers a range of vibration grinding and polishing processes for ferrous metal parts. To obtain a surface with a micro-roughness of  $R_a = 0.32 \mu\text{m}$  with an initial  $R_a = 20 \dots 10 \mu\text{m}$ , the parts should be processed in the following sequence:

– first, in the medium of abrasive granules with a grain size of 12 ... 40 in the presence of an aqueous solution to a purity of  $R_a = 2.5 \dots 1.25 \mu\text{m}$ ;

– then, in the medium of abrasive granules with a grain size of 6 ... 10 in the presence of an aqueous solution to a purity of  $R_a = 1.25...0.63 \mu\text{m}$ ;

– finally, in the medium of a special molded filler and an aqueous solution to a purity of  $R_a = 0.16 \mu\text{m}$ .

The total processing time is 12 ... 14 hours. Naturally, such complex multistage technological processes of vibration treatment have not found wide application in mechanical engineering.

The chemically active solution [7] allows to eliminate multistage overloading of the reservoir contents and to obtain a cleanliness of the treated surface of  $R_a = 0.32 \mu\text{m}$  at the initial  $R_a = 20...10 \mu\text{m}$  in one operation in the medium of abrasive granules AH-2 TY 2-036-02211899-007-97 (Ukrainian standard).

The second stage of processing is required only if it is necessary to obtain a purity of  $R_a = 0.16...0.08 \mu\text{m}$ .

### **Conclusions**

1. The process of metal removal during vibration processing is characterized by the intensity of mechanical and chemical actions and the ability of the material of the processed part to resist the effects of these processes.

2. In connection with the considered model of destruction of the surface layer of the processed part the ratio of micro-cutting and elastic-plastic deformation processes is 30 ... 35 % and 70 ... 65 %, respectively.

3. Unlike abrasive granules used as a working medium in vibration grinding operations, the interaction of metal balls used in vibration polishing operations is accompanied by elastic-plastic deformation and the formation of many processing traces.

4. The use of chemically active solutions in vibration treatment contributes to a more intensive metal removal due to the formation of loose films on the surface of parts, which are easily removed by an abrasive during processing and favorably affects the formation of the micro-relief of the processed surface. In addition, the chemically active solution has anti-corrosion properties and helps to brighten the processed surface.

**References:** 1. *Mitsyk A.V* Rozvytok procesiv obrobky vil'nym abrazyvnym seredovysshem v kolyvnyh rezervuarh i formuvannja i'h fizyko-tehnologichnyh mozlyvostej. Visnyk SNU im. V. Dalja. Sjevjerodonec'k, SNU im. V. Dalja, 2020. № 4 (260). pp. 55 – 65. DOI: <https://doi.org/10.33216/1998-7927-2020-260-4-55-65>. 2. Instrumental'noe obespechenie processov obrabotki detalej v granulirovannyh sredah: monografija / A.P. Babichev, P.D. Motrenko, S.A. Kostenkov, O.A. Rozhnenko, M.A. Tamarkin, V.Ja. Shumjacher; Donskoj gos. tehn. un-t. Rostov-n/D: 2011. 267 p.

3. Mitsyk A.V., Fedorovich V.O., Grabchenko A.I. Mehano-fyzyko-himichne modeljuvannja procesu rujnuvannja poverhni detali u vil'nomu abrazyvnomu seredovyshhi. Rizannja ta instrumenty v tehnologichnyh systemah. Kharkiv, NTU «KhPI», 2020. № 92. pp. 62 – 67. DOI: <http://doi.org/10.20998/2078-7405.2020.92.08>. 4. Babichev A.P. Osnovy vibracionnoj tehnologii / A.P. Babichev, I.A. Babichev. Rostov-n/D: Izdatel'skij centr DGTU, 2008. 694 p. 5. Babichev A.P. Vibracionnaja obrabotka detalej v abrazivnoj. M.: Mashinostroenie, 1968. 92 p. 6. Ob'emnaja vibracionnaja obrabotka / I.E. Burshtejn, V.V. Balickij, A.F. Duhovskij, M.Ja. Dubova i dr.; pod red. I.E. Burshtejna. Moskva: JeNIMS, 1977. 108 p. 7. Kartashov I.N. Obrabotka detalej svobodnymi abrazivami v vibrirujushhiih rezervuarah / I.N. Kartashov, M.E. Shainskij, V.A. Vlasov. Kiev: Vishha shkola, 1975. 188 p.

Андрій Міщик, Володимир Федорович,  
Анатолій Грабченко, Харків, Україна

### **ВЗАЄМОДІЯ АБРАЗИВНОГО СЕРЕДОВИЩА З ОБРОБЛЮВАНОЮ ПОВЕРХНЕЮ ТА ПРОЦЕС ЗНЯТТЯ МЕТАЛУ ПРИ ВІБРООБРОБЦІ В ПРИСУТНОСТІ ХІМІЧНО-АКТИВНОГО РОЗЧИНУ**

**Анотація.** Розглянуто взаємодію гранул робочого середовища з оброблюваною поверхнею деталі. Відзначено, що методи обробки характеризуються динамічним взаємодіям абразивного середовища з оброблюваною поверхнею. Зазначено, що при віброобробці відбувається ударний контакт абразивної гранули з поверхнею деталі, що призводить до утворення характерних слідів при формуванні рельєфу поверхні. Виділено види впливу абразивних зерен гранул робочого середовища на поверхню оброблюваної деталі. Зазначено, що вплив абразивних зерен залежить від геометричних параметрів їх вершин і робочого контуру гранули в цілому. Показано, що глибина сліду від абразивної гранули змінюється в напрямку її руху і визначається швидкістю переміщення, силою і частотою проникнення за час контакту та іншими динамічними факторами. Дано три види впливу абразивного зерна на оброблювану поверхню. Встановлено, що кожне абразивне зерно в процесі обробки з плином часу виконує тільки тертя, потім пластичне відтиснення і далі різання. Показано, що чергування роботи абразивних зерен пов'язано з характером переміщення гранули по поверхні деталі. Розглянуто взаємодію поверхонь тіл при віброобробці. Вказані відмінні ознаки способу віброобробки від інших аналогів. Дано умови утворення поверхневого шару деталі при віброобробці. Проведено аналіз механо-фізико-хімічної моделі процесу мікрорізання в присутності хімічно-активного розчину і наведено порівняння інтенсивності технологій віброобробки сталевих деталей. Показано порівняння технологічних процесів віброобробки сталевих деталей до високих класів чистоти поверхні. Визначено, що хімічно-активний розчин дозволяє усунути багатостадійні переваантаження вмісту резервуару та отримати необхідну чистоту обробленої поверхні за одну операцію віброобробки. Відзначено, що хімічно-активний розчин має корозійні властивості і сприяє освітленню обробленої поверхні.

**Ключові слова:** абразивне середовище; види впливу середовища; поверхневий шар; механо-фізико-хімічна модель; зняття металу; хімічно-активний розчин; технології віброобробки.

V. Molnár, Miskolc, Hungary

## **TRIBOLOGY AND TOPOGRAPHY OF HARD MACHINED SURFACES**

**Abstract.** *In machining automotive industrial parts by hard machining procedures, the topographic characteristics of high accuracy surfaces have high importance. In this paper 2D and 3D surface roughness features of gear bores machined by hard turning and grinding are demonstrated. The 3D roughness parameters, which are considered as more exact than the 2D parameters, were compared to the 2D ones, which are used more widely in industrial practice. The analyzed machining procedure versions were ranked based on the topographic parameters determining the tribological (wear and oil-retention capability) characteristics of the different surfaces.*

**Keywords:** *hard turning; in-feed grinding; 3D surface roughness; tribology.*

### **1. INTRODUCTION**

Due to the advancement of machining technology and the increasingly efficient machining procedures [1], the quality of the machined surfaces has to be described as exactly as possible. The grooves generated by the tool are different when the tool has a linear motion [2] or a rotating tool is applied [3]; these kinematic characteristics lead to different surface topography [4, 5]. Identical or almost identical roughness values can be reached by different machining procedures (e.g. hard turning and grinding); however, because of the different cutting characteristics the surface topography will also be different [6]. At the same time the cutting data, particularly the feed, significantly influence the roughness of the machined surface [7]. The potentially most accurate determination of roughness parameters is required by the diversity of machining procedures [8, 9], the high number of roughness influencing factors, and the comparability of roughness parameters of surfaces machinable by various procedures. In the automotive industry the efficient machining of hard surfaces has a high significance, thus hard machining procedures such as hard turning or grinding were compared in this study. These procedures or procedure versions differ from each other not only in the resulting surface topography, but also in other relevant factors such as economic issues of the machining procedures [10] or the impacts of the cooling and lubrication [11].

There are numerous machining procedures (use of single-point-tool or abrasive tool) for machining hard materials when high accuracy is required. The different procedures can result different surface topographies on the part. The working requirements of the parts can be different, thus the topography characteristics after machining should be analyzed [12, 13].

The lifetime of parts is significantly influenced by the irregularities of working surfaces (micro and macro geometrical errors). Contacting surfaces experience wear, but a suitable machining procedure and/or lubrication can decrease the extent of the wear. The wear of a surface with good oil-retention capability is slower. By analyzing the roughness parameters, conclusions about the tribological characteristics of the surfaces can be drawn [14, 15]. The experiments aimed to analyze the 2D and 3D roughness parameters by which the tribological properties can be characterized.

The core roughness depth ( $R_k$ ) and the core height ( $S_k$ ) are related to the lifetime of the surface. When two surfaces are in contact with each other during relative motion (working surfaces) part of the profile peaks will be sheared. The remaining layer is characterized by a relatively large bearing area and it is the part of the core zone of the surface. The reduced peak height ( $R_{pk}$ ,  $S_{pk}$ ) is the height of the layer worn in the initial wearing phase. The reduced valley depth ( $R_{vk}$ ,  $S_{vk}$ ) is the layer beneath the core zone and correlates with the oil-retention capability of the surface [16]. In terms of wear, lower reduced peak height values are favorable. At the same time, since these parameters are height and depth values, they do not provide information about the area (2D) or the volume (3D) of the peaks or valleys. This is why the peak material portion ( $M_{R1}$  in 2D and  $Sr1$  in 3D) and the valley material portion ( $MR2$  in 2d and  $Sr2$  in 3D) have to be defined. By using the  $R_{pk}$ ,  $R_{vk}$ ,  $MR1$  and  $MR2$  values or the  $S_{pk}$ ,  $S_{vk}$ ,  $Smr1$  and  $Smr2$  values the areas (2D parameters) of the peak ( $A1$ ) and the valley zones ( $A2$ ) and the volumes (3D parameters) of the peak ( $Sa1$ ) and the valley zones ( $Sa2$ ) can be obtained [17, 18]. The area or volume of the profile valleys provide relevant information about the oil-retention capability of a surface. The higher these values are, the more lubricant remains in the surface valleys.

The skewness ( $R_{sk}$ ,  $S_{sk}$ ) is the height distribution of profile points relative to the center line of the profile and provides information about the asymmetric nature of the surface points. Its value is positive if the heights of the peaks are higher than the depths of the valleys and negative when the depths of the valleys are higher. A surface is characterized by higher load bearing capacity and higher wear resistance if the skewness value is negative. The kurtosis ( $R_{ku}$ ,  $S_{ku}$ ) provides information about the peaky feature of a surface. When its value is relatively high ( $>3$ ) a friction surface shows more intense wear. When its value is lower the surface shows higher wear resistance [19].

Using a tribological topography map the tribological characteristics of surfaces can be analyzed. The map includes the skewness and kurtosis values of the machined surfaces and they are placed in a coordinate system. From the tribological point of view a surface is ideal if the point of a surface characterized by these two parameters is located by lower kurtosis (close to 0) and also lower

(negative) skewness values. In Fig. 1 an example for a tribological topography map is shown with points that belong to surfaces machined by the major procedures. Topographies of gear bore surfaces machined by hard turning, grinding and combined (turning and grinding in one clamping) experiments were compared based on roughness parameters which characterize the wear and the oil-retention capability. The differences of the 2D and 3D parameter values were also analyzed.

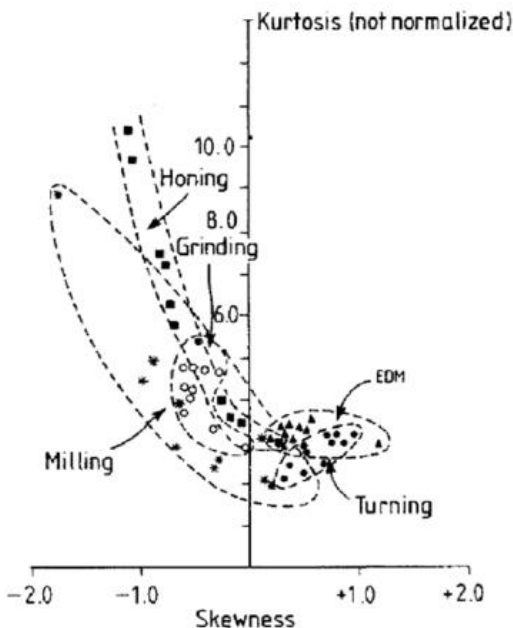


Figure 1 – Tribological topography map [20]

## 2. EXPERIMENTAL SETUP

In the experiments bores of gears were machined by hard turning when three different feeds were applied (T1, T2, T3), by infeed grinding (G1) and using a combination of hard turning and grinding (G2). The technological data of hard turning were:

- Feed (f): 0.1 mm/rev (T1), 0.2 mm/rev (T2), 0.3 mm/rev (T3)
- Depth of cut ( $a_p$ ): 0.2 mm
- Workpiece rpm (n): 615 1/min

In the hard turning pass of the G2 combined operation the feed was set to 0.2 mm/rev when the other parameters were left unchanged.

Parameters of the infeed grinding:

- Feed (f): 0.01 mm/rev
- Wheel width (d): 34 mm
- Allowance (Z): 0.2 mm
- Workpiece rpm ( $n_w$ ): 325 1/min
- Tool rpm ( $n_t$ ): 20000 1/min

In the infeed grinding part of the G2 combined procedure operation the allowance was set to 0.05 mm when the other parameters were left unchanged.

The machining experiments were carried out on a machining center type EMAG VSC 400. In the machining experiment a Sandvik CCGW 09T308 NC2 type insert and an E25T-SCLCR 09-R type tool holder were used. The grinding operations were carried out using a bore grinding wheel type Norton 3AS80J8VET 01\_36X37X13. The workpiece material was 20MnCr5, its hardness was 62–64 HRC. The length of the machined bore was 34 mm and its diameter was 88 mm.

The surface topography was analyzed by measuring 2D and 3D roughness parameters. In the 2D measurement 3 measurements were carried out per workpiece, located at 120° distance from each other. The measurement lengths were 4 mm. In the 3D measurements 2×2 mm areas were scanned. 0.8 mm cut-off and Gauss filter were applied in each measurement, which was carried out by using an inductive sensor. The number of scanned points was 4000 in the 2D and 1 million in the 3D measurement.

### 3. RESULTS AND DISCUSSION

Topographic characteristics of random (ground) and periodic (turned) surfaces (Fig. 2) were analyzed based on 2D and 3D roughness parameters.

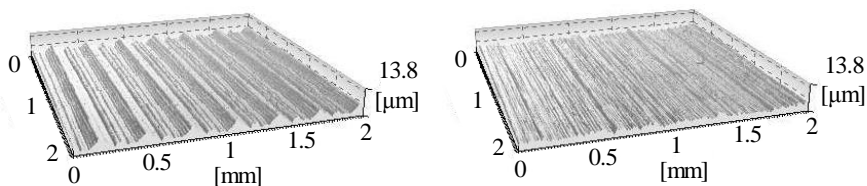


Figure 2 – Periodikus (a) és random (b) felületek (a T3 és G2 eljárásváltozatok)

In Figs. 2 and 3 the measured values of core roughness depth (2D), core height (3D), the reduced peak height and reduced valley depth are summarized. The core roughness depth (2D parameter Rk) varied from 0.12 and 0.19  $\mu\text{m}$ . The core height (3D parameter Sk) varied from 1.39 to 3.27  $\mu\text{m}$ . This means a difference of 3 orders of magnitude. The values of the 2D parameter of the hard turned surfaces showed a slight decrease and those of the 3D parameter a slight

increase with the increase of feed. Compared to version G1, the 2D and 3D values of the ground surface machined in the combined version G2 were 10% and 20% higher, respectively. The values of the reduced peak height (Rpk and Spk) showed identical tendencies and similar rates. The values of the 2D parameter of the reduced valley depth (Rvk) showed similar rates; however, there were some deviations concerning the 3D parameter (Svk): the value of the surface machined by version T3 decreased compared to version T2 instead of the expected increase, and the value of version G2 decreased instead of increasing. In all, the 2D and 3D parameter values result in contradictory conclusions. Based on findings from the literature [21, 22], it can also be presumed in the present study that the results of 3D measurements are more exact than those of 2D measurements because the number of detected points is three orders of magnitude higher. Based on the 3D parameter, from a tribological point of view, it can be stated that the heights of the peaks that are worn in the initial phase of working is the most favorable (minimal) in version T1 (carried out by a feed of 0.1 mm/rev) and the least favorable in version T3 (0.3 mm/rev feed). Based on the depth of valley zone it can be concluded that the oil-retention capability is the most favorable in version G1 and similar in version T2.

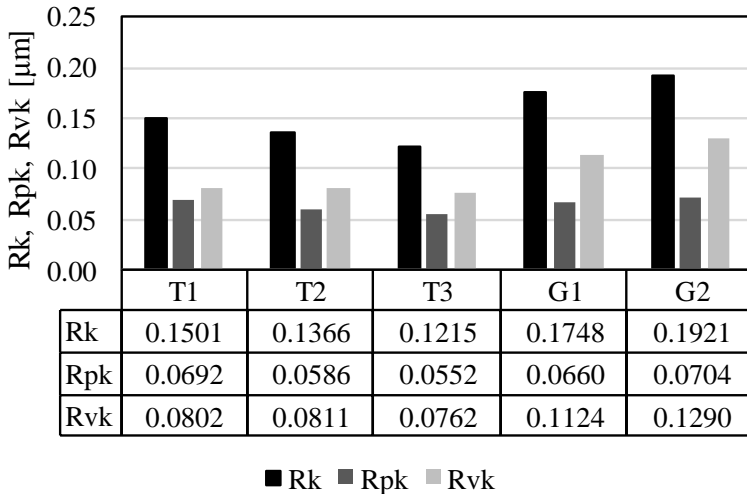


Figure 3 – Core roughness depth (Rk), reduced peak height (Rpk) and reduced valley depth (Rvk)

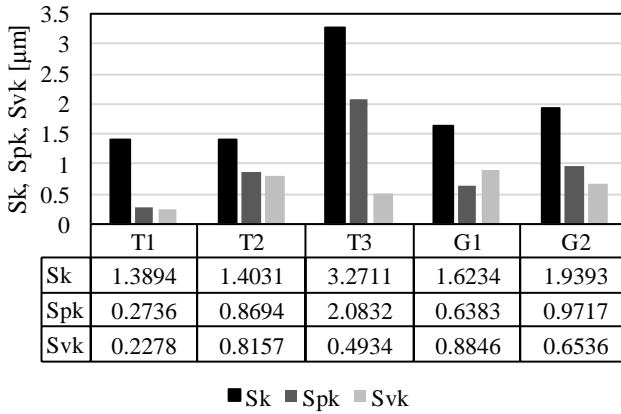


Figure 4 – Core height (Sk), reduced peak height (Spk) and reduced valley depth (Svk)

The peak and valley material portions are summarized in Figs. 4 and 5. MR1 and MR2 are the 2D, Sr1 and Sr2 are the 3D parameters that are required to calculate the areas and volumes of the peak and valley zones. It is shown in the figures that there is only a minimal difference between the analyzed versions: version T3 shows a slight outlying in the Sr1 and Sr2 values. The differences between the 2D values are negligible (e.g. there is only 1.2% difference between the maximum and minimum MR1 values).

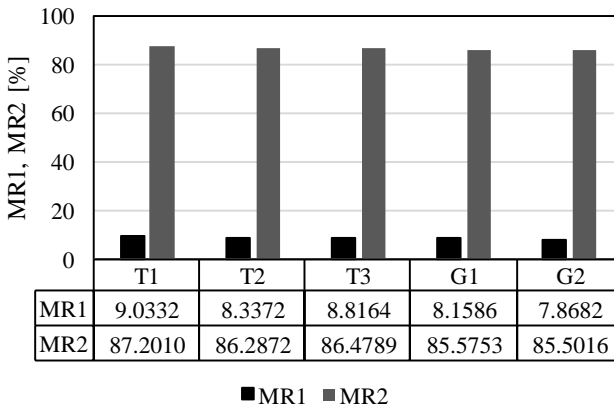


Figure 5 – Peak material portion (MR1) and valley material portion (MR2) 2D roughness parameter values

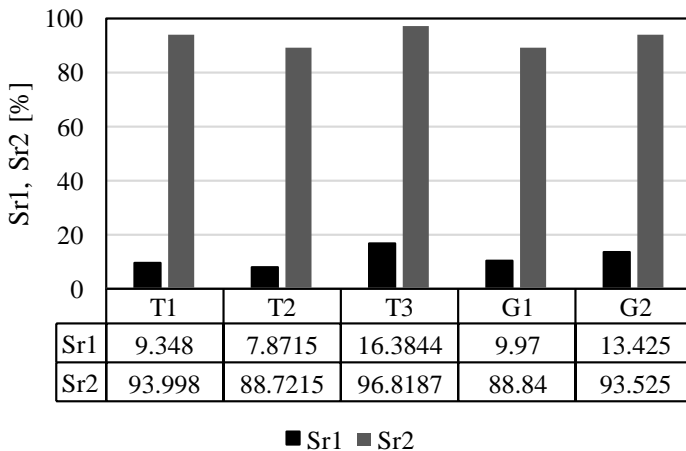


Figure 6 – Peak material portion (MR1) and valley material portion (MR2) 3D roughness parameter values

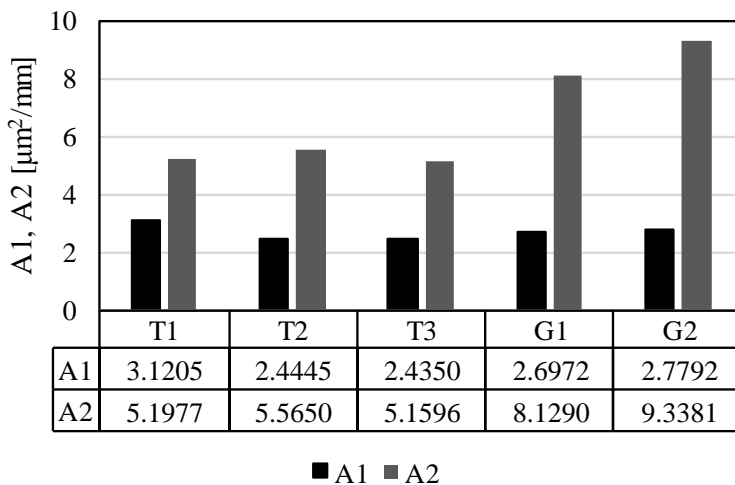


Figure 7 – Area of peak (A1) and valley zone (A2)

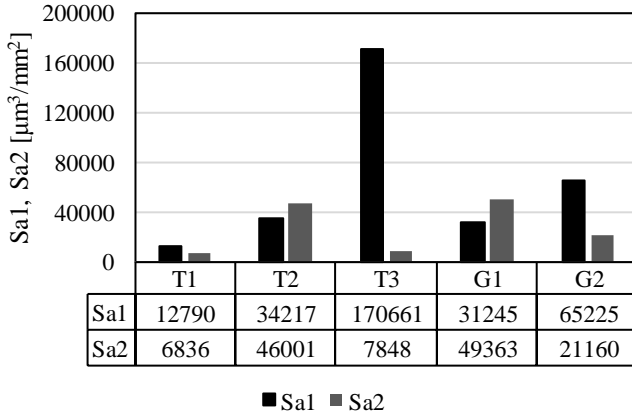


Figure 8 – Volume of peak (Sa1) and valley zone (Sa2)

In Figs. 6 and 7 the areas (2D) and volumes (3D) of peak and valley zones are demonstrated. Comparing the area to the volume data is inadequate because of their different dimensions. However, the comparison of the versions to each other is possible. The 2D parameters A1 and A2 are in line with the parameters Rpk and Rvk and the 3D parameters Sr1 and Sr2 with Spk and Svk. Here the higher accuracy of the 3D parameters can also be assumed. The values of the volume parameters reinforce the above statement that from the wear mechanism’s point of view version T1 is the most favorable and from the oil-retention capability’s point of view versions G1 and T2 are the most favorable.

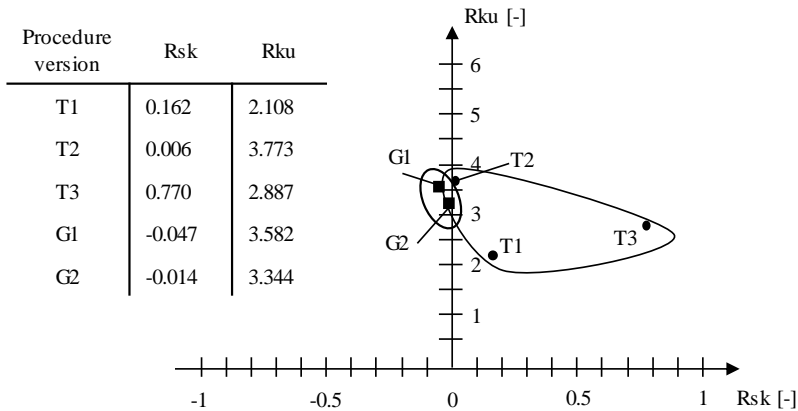


Figure 9 – Tribological topography map for the 2D parameters (skewness, kurtosis)

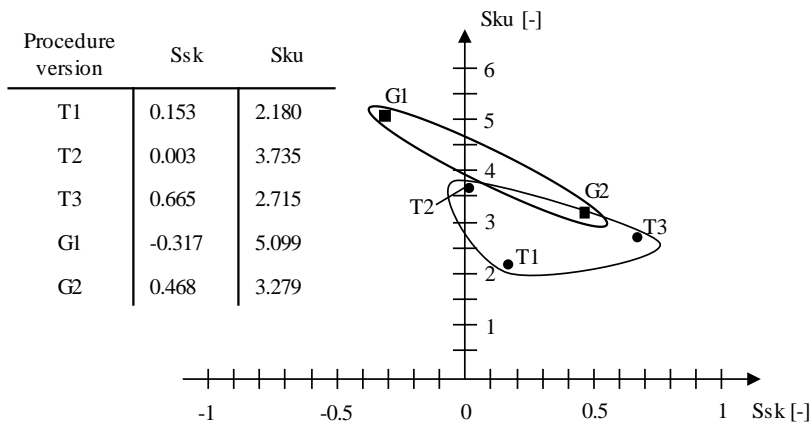


Figure 10 – Tribological topography map for the 3D parameters (skewness, kurtosis)

Based on the 2D (Fig. 8) and 3D (Fig. 9) parameters (skewness and kurtosis) the tribological topography maps of the versions were prepared. The locations of data points of the hard turning versions are in line with the published results. There is no significant difference between the 2D and 3D values. Based on the 2D parameters – considered less exact – the locations of data points of the two ground surfaces are in line with published results. However, for the 3D parameters one difference is experienced: the skewness (Ssk) of version G2 is higher than expected.

### SUMMARY

From a tribological point of view, wear resistance and oil-retention capability are determinant characteristics of machining industrial parts. Analyzing the surface topography of wearing parts is a critical research area. In this paper roughness characteristics of surfaces machined by hard turning, infeed grinding and using a combination were analyzed and compared. Based on the analyzed parameters the following order or ranking (most favorable comes first) was established between the studied versions:

- Reduced peak height, Spk (wear resistance), favored: low  
T1, G1, T2, G2, T3
- Volume of the peak zone, Sa1 (wear resistance), favored: low  
T1, G1, T2, G2, T3
- Skewness, Sks (wear resistance), favored: low  
G1, T2, T1, G2, T3
- Kurtosis, Sku (wear resistance), favored: <3  
T1, T3, G2, T2, G1

- Reduced valley depth, Svk (oil-retention capability), favored: high G1, T2, G2, T3, T1
- Volume of valley zone, Sa2 (oil-retention capability), favored: high G1, T2, G2, T3, T1

Different orders are found for the parameters characterized by various tribological properties: based on the parameters Spk and Sa1 the orders of wear resistance are identical, but the skewness and kurtosis values are not in line with these orders. The reason for this is the different mathematical approaches. Because of this, the roughness parameters to be used have to be selected carefully and the results have to be interpreted with some reservation. The study pointed out that there can be significant differences between the 2D and 3D parameter values obtained by measuring the same surface and this may lead to controversial interpretation of the results.

The study can be extended to more experimental setups or to analyzing various grades of materials.

**References:** 1. *Karpuschewski, B., Kundrak, J., Emmer, T., Borysenko, D.*: A new strategy in face milling-inverse cutting technology, *Solid State Phenomena*, No. 261, 2017, pp.331–338. 2. *Ferencsik, V., Gal, V.*: FE Investigation of Surface Burnishing Technology, *Cutting & Tools in Technological System*, No. 93, 2020, pp.3–8. 3. *Kundrak, J., Gyani, K., Felho, C., Deszpoth, I.*: The effect of the shape of chip cross section on cutting force and roughness when increasing feed in face milling, *Manufacturing Technology*, Vol. 17, No. 3, 2017, pp.335–342. 4. *Sztankovics, I., Kundrak, J.*: The characteristic parameters of the twist structure on cylindrical surfaces machined by turning procedures, *Applied Mechanics and Materials*, No. 693, 2014, pp. 418–423. 5. *Kundrak, J., Sztankovics, I., Gyani, K.*: Analysis of the Theoretical Values of Several Characteristic Parameters of Surface Topography in Rotational Turning, *World Academy of Science Engineering and Technology*, Vol. 8, No. 5, 2014, pp. 907–912. 6. *Kundrak, J. (1996)*: The Scientific Principles of Increasing the Effectiveness of Inner Surfaces' Cutting with CBN Tools, *Dissertation*, p.368. 7. *Kundrak, J., Markopoulos, A.P., Makkai, T., Deszpoth, I., Nagy, A.*: Analysis of the effect of feed on chip size ratio and cutting forces in face milling for various cutting speeds, *Manufacturing Technology*, Vol. 18, No. 3, 2018, pp.431–438. 8. *Sukaylo, V.A., Kaldos, A., Krukovsky, G., Lierath, F., Emmer, T., Pieper, H.J., Kundrak, J., Bana, V.*: Development and verification of a computer model for thermal distortions in hard turning, *Journal of Materials Processing Technology*, Vol. 155, No. 1-3, 2004, pp.1821–1827. 9. *Nagy, A.*: Influence of Measurement Settings on Areal Roughness with Confocal Chromatic Sensor on Face-Milled Surface, *Cutting & Tools in Technological System*, No. 93, 2020, pp.65–75. 10. *Kundrak, J., Varga, G., Deszpoth, I., Molnar, V.*: Some aspects of the hard machining of bore holes, *Applied Mechanics and Materials*, No. 309, 2013, pp.126–132. 11. *Kundrak, J., Varga, G.*: Possibility of reducing environmental load in hard machining, *Key Engineering Materials*, No. 496, 2011, pp.205–210. 12. *Kundrak, J., Mamalis, A.G., Markopoulos, A.*: Finishing of hardened boreholes: Grinding or hard cutting?, *Materials and Manufacturing Processes*, Vol. 19, No. 6, 2004, pp. 979–993. 13. *Kundrak, J.*: Alternative machining procedures of hardened steels, *Manufacturing technology*, Vol. 11, No. 11, 2011, pp. 32–39. 14. *El-Tayeb, N.S.M, Low, K.O., Brevem, P.V.*: On the surface and tribological characteristics of burnished cylindrical Al-6061, *Tribology International*, Vol. 42, 2009, pp. 320–326. 15. *Whittaker, R.K., Hothi, H.S., Eskelinen, A., Blum, G.W., Skinner, J.A., Hart, A.J.*: Variation in Taper Surface Roughness for a Single Design Effects the Wear Rate in Total Hip Arthroplasty, *Journal of Orthopaedic Research*, Vol. 35, 2017, pp.1784–1792. 16. *Gadelmawla, E.S.*,

Kourab, M.M., Maksouf, T.M.A., Elewaa, I.M., Solimand, H.H.: Roughness parameters, Journal of Materials Processing Technology, Vol. 123, 2002, pp.133–145. **17.** ISO 25178-2:2012 Geometrical product specifications (GPS) - Surface texture: Areal - Part 2: Terms, definitions and surface texture parameters. 2012. **18.** Stout, K., Blunt, L.: Three-dimensional Surface, Topography. 2 ed. London: Penton Press, 2000. **19.** Kovacs, Z., Viharos, Z.J., Kodacsy, J.: The effects of machining strategies of magnetic assisted roller burnishing on the resulted surface structure, Materials Science and Engineering, No. 448, 2018, nr.012002. **20.** Whitehouse, D.J.: Handbook of Surface Metrology, Institute of Physics Bristol, UK, 1994. **21.** Struzikiewicz, G., Sioma, A.: Evaluation of Surface Roughness and Defect Formation after the Machining of Sintered Aluminum Alloy AlSi10Mg, Materials, Vol. 13, No. 7, 2020. **22.** Deltombe, R., Kubiak, K.J., Bigerelle, M.: How to Select the Most Relevant 3D Roughness Parameters of a Surface?, Scanning, Vol. 36, No. 1, 2014, pp.150–160.

Віктор Мольнар, Мішкольц, Угорщина

## ТРИБОЛОГІЯ І ТОПОГРАФІЯ ЖОРСТКО ОБРОБЛЕНИХ ПОВЕРХОНЬ

**Анотація.** В автомобільній промисловості ефективна обробка твердих (загартованих) поверхонь має велике значення, тому в цьому дослідженні порівнювалися такі методи обробки, як жорстке точіння і шліфування. Ці процедури або версії процедур відрізняються один від одного не тільки результируючою топографією поверхні, але і іншими важливими факторами, такими як економічні проблеми, пов'язані з процедурами обробки або вплив охолодження і мастила. Різні процедури можуть призвести до різної топографії поверхні деталі. Робочі вимоги до деталей можуть бути різними, тому необхідно аналізувати топографічні характеристики після обробки. Аналізуючи параметри шорсткості, можна зробити висновки про трибологічні характеристики поверхонь. Експерименти були спрямовані на аналіз 2D і 3D параметрів шорсткості, за допомогою яких можна охарактеризувати трибологічні властивості. Використовуючи карту трибологічної топографії, можна проаналізувати трибологічні характеристики поверхонь. Карта включає в себе значення асиметрії та ексцесу оброблених поверхонь, і вони поміщені в систему координат. З трибологічної точки зору поверхня ідеальна, якщо точка поверхні, що характеризується цими двома параметрами, розташована з меншим ексцесом (близьким до 0), а також меншими (негативними) значеннями перекосу. Топографії поверхонь отворів зубчастих коліс, оброблених жорстким точінням, шліфуванням і комбінованим (точіння і шліфування за один запис) експериментально порівнювалися на основі параметрів шорсткості, які характеризують знос і здатність утримувати мастило. Також були проаналізовані відмінності значень 2D і 3D параметрів. Для параметрів, що характеризуються різними трибологічними властивостями, знайдені різні порядки: для параметрів  $S_{pk}$  і  $S_{aj}$  порядки зносостійкості ідентичні, але значення асиметрії та ексцесу не відповідають цим порядкам. Причина цьому - різні математичні підходи. Через це параметри шорсткості, які будуть використовуватися, повинні бути ретельно обрані, щоб їхні результати були інтерпретовані з деякими застереженнями. Дослідження показало, що між значеннями 2D і 3D параметрів, отриманих при вимірюванні однієї і тієї ж поверхні, можуть бути значні відмінності, і це може привести до суперечливої інтерпретації результатів.

**Ключові слова:** жорстке точіння; врізне шліфування; тривимірна шорсткість поверхні; трибологія.

A. Nagy, Miskolc, Hungary

## INVESTIGATION OF THE EFFECT OF AREAL ROUGHNESS MEASUREMENT LENGTH ON FACE MILLED SURFACE TOPOGRAPHIES

**Abstract.** *Surface roughness is of great importance in the manufacturing industry, as it affects surfaces' tribological properties (wear, friction, lubrication, etc.), corrosion resistance, fatigue strength and appearance. Areal roughness measurement, which provides a more comprehensive characterization of surfaces, is becoming increasingly popular, but systematic studies are still lacking, so measurements are often analyzed differently. In this paper, the effect of the measurement length is analyzed in the main measurement direction on areal roughness of face milled surface topographies, which were measured with a confocal chromatic sensor.*

**Keywords:** *surface roughness; areal roughness; measurement length.*

### 1 INTRODUCTION

One of the main quality factors of the machined surfaces of the parts is the surface roughness, as it influences their tribological properties (wear, friction, lubrication, etc.), their corrosion resistance, fatigue strength and their appearance. Two methods have been developed to investigate this, profile analysis and areal roughness analysis. The latter, which was later developed, is becoming more widespread in the scientific community as well as in industry, as 3D surfaces in terms of shape or functionality contain much more data thanks to the main and lateral directional measurement, and the surfaces cannot be characterized as distinctly by traditional 2D profile roughness parameters [1]. This is used for a wide variety of machining methods, some of which are briefly described, focusing on the method of measurement.

Roughness tests are often performed on experimentally machined surfaces worldwide. Eifler et al. [2] studied the roughness of micro-milled surfaces. The surfaces were compared in the measured areas with a F-operator to separate the shape and with an L-filter to filter out the waviness, and the resulting  $600 \times 600 \mu\text{m}^2$  roughness topographies were analyzed with the  $S_a$  and  $S_q$  parameter values. They found that the distance of the milling marks and the tilt angle of the milled surface had a significant effect on the roughness. During ultraprecision turning, Karpát [3] analyzed side surfaces created with a diamond tool. The outliers of the measurement results were filtered out and the topographies were leveled. The roughness was then separated from the waviness with the  $8 \mu\text{m}$  cut-off length of a Gaussian filter to obtain  $144 \times 108 \mu\text{m}^2$  areas for analysis. The effects of cutting edge angles, feed rate, and depth of cut were compared on roughness with parameters  $S_a$ ,  $S_q$ , and  $S_z$ . It was found that the tool with the  $30^\circ$  chamfer formed

the surface with the lowest average roughness of 1 nm with a small depth of cut and feed. Zak [4] compared the textures of surfaces machined to nearly the same average roughness by several methods (hard turning, grinding, burnishing), developing a new approach to characterize surface topographies by area-scale fractal analysis. An area of  $2.4 \times 2.4 \text{ mm}^2$  was measured on each surface and the method of filtration was not mentioned. The surfaces and the effects of machining methods were characterized with the help of several roughness parameters:  $S_a$ ,  $S_z$ ,  $S_{sk}$ ,  $S_{ku}$ , as well as  $S_{mr}$ ,  $S_{mc}$ ,  $S_{xp}$ , and with functional volume indices ( $V_{mp}$ ,  $V_{mc}$ ,  $V_{vc}$ ,  $V_{vv}$ ). He found that the surface made with combined machining (turning and grinding) is better than the hard-turned surface in a functional point of view (load bearing, force sealing), while the grinded surface has a better ability to preserve fluid.

Many researcher groups study the topography of formed surfaces in SLM metal additive manufacturing. In Wüst et al. [5]  $1 \times 1 \text{ mm}^2$  areas were measured and an S-filter and an L-filter were used in the evaluation. The values of the obtained  $S_a$  index were compared with the surfaces machined by the hybrid additive method, where the feed rate increased, the depth of cut decreased the roughness. In another article, Cabanettes et al. [6] compared different machining strategies, characterizing the topographies at several levels (shape, waviness, roughness). A measurement area of  $3.22 \times 1.90 \text{ mm}^2$  was examined on the machined surfaces, the shape error was eliminated with a polynomial filter of order 2 to evaluate the topographies, and no other filter was applied. The surfaces were characterized by the values of the roughness parameters  $S_a$ ,  $S_z$ ,  $S_{al}$ ,  $S_{tr}$ ,  $S_{dq}$  and  $S_{dr}$ . Charles et al. [7] analyzed the effects of different machining parameters on roughness. For this,  $4 \times 4 \text{ mm}^2$  areas were measured, and no filtering was mentioned on the topographies during evaluation. Surfaces have frequently been characterized by the average roughness  $S_a$ , which is becoming increasingly popular (including in additive machining).

The brief literature review above shows that the investigations of the settings of roughness measurement (size of the measured area, the filtering of topographies) on surfaces machined by different methods are carried out in various ways, and information is obtained from different selections of roughness indices for characterization and comparison. Based on the reviewed literature, it means that there is no unified method of areal roughness measurement, and thus the surfaces produced in different ways cannot actually be compared.

This article is a continuation of a previous study [8] and its aim is to analyze the effects of roughness measurement settings on the values of areal roughness parameters in order to select unified measurement conditions for later studies. In this paper, I examine whether and to what extent the roughness values are affected by varying the measurement length as a function of the feed rate which creates the periodicity. This is due to the fact that few researchers have addressed this, despite the relatively large number of roughness analyses. In our research group, for

example, previous investigations have been carried out on several features of face milled surfaces [9], analyzed changes in theoretical roughness [10], or the effect of the feed rate on roughness [11,12].

## 2 EXPERIMENTAL CONDITIONS

The experiments were performed on a PerfectJet MCV-M8 vertical milling machine on two C45 grade workpieces on which 50 mm long flat surfaces were produced by symmetrical face milling under dry conditions. Specimens were machined with a single Sandvik R215.44-15T308M-WL (grade GC4030) coated carbide insert in a Sandvik R252.44-080027-15M milling head on the machine, with the following cutting data set: constant cutting speed ( $v_c=300$  m/min) and depth of cut ( $a_p=0.8$  mm), variable feed rates ( $f_z=0.1 / 0.3$  mm/rev.). Due to the perpendicular position of the tool axis and the machined surface, double milling marks formed on the surfaces.

It was previously found that among cutting data the feed rate has the greatest influence on roughness [11], which is why we examine the roughness for the measurement length at several feeds. The reason for choosing the above values is that ISO 4288:1998 specifies different measurement and cut-off lengths for these feed rate values for surfaces with a periodic profile. The values selected accordingly are also recommended in ISO 25178-3:2012. Thus, this investigation is performed on several workpieces representing different standard cut-off lengths.

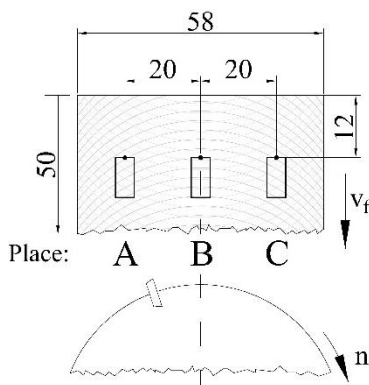


Figure 1 – Measuring places on the topographies

The instrument used for the measurement was an AltiSurf 520 type 3D surface roughness measuring device with a confocal chromatic sensor (CL2). Three measurement distances were recorded at the same distance, of which the middle area (B) was aligned to the milling symmetry plane (Fig. 1). It is necessary to examine several areas on the surfaces at the same time because all parts of functional surfaces

are connected to their counterpart at once, where roughness plays an important role. In addition, due to kinematic conditions, face milling is characterized by a variety of roughness impressions, so that roughness differs on different parts of the surface [12]. The measured topographies were uniformly 4 mm wide (perpendicular to the feed direction), and the length was varied (in the feed direction) determined on basis of the feed. These are characterized by the value  $p$ , which shows the feed per tooth in the measurement length.

Table 1 – Roughness values measured on specimen of  $f_z=0.1$  mm/rev

<b>p [-]</b>	<b>3</b>	<b>4</b>	<b>5</b>	<b>7</b>	<b>9</b>	<b>10</b>	<b>15</b>	<b>20</b>	<b>25</b>	<b>30</b>	
<b>length[mm]</b>	<b>0.3</b>	<b>0.4</b>	<b>0.5</b>	<b>0.7</b>	<b>0.9</b>	<b>1</b>	<b>1.5</b>	<b>2</b>	<b>2.5</b>	<b>3</b>	
	<b>A</b>	0.436	0.438	0.440	0.443	0.442	0.445	0.445	0.445	0.448	0.448
<b>S<sub>a</sub> [μm]</b>	<b>B</b>	0.417	0.423	0.427	0.430	0.430	0.434	0.433	0.433	0.434	0.434
	<b>C</b>	0.356	0.363	0.363	0.361	0.360	0.361	0.361	0.359	0.361	0.360
	<b>A</b>	0.516	0.519	0.521	0.523	0.523	0.525	0.526	0.525	0.529	0.528
<b>S<sub>q</sub> [μm]</b>	<b>B</b>	0.483	0.491	0.496	0.497	0.497	0.501	0.500	0.500	0.502	0.502
	<b>C</b>	0.432	0.441	0.440	0.438	0.437	0.439	0.439	0.437	0.439	0.438
	<b>A</b>	2.886	2.916	3.000	2.995	2.984	3.087	3.198	3.259	3.294	3.272
<b>S<sub>z</sub> [μm]</b>	<b>B</b>	2.336	2.505	2.518	2.556	2.656	2.599	2.634	2.646	2.645	2.664
	<b>C</b>	2.142	2.343	2.332	2.342	2.381	2.450	2.420	2.406	2.437	2.579
	<b>A</b>	0.518	0.518	0.521	0.510	0.514	0.509	0.507	0.504	0.495	0.497
<b>S<sub>sk</sub> [-]</b>	<b>B</b>	0.440	0.456	0.481	0.462	0.452	0.450	0.455	0.453	0.457	0.457
	<b>C</b>	0.583	0.584	0.582	0.583	0.587	0.584	0.586	0.585	0.585	0.585
	<b>A</b>	2.194	2.202	2.204	2.181	2.186	2.188	2.185	2.172	2.167	2.170
<b>S<sub>ku</sub> [-]</b>	<b>B</b>	1.991	2.021	2.027	2.005	1.983	1.980	1.985	1.968	1.991	1.986
	<b>C</b>	2.211	2.243	2.241	2.235	2.236	2.233	2.231	2.226	2.234	2.233

In ISO 4288:1998, for surfaces with a periodic profile, the measurement lengths were determined so that the profile contained 10–25 times the mean width of the profile elements ( $R_{Sm}$ ) [13]. This range, if a long enough surface is available for the measurement, proves to be sufficient in most cases so that there is neither too little nor too many outliers (due to machining errors) relative to the total measurement length, which would skew the results. Based on this, I chose values which are multiples of the feed; between  $p=3$ –30 for this study.

The evaluation was carried out with AltiMap Premium software, where after leveling the topographies and eliminating the outliers, I set the cut-off lengths according to the above-mentioned standard (at 0.25 and 0.8 mm, respectively).

### 3 RESULTS AND DISCUSSION

Tables 1 and 2 show the measurement results on the surfaces of the two specimens for the most commonly used 3D roughness parameters [14], arranged according to the three measurement places and the different measurement lengths. Each measurement was repeated three times, the reported values being the arithmetic means of the three results. The relative differences of the results by parameter and measurement location are shown in diagrams in Figure 2 for the two workpieces.

The diagrams show similar characteristics. The most important finding is that with the increase of the measurement length, the difference in the values is noticeable initially, after that the measured values show little deviation. This means that any value of  $p$  can be set, as the measurement length hardly affects the measured values.

Table 2 – Roughness values measured on specimen of  $f_z=0.3$  mm/rev.

<b>p [-]</b>	<b>3</b>	<b>4</b>	<b>5</b>	<b>7</b>	<b>9</b>	<b>10</b>	<b>15</b>	<b>20</b>	<b>25</b>	<b>30</b>	
<b>length[mm]</b>	<b>0.9</b>	<b>1.2</b>	<b>1.5</b>	<b>2.1</b>	<b>2.7</b>	<b>3</b>	<b>4.5</b>	<b>6</b>	<b>7.5</b>	<b>9</b>	
<b>S<sub>a</sub> [μm]</b>	<b>A</b>	1.858	1.859	1.860	1.861	1.861	1.859	1.856	1.854	1.854	1.854
	<b>B</b>	2.238	2.244	2.245	2.244	2.249	2.241	2.248	2.249	2.250	2.251
	<b>C</b>	1.059	1.060	1.060	1.064	1.064	1.064	1.066	1.068	1.068	1.069
<b>S<sub>q</sub> [μm]</b>	<b>A</b>	2.131	2.131	2.132	2.134	2.134	2.129	2.128	2.126	2.126	2.125
	<b>B</b>	2.546	2.553	2.553	2.552	2.559	2.548	2.558	2.558	2.560	2.562
	<b>C</b>	1.410	1.411	1.410	1.413	1.413	1.414	1.415	1.416	1.416	1.417
<b>S<sub>z</sub> [μm]</b>	<b>A</b>	8.060	8.001	8.021	7.981	8.171	8.200	8.161	8.177	8.185	8.265
	<b>B</b>	9.047	9.037	8.985	8.895	8.965	8.999	9.034	8.986	8.940	9.171
	<b>C</b>	7.391	7.385	7.379	7.514	7.642	7.679	7.612	7.642	7.633	7.689
<b>S<sub>sk</sub> [-]</b>	<b>A</b>	0.557	0.554	0.554	0.553	0.551	0.547	0.545	0.544	0.544	0.545
	<b>B</b>	0.458	0.452	0.446	0.440	0.438	0.421	0.436	0.436	0.437	0.440
	<b>C</b>	1.311	1.308	1.308	1.298	1.298	1.295	1.289	1.280	1.277	1.279
<b>S<sub>ku</sub> [-]</b>	<b>A</b>	1.999	1.997	1.996	1.996	1.993	1.987	1.990	1.988	1.988	1.989
	<b>B</b>	1.866	1.861	1.855	1.852	1.849	1.834	1.847	1.844	1.842	1.845
	<b>C</b>	4.235	4.220	4.216	4.193	4.191	4.182	4.170	4.147	4.140	4.141

The values of the arithmetic mean roughness  $S_a$  and the root-mean-square average roughness  $S_q$  show the same characteristic on a workpiece and at a measuring place. With increasing  $p$ , in most cases the values first increase ( $p \leq 12.5$ ) and then remain nearly the same. Although with a larger deviation, the same can be stated for the maximum height parameter  $S_z$ . The values of the dimensionless

skewness  $S_{sk}$  and kurtosis  $S_{ku}$  initially decrease, and then at  $p \leq 15$  they are unaffected by the length.

In Tables 3 and 4, the deviations of the values are reported according to the indicated  $p$ - $p$  interval, the signed  $S_i$  roughness parameter, and the shown measurement location, using the following difference (1) and percentage (2) formulas:

$$\text{Differences of values} = \max(S_i) - \min(S_i) \tag{1}$$

$$\text{Percentage value differences} = \frac{\max(S_i) - \min(S_i)}{\text{average}(S_i)} [\%] \tag{2}$$

Since the values stabilized in most cases with increasing  $p$  in Figure 2, the ranges in the tables were aligned to the largest  $30 \times$  length examined. This is because the longer the length, in theory the better the irregularities are distributed on the topographies, the values are more averaged, which is generally expected for the parameters  $S_a$  and  $S_q$ .

Tables 3 and 4 show decreasing values in each case (one parameter, one measurement place) together with the narrowing of the ranges. This makes it clear that the longer measurement length (in the examined range) results in a smaller deviation in value, i.e., the measurement results have lower error values in the narrower intervals.

Table 3 – Differences in roughness values for  $f_z=0.1$  mm/rev

P-P interval		3-30		10-30		15-30		20-30		25-30	
$S_a$ [ $\mu\text{m}$ ]	A	0.012	2.67%	0.006	1.34%	0.004	0.82%	0.003	0.72%	0.001	0.15%
	B	0.018	4.23%	0.003	0.75%	0.002	0.55%	0.002	0.47%	0.001	0.16%
	C	0.007	2.05%	0.002	0.54%	0.002	0.53%	0.002	0.53%	0.001	0.21%
$S_q$ [ $\mu\text{m}$ ]	A	0.012	2.36%	0.006	1.17%	0.003	0.65%	0.003	0.61%	0.001	0.10%
	B	0.020	3.92%	0.003	0.67%	0.003	0.54%	0.003	0.54%	0.001	0.13%
	C	0.009	2.08%	0.002	0.51%	0.002	0.51%	0.002	0.51%	0.001	0.21%
$S_z$ [ $\mu\text{m}$ ]	A	0.457	14.66%	0.290	8.97%	0.145	4.42%	0.084	2.54%	0.024	0.74%
	B	0.331	12.79%	0.070	2.67%	0.033	1.26%	0.023	0.85%	0.023	0.85%
	C	0.437	18.23%	0.182	7.40%	0.172	7.00%	0.172	6.96%	0.142	5.64%
$S_{sk}$ [-]	A	0.026	5.07%	0.017	3.43%	0.012	2.39%	0.009	1.71%	0.002	0.41%
	B	0.041	8.96%	0.011	2.47%	0.008	1.83%	0.008	1.83%	0.003	0.68%
	C	0.004	0.77%	0.003	0.44%	0.002	0.39%	0.001	0.15%	0.001	0.15%
$S_{ku}$ [-]	A	0.043	1.98%	0.027	1.24%	0.023	1.07%	0.011	0.49%	0.003	0.14%
	B	0.064	3.20%	0.028	1.43%	0.028	1.43%	0.028	1.43%	0.008	0.43%
	C	0.032	1.45%	0.012	0.52%	0.012	0.52%	0.012	0.52%	0.001	0.05%

Table 4 – Differences in roughness values for fz=0.3 mm/rev

P-P interval		3-30		10-30		15-30		20-30		25-30	
S <sub>a</sub> [μm]	A	0.008	0.45%	0.007	0.37%	0.002	0.11%	0.001	0.03%	0.000	0.01%
	B	0.013	0.56%	0.010	0.43%	0.006	0.27%	0.004	0.19%	0.004	0.19%
	C	0.010	0.95%	0.005	0.45%	0.003	0.25%	0.001	0.10%	0.001	0.07%
S <sub>q</sub> [μm]	A	0.010	0.48%	0.008	0.36%	0.003	0.13%	0.001	0.03%	0.000	0.02%
	B	0.016	0.64%	0.014	0.56%	0.010	0.37%	0.006	0.24%	0.006	0.24%
	C	0.007	0.50%	0.003	0.22%	0.001	0.09%	0.001	0.04%	0.001	0.04%
S <sub>z</sub> [μm]	A	0.284	3.49%	0.130	1.59%	0.104	1.26%	0.088	1.07%	0.085	1.03%
	B	0.297	3.30%	0.247	2.75%	0.231	2.56%	0.231	2.56%	0.231	2.56%
	C	0.311	4.10%	0.089	1.16%	0.078	1.02%	0.056	0.73%	0.056	0.73%
S <sub>sk</sub> [-]	A	0.014	2.46%	0.007	1.31%	0.002	0.31%	0.001	0.25%	0.000	0.08%
	B	0.037	8.42%	0.019	4.44%	0.015	3.39%	0.012	2.69%	0.008	1.91%
	C	0.034	2.63%	0.021	1.60%	0.012	0.93%	0.003	0.24%	0.002	0.14%
S <sub>ku</sub> [-]	A	0.012	0.61%	0.005	0.26%	0.003	0.16%	0.002	0.08%	0.000	0.03%
	B	0.032	1.71%	0.014	0.77%	0.010	0.52%	0.007	0.40%	0.007	0.37%
	C	0.095	2.28%	0.045	1.09%	0.031	0.75%	0.008	0.19%	0.002	0.05%

The increase of the feed rate globally does not affect the deviation values. However, the magnitudes of the percentage deviations are usually smaller, as can be expected from the basis of the larger roughness values (S<sub>a</sub>, S<sub>q</sub>, S<sub>z</sub>). In the case of S<sub>sk</sub> and S<sub>ku</sub>, they do not necessarily decrease.

As for the roughness values, the differences are the greatest for the S<sub>z</sub> index. These are quite large over the entire study range; 0.25–0.5 μm and with it, even 19% is possible, but by increasing the length, even in the case of p≥10 S<sub>z</sub> remains below 0.3 μm and 9%.

In terms of S<sub>a</sub>, S<sub>q</sub> indices, deviations of less than 1% can already be achieved for p≥15. In the same way, they remain below 7% for S<sub>z</sub>, 3.5% for S<sub>sk</sub>, and 1.5% for S<sub>ku</sub>. These magnitudes of the difference are small, and also, in the three intervals designated between p=15–30, the decrease of the values in the table analyzed by row is not significant. It can also be seen to what extent the change of the measurement length influences the values of the examined roughness parameters; these are in descending order: S<sub>z</sub>, S<sub>sk</sub>, S<sub>ku</sub>, S<sub>q</sub>, S<sub>a</sub>.

For the measurement locations, the following relations can be seen to each roughness index. For S<sub>a</sub>, the deviation is maximal in place **B**, and these values in the side places are smaller and are close to each other. In the case of the S<sub>q</sub> index, the differences are always minimal, at 0.2–2.1% at location **C**, the deviations at **A** and **B** are very similar. For the S<sub>sk</sub> and S<sub>ku</sub> parameters, the smaller differences are found at the lateral measurement places, the maximal values for the kurtosis are in the middle place at the lower feed, and on the exit side at the higher feed rate. The

ratio of the values of  $S_z$  varies between measurement sites for the  $p$ - $p$  ranges, here any regularity cannot be identified. Thus, if the five examined parameters are considered together, the relationship between the measurement locations varies regardless of the feed, so the deviation is not regular.

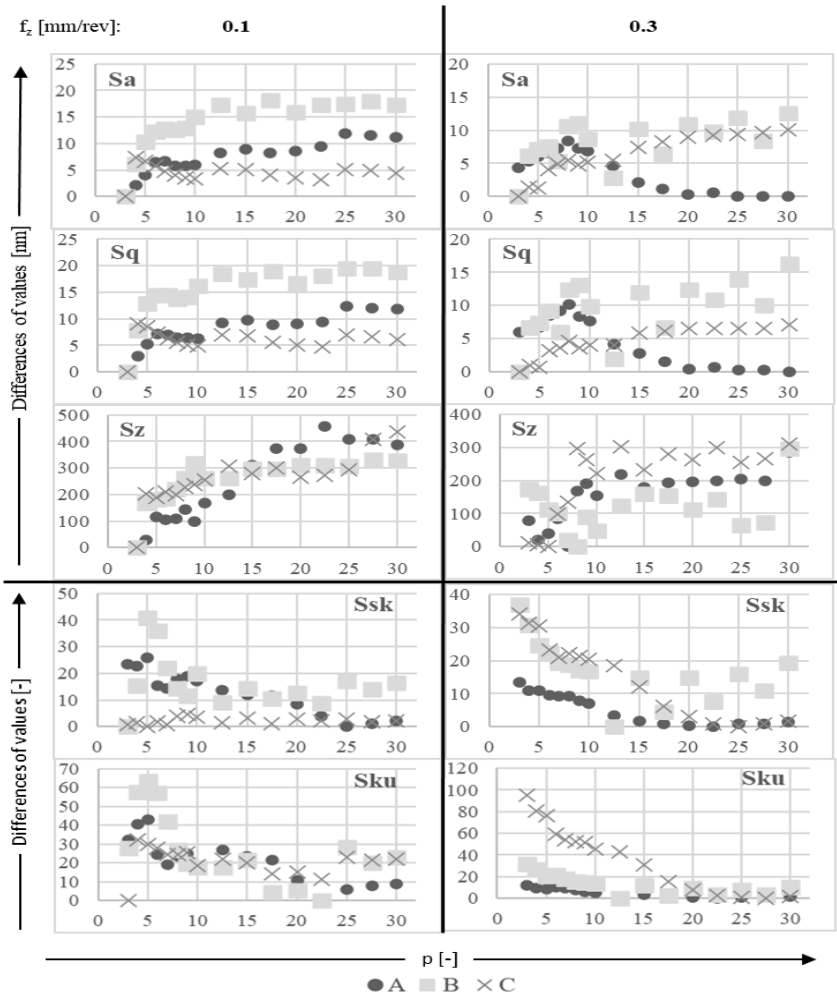


Figure 2 – Relative differences in roughness values by parameter and measurement location

## 4 CONCLUSIONS

In the present article, we examined the effect of the measurement length on the values of areal roughness parameters at symmetrically face milled surfaces at two feed rates. In doing so, the measurement length was set as a multiple of the feed per tooth and denoted by  $p$ . The analysis was performed based on the values of five roughness parameters.

We found that at low  $p$  values the roughness parameter values changed significantly, while at  $p \geq 15$  they are almost the same. Above  $p \geq 15$  on both specimens the differences are maximum 1% for  $S_a$  and  $S_q$ , 7% for  $S_z$ , 3.5% for  $S_{sk}$  and 1.5% for  $S_{ku}$ . Based on this, when measuring areal roughness a value of at least 15 times  $p$  is recommended.

Among the examined roughness parameters, the values of  $S_z$  showed the largest differences, reaching up to 20% in the whole study range, however, the ratio was reduced to 9% even in the case of  $p \geq 10$ . The increase of the feed rate generally resulted in a slight change in the deviations. The degree of influence of the measurement length on the areal roughness parameters was found to be (in descending order):  $S_z$ ,  $S_{sk}$ ,  $S_{ku}$ ,  $S_q$ , and finally  $S_a$ .

**References:** 1. *Pomberger, S., Stoschka, M., Leitner, M.*: Cast surface texture characterisation via areal roughness, *Precision Engineering* vol.60 (2019) pp.465-481. 2. *Eifler, M., Klauer, K., Kirsch, B., Seewig, J., Aurich, J. C.*: Micro-milling of areal material measures—influences on the resulting surface topography, *Procedia CIRP* vol.71 (2018) pp.122-127. 3. *Karpat, Y.*: Influence of diamond tool chamfer angle on surface integrity in ultra-precision turning of single crystal silicon, *The International Journal of Advanced Manufacturing Technology* vol.101(5) (2019) pp.1565-1572. 4. *Zak, K.*: Areal field and fractal based characterization of hard surfaces produced by different machining operations, *Journal of Machine Engineering* vol.16(1) (2016) pp.24-32. 5. *Wüst, P., Edelmann, A., Hellmann, R.*: Areal surface roughness optimization of maraging steel parts produced by hybrid additive manufacturing, *Materials* vol.13(2) (2020) ArtNo:418. 6. *Cabanettes, F., Joubert, A., Chardon, G., Dumas, V., Rech, J., Grosjean, C., Dimkovski, Z.*: Topography of as built surfaces generated in metal additive manufacturing: a multi scale analysis from form to roughness, *Precision Engineering* vol.52 (2018) pp.249-265. 7. *Charles, A., Elkaseer, A., Thijs, L., Hagenmeyer, V., Scholz, S.*: Effect of process parameters on the generated surface roughness of down-facing surfaces in selective laser melting, *Applied Sciences* vol.9(6) (2019) ArtNo:1256. 8. *Nagy, A.*: Influence of Measurement Settings on Areal Roughness with Confocal Chromatic Sensor on Face-milled Surface, *Rezanie i Instrumenty v Tekhnologicheskikh Sistemah* vol.93 (2020) pp.65-75. 9. *Kundrák, J., Gyáni, K., Felhő, C., Deszpoth, I.*: The effect of the shape of chip cross section on cutting force and roughness when increasing feed in face milling, *Manufacturing Technology* vol.17(3) (2017) pp.335–342. 10. *Kundrák, J., Felhő, Cs.*: 3D Roughness Parameters of Surfaces Face Milled by Special Tools, *Manufacturing Technology* vol.16(3) (2016) pp.532-538. 11. *Varga, G., Kundrák, J.*: Effects of technological parameters on surface characteristics in face milling, *Solid State Phenomena* vol.261 (2017) pp.285-292. 12. *Nagy, A., Kundrák, J.*: Changes in the values of roughness parameters on face-milled steel surface, *Rezanie i Instrumenty v Tekhnologicheskikh Sistemah* vol.92 (2020) pp.85-95. 13. *David Whitehouse*: Surfaces and their Measurement. Butterworth-Heinemann, Oxford, 2004. 14. *Todhunter, L. D., Leach, R., Lawes, S.*

Blateyron, F.: Industrial survey of ISO surface texture parameters. CIRP Journal of Manufacturing Science and Technology, vol.19. (2017) pp. 84-92.

Антал Надь, Мішкольц, Угорщина

## ДОСЛІДЖЕННЯ ВПЛИВУ ДОВЖИНИ ВИМІРЮВАННЯ ШОРСТКОСТІ НА ТОПОГРАФІЇ ПОВЕРХНІ ПІСЛЯ ТОРЦЕВОГО ФРЕЗЕРУВАННЯ

**Анотація.** *Огляд літератури показує, що дослідження змін у налаштуваннях вимірювання шорсткості (розмір вимірюваної області, фільтрація топографії) на поверхнях, оброблених різними методами, виконуються різними способами, і інформація для характеристики і порівняння складається з різних наборів показників шорсткості. Це означає, що не існує єдиного методу вимірювання шорсткості поверхні, і тому поверхні, отримані різними способами, фактично не можуть бути співставлені. У цій статті досліджується ступінь впливу зміни довжини вимірювання на значення шорсткості в залежності від величини швидкості подачі, яка створює періодичність. Це пов'язано з тим, що не всі дослідники зверталися до цього, незважаючи на відносно велику кількість аналізів шорсткості. Для досліджень використовувався прилад для 3D вимірювання шорсткості поверхні типу AltiSurf 520 з конфокальним хроматичним датчиком (CL2). Три ділянки були записані на одній і тій же відстані, з яких середня область була вирівняна по площині симетрії фрезерування. Важливо було одночасно досліджувати кілька ділянок на поверхнях, тому що всі частини функціональних поверхонь одночасно з'єднані зі своїми аналогами, де шорсткість відіграє важливу роль. Оцінка проводилася за допомогою програмного забезпечення AltiMap Premium, де після вирівнювання топографії та виключення викидів були встановлені відрізки довжини відповідно до стандарту для двох швидкостей подачі. При цьому довжина вимірювання була встановлена як кратна подачі на зуб і позначена буквою  $r$ . Аналіз проводився на основі значень п'яти параметрів шорсткості. Виявлено, що при низьких значеннях  $r$ , значення параметрів шорсткості істотно змінюються, а при  $r \geq 15$  вони практично не відрізняються. Вище  $r \geq 15$  для досліджуваних зразків різниця становить максимум 1% для  $S_a$  і  $S_q$ , 7% для  $S_z$ , 3,5% для  $S_{sk}$  і 1,5% для  $S_{ku}$ . Виходячи з цього, при вимірюванні шорсткості поверхні рекомендується значення не менше  $r \geq 15$ . Серед досліджених параметрів шорсткості значення  $S_z$  показало найбільшій відмінності, досягаючи 20% у всьому досліджуваному діапазоні, проте це співвідношення зменшилося до 9% навіть в разі  $r \geq 10$ . Збільшення швидкості подачі зазвичай призводило до невеликої зміни відхилень. Ступінь впливу довжини вимірювання на параметри шорсткості поверхні виявилася (в порядку убавання):  $S_z$ ,  $S_{sk}$ ,  $S_{ku}$ ,  $S_q$  і, нарешті,  $S_a$ .*

**Ключові слова:** *шорсткість профілю; шорсткість поверхні; довжина вимірювання.*

I. Sztankovics, Miskolc, Hungary

## **THE EFFECT OF THE CIRCULAR FEED ON THE SURFACE ROUGHNESS AND THE MACHINING TIME**

**Abstract.** *The surface roughness is analysed in different feeds and turning procedures (rotational and conventional) in this paper. Cutting experiments were made on different cutting speeds and feed rates with 2 cutting tool with helical edge geometry and 1 traditional turning tool. The measured 2D surface roughness values were compared between the different cutting tools. The benefit of the circular feed application is showed by the decrease of roughness parameters and machining time.*

**Keywords:** *machining time; rotational turning; surface roughness.*

### **5. INTRODUCTION**

The produced surface quality and the efficiency of the machining depends on the applied cutting procedure. Kunderák et al. showed in studying finishing procedures of bore machining that the same surface roughness can be achieved by various kinematic relations, however the machining time will be different depending on the procedure [1]. Varga et al. analysed the effect of burnishing after grinding [2], which leads to better surface topography, however the machining time will be consequently higher. Qehaja et al. studied the dry turning process [3], where they concluded that the feed rate has a high influence on the machining time and surface roughness. Niaki et al. analysed different tool grades and showed that the stability of the cutting edge also has a high impact on the generated surface. The application of the application of unconventional machining methods are shown in the work of Berenji et al. [4]. They determined that the application of different procedures can lead to better surface quality while also increasing the efficiency. An edge with helical geometry and a tangential circular feed are applied in rotational turning [5]. Therefore, the applied kinematics and edge geometry has a major effect on the surface quality and the efficiency. The aim of this paper is to analyse roughness values and the machining time in cutting of cylindrical surfaces with different kinematics and edge geometry (rotational and longitudinal turning).

### **6. EXPERIMENTAL CONDITIONS**

In this study, the experimental work was carried out on a Perfect-Jet MCV-M8 machining centre. The cutting tool is clamped to the machine table and the experimental workpiece is fixed in the tool holder of the machine. The fast rotation of the spindle assured the main cutting movement, while the CNC controlled circular motion of the tool around the rotating workpiece resulted the secondary

feed motion. The clamped tool with the helical cutting edge for rotational feed and the workpiece can be seen in Figure 1.

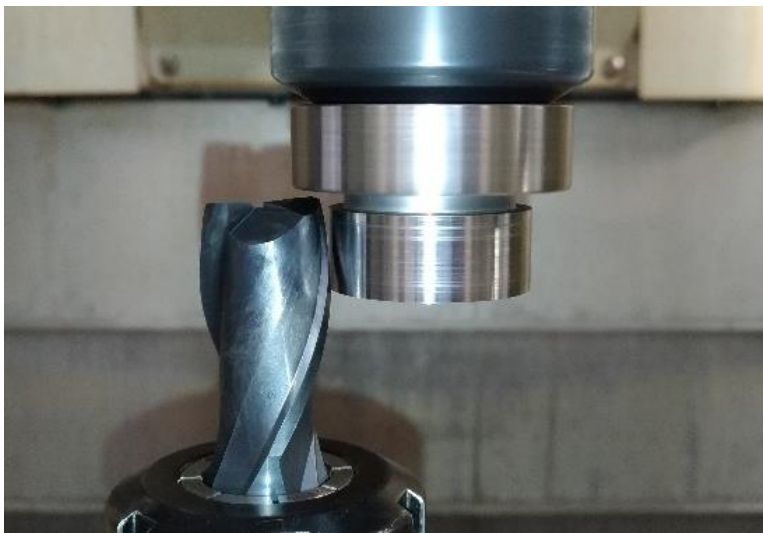


Figure 1 – Geometrical and kinematical relations of rotational turning

A heat-treated C45 steel grade is machined during the experiments, which had a 12 mm length  $\text{Ø}40$  mm diameter surface. The circular feed was realized by two rotational turning tools: Fraisa P5300682 ( $\lambda_s = 30^\circ$ , notation: A) and Sandvik Coromant R215.38-20050-AC38L ( $\lambda_s = 50^\circ$ , notation: B). The result of the rotational turning are compared with a standard longitudinal turning tool (CNMG 120412-PM insert in DCLNL 2525 M 12 holder, notation: C). The experiments are carried out with 200 m/min and 250 m/min cutting speed ( $v_c$ ), 0.1 mm depth of cut and five values of feed ( $f$ ) for each cutting tool ( $f = 0.1$  mm, 0.2 mm, 0.4 mm, 0.6 mm, 0.8 mm). The machined surfaces are measured by a Mitutoyo SurfTest SJ-301 2D roughness measuring device on three generatrix of the cylindrical part. The measured length and cut-off length are adjusted according to DIN EN ISO 4288.

## **7. EXPERIMENTAL RESULTS AND DISCUSSION**

The roughness measurement results of the Arithmetical mean deviation of the assessed profile ( $R_a$ ) and the Average peak to valley height of the profile ( $R_z$ ) are shown in Table 1 for Tool A, Table 2 for Tool B and Table 3 for Tool C.

Table 1 – Roughness measurement results for Tool A

$v_c$ [m/min]	$f$ [mm]	$R_{a,1}$ [ $\mu\text{m}$ ]	$R_{a,2}$ [ $\mu\text{m}$ ]	$R_{a,3}$ [ $\mu\text{m}$ ]	$R_{z,1}$ [ $\mu\text{m}$ ]	$R_{z,2}$ [ $\mu\text{m}$ ]	$R_{z,3}$ [ $\mu\text{m}$ ]
200	0.1	0.47	0.45	0.48	3.22	2.83	3.05
	0.2	0.47	0.48	0.49	3.82	3.79	3.73
	0.4	0.54	0.55	0.57	3.58	3.54	3.45
	0.6	0.73	0.69	0.74	5.18	5.19	5.67
	0.8	1.2	1.39	1.28	7.42	7.16	7.24
250	0.1	0.45	0.44	0.44	3.04	2.95	3.07
	0.2	0.45	0.45	0.44	3.81	3.80	3.78
	0.4	0.6	0.63	0.61	4.6	4.49	4.27
	0.6	0.76	0.74	0.78	5.95	5.19	5.39
	0.8	1.1	1.18	1.08	6.89	7.32	6.87

Table 2 – Roughness measurement results for Tool B

$v_c$ [m/min]	$f$ [mm]	$R_{a,1}$ [ $\mu\text{m}$ ]	$R_{a,2}$ [ $\mu\text{m}$ ]	$R_{a,3}$ [ $\mu\text{m}$ ]	$R_{z,1}$ [ $\mu\text{m}$ ]	$R_{z,2}$ [ $\mu\text{m}$ ]	$R_{z,3}$ [ $\mu\text{m}$ ]
200	0.1	0.53	0.46	0.47	3.46	2.91	2.74
	0.2	0.39	0.39	0.36	3.21	3.40	2.66
	0.4	0.93	0.90	0.87	4.79	4.66	4.50
	0.6	2.01	1.91	1.91	9.86	9.36	8.94
	0.8	4.75	3.99	3.93	19.59	17.73	18.8
250	0.1	0.34	0.34	0.33	2.62	2.77	2.86
	0.2	0.34	0.34	0.32	2.24	2.12	2.08
	0.4	0.73	0.68	0.71	4.16	4.21	3.95
	0.6	2.28	2.33	2.38	10.54	10.84	10.71
	0.8	3.65	3.64	3.66	16.58	16.52	16.51

Table 3 – Roughness measurement results for Tool C

$v_c$ [m/min]	$f$ [mm]	$R_{a,1}$ [ $\mu\text{m}$ ]	$R_{a,2}$ [ $\mu\text{m}$ ]	$R_{a,3}$ [ $\mu\text{m}$ ]	$R_{z,1}$ [ $\mu\text{m}$ ]	$R_{z,2}$ [ $\mu\text{m}$ ]	$R_{z,3}$ [ $\mu\text{m}$ ]
200	0.1	0.49	0.49	0.48	2.01	1.91	1.76
	0.2	0.96	0.99	0.94	4.44	5.00	4.46
	0.4	3.36	3.27	3.27	13.52	13.44	13.35
	0.6	6.68	6.49	6.57	25.74	25.54	25.67
	0.8	10.66	10.78	10.53	40.37	40.15	40.52
250	0.1	0.48	0.48	0.47	1.93	1.93	1.85
	0.2	0.99	0.92	1.02	4.77	4.42	4.84
	0.4	2.97	3.09	3.08	12.61	12.38	12.61
	0.6	6.69	6.65	6.86	26.08	26.16	26.55
	0.8	10.15	9.96	9.85	38.83	38.59	38.83

The mean values for the different setups are calculated and shown in Table 4. The machining times ( $t_m$ ) are also determined for the comparison of productivity by the application of the results of previous studies [6]. This parameter means the required time to produce the machined surface, therefore it can be used for the comparison of productivity of turning procedures with different kinematics.

The results of the roughness evaluations are shown in Figure 2. The values increase only in a small extent on surfaces machined by Tool A, which has a 30° inclination angle. On lower feeds ( $f \leq 0.4$  mm) the growth is almost negligible, while increasing the feed from 0.4 mm to 0.8 mm results in an almost two-fold increase in the roughness parameters on various speeds. Machining by Tool B resulted in a nearly constant surface roughness on 0.1 mm and 0.2 mm feeds. The increase of the roughness values can be observed from 0.2 mm feed, from where the alteration can be described as an exponential growth. If the feed is higher than this limit, a 0.2 mm increase in the feed results in a nearly two-fold increase in  $R_a$  and  $R_z$  for both  $v_c$ .

Table 4 – Mean values of the roughness parameters and the machining times

Tool	f [mm]	$v_c = 200$ m/min			$v_c = 250$ m/min		
		$R_{a,a}$ [µm]	$R_{z,a}$ [µm]	$t_m$ [s]	$R_{a,a}$ [µm]	$R_{z,a}$ [µm]	$t_m$ [s]
A	0.1	0.466	3.033	4.53	0.443	3.02	3.86
	0.2	0.48	3.78	2.76	0.446	3.796	2.20
	0.4	0.553	3.523	1.36	0.613	4.453	1.09
	0.6	0.72	5.346	0.90	0.76	5.51	0.72
	0.8	1.29	7.273	0.67	1.12	7.026	0.53
B	0.1	0.486	3.036	5.65	0.336	2.75	4.50
	0.2	0.38	3.09	2.95	0.333	2.146	2.35
	0.4	0.9	4.65	1.39	0.706	4.106	1.11
	0.6	1.943	9.386	0.82	2.33	10.696	0.73
	0.8	4.223	18.706	0.61	3.65	16.536	0.49
C	0.1	0.486	1.893	4.01	0.476	1.903	3.19
	0.2	0.963	4.633	1.92	0.976	4.676	1.53
	0.4	3.3	13.436	0.92	3.046	12.533	0.73
	0.6	6.58	25.65	0.59	6.733	26.263	0.47
	0.8	10.656	40.346	0.43	9.986	38.75	0.34

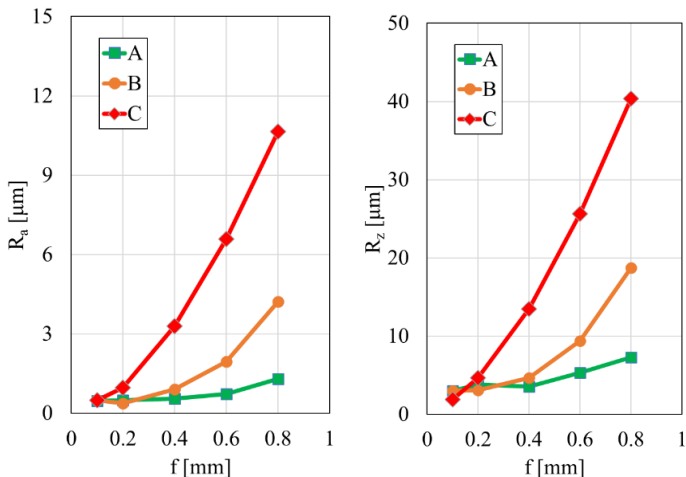


Figure 2 – Mean values of the roughness parameters ( $v_c = 200$  m/min)

The results of the measurements made on surfaces machined by a traditional turning tool are not presented any nearly constant roughness values on the studied setups. Here the exponential growth starts from 0.1 feed.

The comparison of different tools leads into the following conclusions. Machining with 0.1 mm feed resulted in nearly the same  $R_a$  values for the three cutting tools, however the measured  $R_z$  parameters showed differences. The average peak to valley height of the profile was lowest in traditional turning from which a 1.5-fold higher results measured after machining with rotational turning. I got this outcome because on this feed not the geometry of the cutting tool is significant in the surface texture generation, but the secondary deformations, material structure etc. However, the order of the cutting tools changes on 0.2 mm feed. The lowest roughness was achieved by Tool B, while Tool C becomes the worst. From this feed, the cutting edge geometry starts to play more important role on the surface texture. On 0.4 mm, 0.6 mm and 0.8 mm feeds the lowest roughness values measured on surfaces machined by Tool A, while the highest roughness is produced by Tool C. It can be also seen that the results from machining by Tool C can be achieved with nearly 2 times higher feeds with tool B and 3 times higher feeds with tool A. That means that rotational turning is more efficient: more surfaces can be machined during the same period. This is further analysed in Figure 2, where the roughness values are shown in function of the machining time. It can be seen, that the production of especially smooth surfaces ( $R_a < 0.4 \mu\text{m}$ ,

$R_z < 3.5 \mu\text{m}$ ) needs more time (thus 0.1 mm feed). However, to get a finished surface ( $R_a < 1.0 \mu\text{m}$ ,  $R_z < 6.0 \mu\text{m}$ ), rotational turning requires half of time machining time than traditional turning. The difference between the ratio of feeds and machining time is caused by the higher needed run-in and run-out time in circular feed.

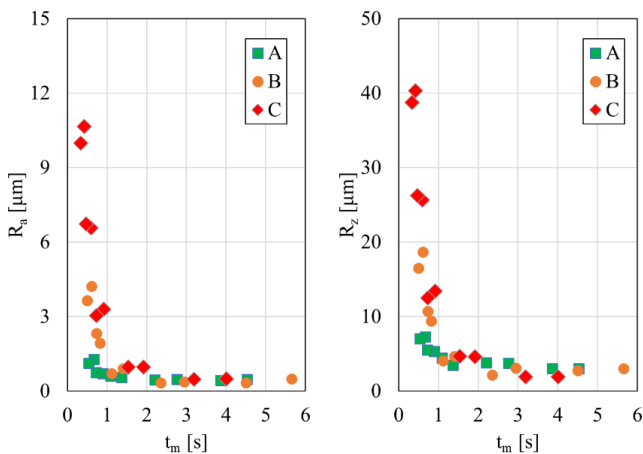


Figure 3 – Roughness measurement results in function of the machining time

## SUMMARY

The Arithmetical mean deviation of the assessed profile and the Average peak to valley height of the profile surface roughness parameters and the machining times are compared on different feeds in machining by traditional and rotational turning. Cutting experiments were made with five feeds, two cutting speeds and three cutting tools. From the mean values of the measured  $R_a$  and  $R_z$  values it is concluded that the application of rotational turning results in a significantly lower surface roughness than the values of traditionally machined surfaces. Comparing the needed machining time showed that 0.5-fold lower machining time needed in rotational turning to achieve a nearly ground surface.

## ACKNOWLEDGEMENTS

Project no. NKFI-125117 has been implemented with the support provided from the National Research, Development and Innovation Fund of Hungary, financed under the K\_17 funding scheme.

The described study was carried out as part of the EFOP-3.6.1-16-00011 “Younger and Renewing University – Innovative Knowledge City – institutional

development of the University of Miskolc aiming at intelligent specialisation” project implemented in the framework of the Szechenyi 2020 program. The realization of this project is supported by the European Union, co-financed by the European Social Fund.

**References:** 1. Kunderak, J., Deszpoth, I., Molnar, V.: Comparative Study Of Material Removal In Hard Machining Of Bore Holes. *Tehnicki Vjesnik-Technical Gazette* 21 (1), pp. 183–189., 2014; 2. Varga, G., Ferencsik, V.: Examination of 3D Surface Topography of Diamond Burnished C45 Workpieces. *Rezanie I Instrumenty V Tekhnologicheskikh Sistemah* 90 (1), pp. 153–162., 2019; 3. Qehaja, N., Jakupi, K., Bunjaku, A., Bruçi, M., Osmani, H.: Effect of Machining Parameters and Machining Time on Surface Roughness in Dry Turning Process. *Procedia Engineering*, Vol 100, pp. 135-140, 2015; 4. Niaki, F. A., Haines, E., Dreussi, R., Weyer, G.: Machinability and Surface Integrity Characterization in Hard Turning of AISI 4320 Bearing Steel Using Different CBN Inserts. *Procedia Manufacturing*, Vol 48, pp 598-605, 2020; 5. Berenji, K. R., Kara, M. E., Budak, E.: Investigating High Productivity Conditions for Turn-Milling in Comparison to Conventional Turning. *Procedia CIRP*, Vol 77, pp. 259-262, 2018; 6. Kunderák, J., Gyáni, K., Deszpoth, I., Sztankovics, I.: Some topics in process planning of rotational turning. *ENGINEERING REVIEW* 34:1 pp. 23-32., 2014.

Іштван Станкович, Мішкольц, Угорщина

## ВПЛИВ КРУГОВОЇ ПОДАЧІ НА ШОРСТКІСТЬ ПОВЕРХНІ І ТРИВАЛІСТЬ ОБРОБКИ

**Анотація.** Метою даної роботи є аналіз значень шорсткості і часу обробки при різанні циліндричних поверхонь з різною кінематикою і геометрією крайок (обертальне і поздовжнє точіння). В даному дослідженні експериментальні роботи проводилися на обробному центрі Perfect-Jet MCV-M8. Різальний інструмент затискається на столі верстата, а експериментальна заготовка фіксується в тримачі інструменту. Швидке обертання шпинделя забезпечувало основний рух різання, в той час як керований ЧПУ круговий рух інструменту навколо заготовки, що обертається під час обробки, здійснював рух вторинної подачі. Порівняння різних інструментів дозволяє зробити наступні висновки. Обробка з подачею 0,1 мм дала майже однакові значення  $R_a$  для трьох різальних інструментів, проте виміряні параметри  $R_z$  показали відмінності. Середня висота профілю від піку до западини була найменшою при традиційному точінні, а після обробки з обертальним точінням результати були в 1,5 рази вище. Цей результат було отримано тому, що на цій подачі важлива не геометрія різального інструменту в створенні текстури поверхні, а вторинні деформації, структура матеріалу і т.п. Однак порядок різальних інструментів змінюється при подачі 0,2 мм. Найменша шорсткість була досягнута інструментом В, а інструмент С — найгіршим. З цієї подачі геометрія різального крайки починає грати більшу важливу роль в текстурі поверхні. На 0,4 мм, 0,6 мм і 0,8 мм припадають найнижчі значення шорсткості, виміряні на поверхнях, оброблених за допомогою інструменту А, в той час як найвища шорсткість досягається за допомогою інструменту С. Також можна бачити, що результати обробки за допомогою інструменту С можуть бути досягнуті з подачі майже в 2 рази вище для інструменту В і в 3 рази вище для інструменту А. Це означає, що обертальне точіння більш ефективне: за той же період можна обробити більше поверхонь. Видно, також, що для виготовлення особливо гладких поверхонь ( $R_a < 0,4$  мкм,  $R_z < 3,5$  мкм) потрібно більше часу (таким чином, подача 0,1 мм). Однак для отримання чистої поверхні ( $R_a < 1,0$  мкм,  $R_z < 6,0$  мкм) обертальне точіння вимагає вдвічі менше часу обробки, ніж традиційне. Різниця між співвідношенням подачі і часом обробки викликана більш високим необхідним часом припрацювання і вибідання при круговій подачі.

**Ключові слова:** час обробки; обертальне точіння; шорсткість поверхні.

R. Strelchuk, Kharkiv, Ukraine

## **SURFACE ROUGHNESS MODELING DURING ELECTRIC DISCHARGE GRINDING WITH VARIABLE POLARITY OF ELECTRODES**

**Abstract.** *The article presents the probabilistic-statistical modeling of surface roughness in the process of electric discharge grinding with the variable polarity of electrodes. The correlation between electric modes of machining and indicators of the quality of the machined surface was established. A probabilistic-statistical model of part surface roughness formed during grinding is obtained, which establishes the correlation between high-altitude surface parameters and electrical machining modes. The developed model makes it possible to calculate the height parameters of the part roughness depending on the electrical modes of grinding. The height of microroughness is determined by the same machining conditions as the depth of erosion pits. It is possible to obtain low roughness if electrical machining modes are reduced.*

**Keywords:** *spatial position of erosion pits; statistical dimensions; roughness parameters; electrical modes.*

**Introduction.** The process of electrical discharge grinding with the variable electrode polarity allows obtaining the required qualitative and quantitative parameters with a significant reduction in the specific consumption of the diamond wheel and the costs of various types of energy [1, 2]. This is explained by the fact that changing in time on the polarity of the electrodes and the corresponding pulse repetition rate ensures stable conditions of the grinding process. By changing the pulses repetition rate, their duty ratio and power with a corresponding change in the polarity of electrodes, it is possible to regulate directly the process itself, up to an equilibrium state, ensuring equal manifestation of electrophysical and electrochemical (even at their insignificance) processes for both electrodes. The process of interaction between the cutting tool and the surface of the machined material under conditions of electrical discharge grinding with the variable polarity of electrodes has not been studied. In this connection, surface roughness modeling was carried out in the paper and the features and regularities of interaction between the cutting tool and the surface of the machined material were established.

**Literature Review.** The interaction of the diamond wheel with the surface of the machined material during electrical discharge grinding is a complex electrophysical system [3,4]. It is simultaneously a place of micro-cutting and the action of discharges in the interelectrode gap. When voltage is applied in this area, an electric current arises and passes through the current-conducting bridge circuits overlapping the interelectrode gap, the working fluid having some electric conductivity, and through the channel of the arising discharge during its action.

To determine the surface roughness, probabilistic-statistical modeling was

performed. During electrical discharge grinding, the roughness of the machined surface is formed as a result of the formation of individual pits that overlap each other. Each pit can be represented as a spherical segment. Since the spherical segment has geometric symmetry relative to the vertical axis, the issue of pits formation was considered in a two-dimensional formulation. The section of the pit is a circular segment, the arc radius of which is equal to the radius of the spherical segment.

**Research Methodology.** Taking into account the stochastic nature of the pit formation process, the method of probabilistic-statistical modeling (Monte Carlo method) was used to determine the surface roughness, which involves the following. The individual vertex and cavity of irregularities of the machined surface are formed by superimposing two repeatedly modeled pits (Fig. 1). For this purpose, the values of geometrical parameters of the pits ( $d_n$  and  $h_n$ ) and the values of parameters of the intersection of the pits were played out with a random number generator according to the law of normal distribution and their marginal values were obtained.

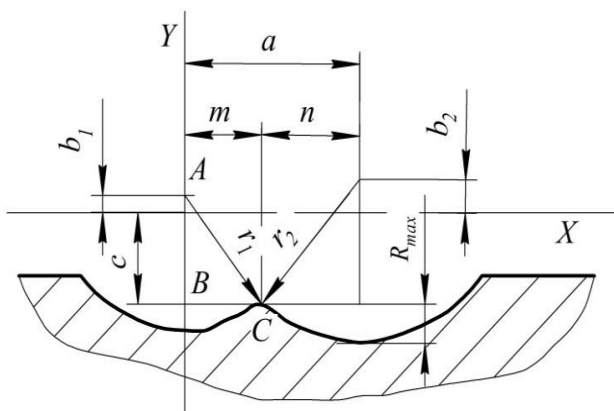


Figure 1 – Scheme for calculating the roughness of the machined surface

The roughness of the machined surface  $R_{max}$  was calculated by the formula:

$$R_{max} = r_{max} - b_{max} - c_{min}, \quad (1)$$

where  $r_{max}$  is the largest value of the arc radius;  $b_{max}$  is the largest value of the distance between the X axis and the center of the larger arc of all realizations;  $c_{min}$  is the smallest value of the distance between the intersection point of the arcs and the X axis of all realizations.

Let us define the parameter  $c$  at the intersection of two pits. The distance along the  $X$  axis between the centers of two intersecting arcs  $a$  is determined from the range from  $a_{min}$  to  $a_{max}$  and can be found as

$$a = m + n, \tag{2}$$

where  $m$  is the distance between the center of the first arc and the intersection point of the arcs;  $n$  is the distance between the center of the second arc and the intersection point of the arcs.

From triangles  $ABC$  and  $A_1B_1C$  we have:

$$r_1^2 = m^2 + (b_1 + c)^2 \tag{3}$$

$$r_2^2 = n^2 + (b_2 + c)^2 \tag{4}$$

where  $r_1, r_2$  are the radii of two intersecting arcs;  $b_1, b_2$  are the distances between the  $X$  axis and the centers of two arcs.

Solving equations (3) and (4) we obtain:

$$m = \sqrt{r_1^2 - (b_1 + c)^2},$$

$$n = \sqrt{r_2^2 - (b_2 + c)^2}.$$

Summing  $m$  and  $n$ , we have:

$$m + n = \sqrt{r_1^2 - (b_1 + c)^2} + \sqrt{r_2^2 - (b_2 + c)^2}. \tag{5}$$

Given (2), expression (5) can be reduced to the form:

$$\sqrt{r_1^2 - (b_1 + c)^2} + \sqrt{r_2^2 - (b_2 + c)^2} - a = 0.$$

The parameter  $c$  cannot be found explicitly from the obtained expression, so a numerical method is used to solve it.

It is known [5] that the relation between the depth and the diameter of an erosion pit has the following form:

$$\frac{d_{\pi}}{h_{\pi}} = 3 \dots 4. \tag{6}$$

From the  $ABC$  triangle (Fig. 2) we have

$$r^2 = \left(\frac{d_{\pi}}{2}\right)^2 + k^2. \tag{7}$$

On the other hand

$$r = k + h_{\pi}$$

Hence

$$k = r - h_{\pi} \tag{8}$$

Given (8) and (6), expression (7) can be represented as

$$5h_{\pi}^2 - 2h_{\pi}r = 0.$$

Solving this equation, we find the dependence of the arc radius  $r$  on the depth of the pit  $h_{\pi}$ :

$$r = 2.5h_{\pi} \tag{9}$$

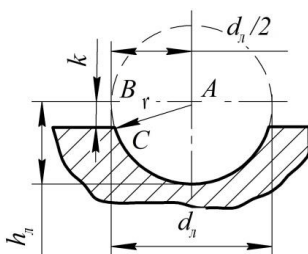


Figure 2 – Scheme for calculating the arc radius of the electrical discharge pit

Let us determine the maximum distance  $a_{max}$  on the X axis between the centers of the two intersecting arcs. In this case, the intersection point is on the outer machined surface (Fig. 3).

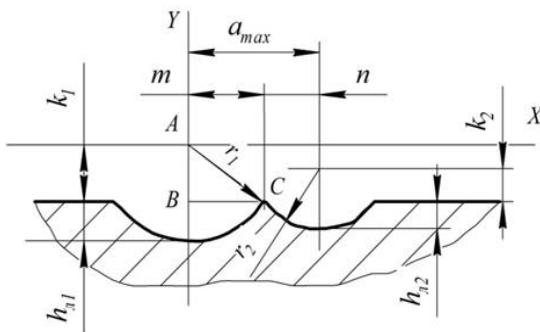


Figure 3 – Scheme for determining the  $a_{max}$  parameter

From equation (9) we express  $h_n$  as

$$h_n = 0.4r. \quad (10)$$

Substituting (10) into (8), we obtain:

$$k = 0.6r. \quad (11)$$

The  $a_{max}$  parameter is defined as

$$a_{max} = m + n. \quad (12)$$

From the triangle  $ABC$  we have:

$$r_1 = m^2 + k_1^2.$$

Hence

$$m = \sqrt{r_1^2 - k_1^2}.$$

Given relation (11), we obtain:

$$m = 0.8r_1. \quad (13)$$

Similarly:

$$n = 0.8r_2. \quad (14)$$

Substituting dependences (13) and (14) into equation (12), we obtain the final expression for determining  $a_{max}$ :

$$a_{max} = 0.8(r_1 + r_2).$$

Let us determine the minimum distance  $a_{min}$  on the  $X$  axis between the centers of the two intersecting arcs. The point of intersection of the two arcs is on the inner surface of the machined material (Fig. 4).

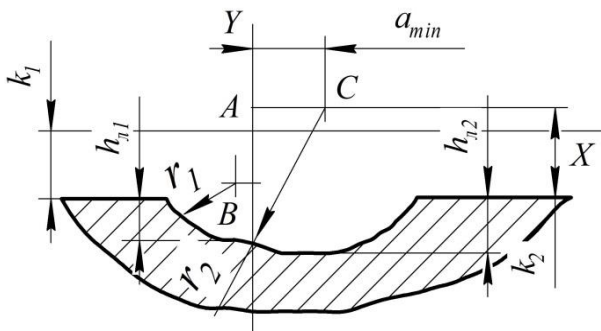


Figure 4 – Scheme for determining the parameter  $a_{min}$ .

From the triangle  $ABC$  we have:

$$r_2^2 = (h_{\pi 1} + k_2)^2 + a_{min}^2$$

Given relations (10) and (11), we can write:

$$r_2^2 = 0.16r_1^2 + 0.48r_1r_2 + 0.36r_2^2 + a_{min}^2$$

Solving this equation concerning  $a_{min}$  we obtain:

$$a_{min} = \sqrt{0.64r_2^2 - 0.48r_1r_2 - 0.16r_1^2}$$

Let us assume that the center of the arc with minimum radius  $r_{min}$  is on the  $X$  axis. Then, considering relation (6), the center of the arc with a larger radius will be higher on the  $Y$  axis. On this basis, let us define parameter  $b$  (Fig. 5).

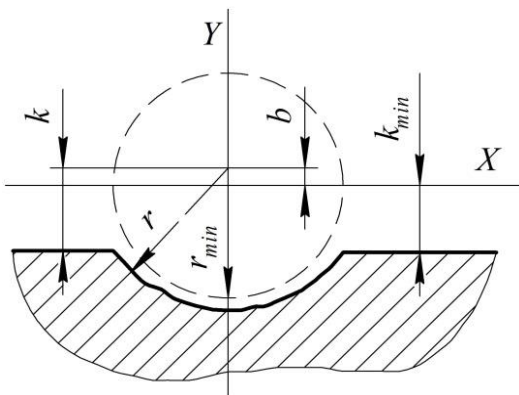


Figure 5 – Scheme for determining the parameter  $b$

Let us express  $b$  through  $k$  and  $k_{min}$ , and given (11), we obtain:

$$b = 0.6(r - r_{min}).$$

**Results.** Following the above-specified method, we have developed a calculation algorithm, the scheme of which is shown in Fig. 6. The calculation sequence is as follows. The values of electrical modes are set: voltage  $U$ , current rate  $I$ , pulse duration  $T$ . Then, the expectation of the erosion pit depth  $h_n$  and the standard deviation are calculated. Then the values of  $r_{max}$ ,  $r_{min}$ , and  $b_{max}$  are determined. After that, with the help of a random number generator, the parameters

$h_{n1}, h_{n2}, r_1, r_2, a, b_1, b_2,$  and  $c$  are played out according to the normal distribution law. The number of repetitions is taken as equal to 1,000. Then the value of  $c_{min}$  is determined. After that, surface roughness parameters are calculated:  $R_{max}, R_a, R_z.$

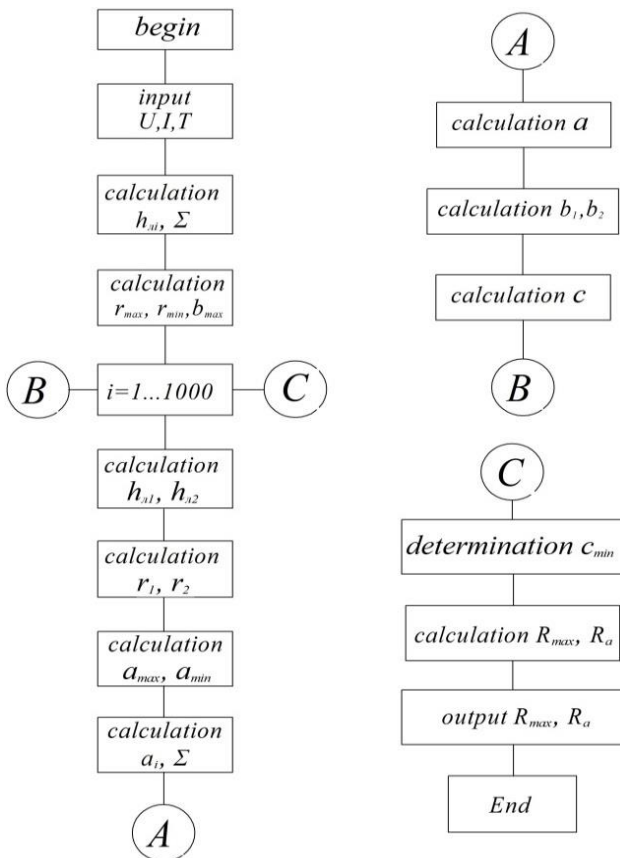


Figure 6 – Scheme of the algorithm for calculating the roughness parameters of the machined surface.

**Conclusions.** The developed model, considering the spatial position of erosion pits, their statistical dimensions, allows calculating the roughness parameters, which, eventually, make it possible to predict the durability of the formed part. The process of electrical discharge grinding with the variable polarity

of electrodes allows reducing roughness parameters, which leads to an increase in durability and reliability of the machined part operation.

**References:** 1. *Strelchuk R.M., Uzunian M.D.* Sposib elektroeroziinohoalmaznogo shlifuvannia zi zminnoiu poliarnistiu elektrodiv, Patent UA, no. 131894, 2019. 2. *Montes, J., Cuevas, F., Reina, F.* Modelling and Simulation of the Electrical Resistance Sintering Process of Iron Powders // *Met. Mater. Int.* 26, pp. 1045–1059 (2020). 3. *D'Urso, G., Maccarini, G., Ravasio, C.* Influence of electrode material in micro-EDM drilling of stainless steel and tungsten carbide // *Int J. Adv. Manuf. Technol.* 85, pp. 2013–2025 (2016). 4. *Giridharan, A., Samuel, G.* Investigation into erosion rate of AISI 4340 steel during wire electrical discharge turning process // *Machining Science and Technology*, pp. 287–298, (2018). 5. *R.Andreani, G.Haeser, J.M.Martínez* // On sequential optimality conditions for smooth constrained optimization, *Optimization* 60 (2011), pp. 627–641.

Роман Стрельчук, Харків, Україна

## МОДЕЛЮВАННЯ ШОРСТКОСТІ ПОВЕРХНІ ПРИ ЕЛЕКТРОЕРОЗІЙНОМУ ШЛІФУВАННІ ЗІ ЗМІННОЮ ПОЛЯРНІСТЮ ЕЛЕКТРОДІВ

**Анотація.** *Електроерозійне алмазне шліфування зі змінною полярністю електродів дозволяє обробляти важкооброблювані матеріали. Процес формування обробленої поверхні залежить, не тільки від електричних режимів обробки, а ще й від матеріалу заготовки, від робочої рідини і т.п. Ці параметри не пов'язані, отже, кожен з них дає свій вплив на хід процесу. Тому дослідження закономірностей зміни шорсткості в залежності від електричних режимів обробки виконувалося з використанням імовірно-статистичного моделювання. У статті проведено імовірно-статистичне моделювання шорсткості поверхні в процесі електроерозійного шліфування зі змінною полярністю електродів. Встановлено взаємозв'язок між електричними режимами обробки і показниками якості обробленої поверхні. Отримано імовірно-статистичну модель шорсткості поверхні деталі, що формується при шліфуванні, яка встановлює взаємозв'язок між висотними параметрами поверхні та електричними режимами обробки. Розроблена модель, дозволяє розрахувати висотні параметри шорсткості деталі в залежності від електричних режимів шліфування. Висота мікронерівностей визначається тими ж умовами обробки, що і глибина ерозійних лунок. Отримання низької шорсткості можливо при зниженні електричних режимів обробки. Використання розробленого алгоритму розрахунку супроводжується великою кількістю обчислень і застосуванням досить складних математичних процедур: рішенням рівнянь чисельними методами, генерацією випадкових чисел та ін. Дані обчислення доцільно проводити в програмних пакетах. У зв'язку з цим виникає необхідність розробки алгоритмів реалізації створеної математичної моделі в програмних пакетах: моделювання шорсткості обробленої поверхні; визначення положення вершини ерозійної лунки, що розглядається в площині формування поперечного мікропрофілю деталі при різних електричних режимах шліфування; розрахунок математичного очікування глибини ерозійної лунки.*

**Ключові слова:** *просторове положення ерозійних лунок; статистичні розміри; параметри шорсткості; електричні режими.*

V. Tihenko, V. Lebedev,  
T. Chumachenko, Odessa, Ukraine

## **AUTOMATIC CONTROL OF TEMPERATURE AND POWER CONDITIONS DURING ROUGH GRINDING OF SLABS**

**Abstract.** *The production of high-quality rolled products (slabs), the formation of its surface phase-structural composition, texture, stress state during rough grinding depends on the temperature in the area of contact between the wheel and the slab. During processing, due to geometric errors of the rolled surface, as well as due to local changes in hardness, periodic fluctuations of the instantaneous depth of cut occur, which can be determined indirectly by controlling one of the technological parameters, for example, the power spent on grinding, with subsequent recalculation it to online temperature values. The grinding temperature is described as a control object in the form of an aperiodic link. Computer simulation has confirmed the efficiency of the system for maintaining the specified temperature of slab grinding under various operating conditions that simulate the situations of real production.*

**Keywords:** *rough grinding; slab grinding temperature control; aperiodic link.*

### **Introduction.**

A significant part of Ukrainian exports are still products of the metallurgical industry, including rolled products.

When supplying metal products for export, Ukrainian metallurgical enterprises face tough competition from foreign manufacturers.

To obtain high-quality rolled products, the surface layer of billets (slabs) containing small cracks, cavities and scale must be cleaned right in the shops of metallurgical enterprises. The output of mill scale is on average 1 - 3% of the mass of finished rolled products.

There are various methods of cleaning (chemical, electrochemical and mechanical), however, in many cases, the processing of the surface layer with abrasive wheels on a roughing and grinding machine is used.

Rough grinding machines differ significantly from grinding machines for general machine-building use in terms of technological requirements for them. This difference lies in the fact that they implement an "elastic" grinding scheme, in contrast to the "rigid" one on conventional grinding machines. "Elastic" grinding scheme - processing with a constant pressing force of the wheel to the rolled steel is intended for the implementation of the process of removing metal of constant thickness from the surface of the workpiece. In practice, inconsistency in the grinding depth is often observed, which is noticeable by changes in the width of the "line" being ground.

The workpiece to be processed is fixed on a moving table, and a headstock with a grinding wheel is lowered onto it from above. The speed of the table with the workpiece can be varied in the range from 5 to 60 m / min. The clamping force of the grinding wheel during roughing can reach 10,000 N.

Since metal defects are concentrated mainly in the surface layer of the workpieces, only the surface layer must be removed to reduce metal waste during peeling. This will reduce the unproductive consumption of expensive metal, which is especially important when roughing alloy steels.

In roughing and grinding machines, the control action can be exerted on the drive for the longitudinal movement of the table, however, the large masses of the table and the workpiece make this channel very inertial and not very suitable for the system for maintaining the grinding depth.

It is expedient to control the drive for moving the grinding head in the direction perpendicular to the surface to be treated.

The temperature arising in the contact area of the grinding wheel with the slab can reach 1200 - 1300°C and cause grinding defects (burns) - deep changes in the phase-structural composition of the surface layer, which creates favorable conditions for the formation of residual stresses and, as a result, cracks [1] ... As is known from the literature [2], thermal grinding defects reduce the durability by 3–4 times. During processing, due to geometric errors of the slab surface, as well as due to local changes in hardness, periodic fluctuations of the instantaneous depth of cut occur, which causes periodic changes in the value of the contact temperature of grinding, as a result of which thermal defects of the surface layer can occur, such as phase and structural transformations that sharply reduce the performance of the surface layer.

The most rational way out of this situation is to automatically maintain the contact temperature of grinding at a safe level. This can be done by compensating for fluctuations in the depth of the cut with other components of the processing modes. Thus, the purpose of this work is to consider a mathematical model of the process of automatic control of the contact temperature of grinding the surface of slabs.

To achieve this goal, it is necessary to solve the following tasks: select a control object, select a controlled value, select control laws, develop an algorithm and a block diagram of the control process.

This task can be accomplished with the help of an analytical study of the process of heat generation during grinding, considering the process of cutting with an abrasive grain with its contradictory laws [3,5].

It would be more rational to choose the grinding temperature as a controllable value; however, practically insurmountable difficulties arise in the practical implementation of this choice. In order to obtain information about the grinding temperature of a particular slab at an arbitrary cutting moment, it is necessary that

there is a temperature sensor in the grinding wheel, which cannot be installed in the wheel without violating the integrity of the latter, which cannot be done during the production process for safety reasons.

A large number of works have been devoted to the issues of adaptive control of the grinding process, *however, the issue of controlling the temperature regime of grinding is practically not considered.*

In the source [1] the authors consider the mathematical modeling of abrasive processing processes, in [2] the source describes the processes of temperature formation during grinding, in the work [3] discloses general issues and theoretical provisions of the adaptive control of the grinding process, in [4] the work considers adaptive feed control, [5] the work is devoted to general issues of adaptive control and optimization issues, [6] - issues of control and optimization of the external grinding process, in [7] - issues of adaptive control of metal-cutting machines, [8] the work is devoted to general issues of saving tools and increasing labor productivity in the use of adaptive control, in [9] the work considers the issue of controlling the transverse feed during grinding, in [10, 11] - the process of adaptive control of grinding forces, in [12] the work considers the effect of temperature fields of the grinding temperature on the stress state of the coatings applied to the part, but in The request for adaptive temperature control is not affected.

From the literature review, it can be concluded that the issues of controlling the grinding temperature have not yet been fully considered.

### **Research Methodology.**

Information about the temperature value can be obtained indirectly by monitoring one of the technological parameters, for example, the power consumed for grinding, with its subsequent conversion into temperature values in the online mode. As shown in [2], the surface temperature during grinding can be related to the power by the following relationship

$$\Theta = \frac{1,12 \cdot \eta \cdot Q \cdot \sqrt{\tau}}{\varepsilon \cdot F},$$

where  $\eta$  is a coefficient indicating what proportion of heat is transferred to the part;  $Q$  - grinding power, W;  $\varepsilon$  - coefficient of thermal activity of the part, J / m<sup>2</sup> deg s<sup>0.5</sup>;  $F$  is the area of the contact patch of the wheel with the part, m<sup>2</sup>;  $\tau$  is the contact time of the wheel with an arbitrary point of the ground surface, sec.

After some transformations we have:

$$\Theta = \frac{0,896 \cdot Q}{\sqrt{v_s} \cdot F \cdot \varepsilon} \text{ or } \Theta = k \cdot Q,$$

$$k = \frac{0,896}{\sqrt{v_s \cdot F \cdot \varepsilon}} = \frac{0,896}{\sqrt{D \cdot t \cdot v_s \cdot S \cdot \varepsilon}}$$

where  $D$  is the diameter of the wheel, m;  $t$  is the depth of grinding, m;  $v_s$  - part speed, m / s;  $S$  - the value of the cross feed, m.

The dependence of temperature on time during grinding is described by the expression [2]

$$\Theta_\tau = \Theta_{\max} \left[ 1 - \exp\left(-\frac{v_u^2 \cdot \tau}{4 \cdot a}\right) \right], \quad (1)$$

where  $\Theta_{\max}$  – is the maximum temperature, °C;  $v_u$  — speed of the heat source, m / s;  $\tau$  is the current time, s;  $a$  - coefficient of thermal diffusivity of the grinded material, m<sup>2</sup> / s.

Assuming that the time constant of the temperature rise process is:

$$\frac{4a}{v_u^2} = T,$$

We have:

$$\Theta_\tau = \Theta_{\max} \left( 1 - e^{-\frac{\tau}{T}} \right),$$

and in operator form:

$$\omega_p = \frac{\Theta_{\tau(p)}}{\Theta_{\max(p)}} = \frac{1}{T_p + 1}.$$

Thus, the grinding temperature in the control system can be represented as an aperiodic link.

In general, the block diagram of the control system can be as shown in Fig. 1.

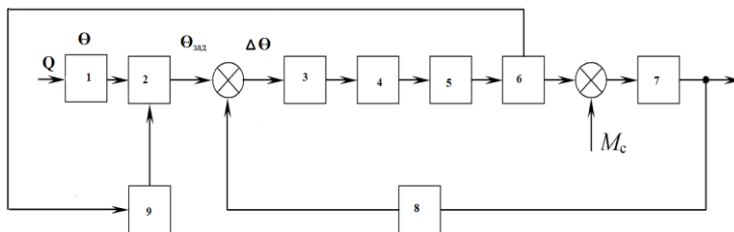
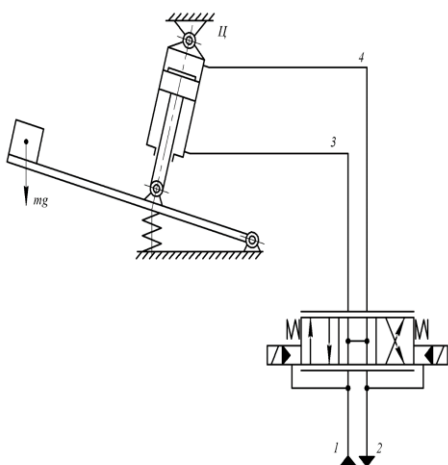


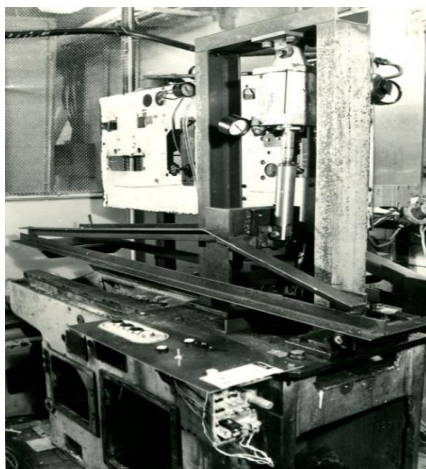
Figure 1 – Block diagram of the grinding temperature maintenance system  
 1 – block for converting power to temperature; 2 – grinding temperature regulator;  
 3 – amplifier; 4 – hydraulic valve with proportional control;  
 5 – hydraulic cylinder; 6 – processing process; 7 – grinding wheel drive;  
 8 – the sensor of the calculated temperature by power; 9 – table speed sensor

The drive for the movement of the grinding head can be pneumatic or hydraulic, but the hydraulic drive has higher dynamic properties.

A fragment of the hydraulic circuit of the drive is shown in Fig. 2 (a). For experimental verification of the characteristics of the control system, a special stand was used (Fig. 2 (b)), which consisted of a welded portal and a rotary frame, the flywheel masses of which corresponded to the reduced flywheel masses of the machine spindle drive.



a)



b)

Figure 2 – Diagram of the hydraulic drive (a) and a stand for experimental research (b)

The body of the hydraulic cylinder and its rod were hinged, respectively, with a portal and a frame. Under the influence of the cylinder, the frame rotated around an axis mounted on the base of the portal.

At the end of the frame opposite to the pivot axis, there was a load imitating the mass of the grinding headstock.

The graph of computer simulation of working off the task by the automatic control system at various gain rates  $K_{amp}$  is shown in Fig. 3.

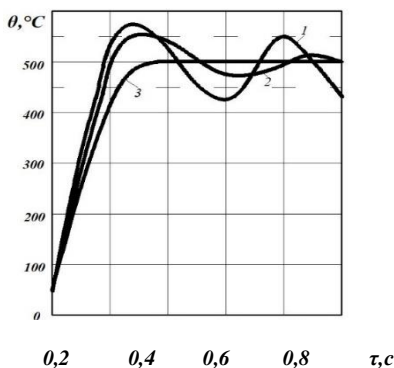


Figure 3 – Computer simulation of the maintenance task constant temperature of slab grinding by an automatic control system with a hydraulic drive:

1 –  $K_{amp} = 640$ ; 2 –  $K_{amp} = 480$ ; 3 –  $K_{amp} = 320$

## Results.

As a result of the study, a model of a system for adaptive control of the temperature of grinding slabs during their cleaning has been proposed. The system under consideration makes it possible to obtain a high-quality surface layer during rough grinding of slabs.

## Conclusions.

Computer simulation has confirmed the operability of the system for maintaining the specified temperature of slab grinding under various operating conditions that simulate the situations of real production.

The use of the system for maintaining the grinding temperature on roughing-grinding machines makes it possible to automate the process of abrasive cleaning, reduce the non-productive consumption of expensive billet metal, and increase the competitiveness of domestic producers of rolled metal products.

**References:** 1. Chirkov G. V. Matematicheskoe modelirovanie rezhimov rezaniya pri obrabotke materialov abrazivnymi instrumentami. *Tekhnologiya mashinostroeniya*. - 2004. - N 6. - pp.58–61. 2. Lebedev V., Klimenko N., Uryadnikova I., Chumachenko T., Ovcharenko A. The definition of amount of heat released during metal cutting by abrasive grain and the contact temperature of the surface being grinded. *Eastern-European Journal of Enterprise Technologies*. 2016. No 5/7(83) 2016. — pp. 43–50. 3. Amitay G, Malkin S, Koren Y. Adaptive control optimization of grinding. trans. *The American society of mechanical engineers*. Vol. 103, No 1, pp. 131–136, Feb.1981. 4. ACM – Adaptive Control & Monitoring. Adaptive feed rate control and monitoring. siemens.com 2008 <https://assets.new.siemens.com/siemens/assets/api/uuid:9b3f1c78-227b-488b-84cc-e39127a0fec7/versionvondfmc-b10081-00acmde-72.pdf>. 5. Ken Thayer. Grinding theory and adaptive control optimization. *Manufacture equipment and accessories*. October 5. 2018

<https://insights.globalspec.com/article/10106/grinding-theory-and-adaptive-control-optimization>.

6. Xiu-Shou H. The Research of a Practical Adaptive Control System for on External Cylindrical Grinding Process. In: Tobias S.A. (eds) *Proceedings of the Twenty-Fifth International Machine Tool Design and Research Conference*. Palgrave, London 1985. pp. 169–175. [https://doi.org/10.1007/978-1-349-07529-4\\_18](https://doi.org/10.1007/978-1-349-07529-4_18). 7. Petrakov Iu.V. Adaptive control system for CNC machine-tools. 2016 Zavershennye nauchno-issledovatel'skie raboty <https://report.kpi.ua/en/node/1082> 8. Larry Hafil. Adaptive Controls Save Tools and Time. *Technology Advances Supercharge an Old Process*. JAN 23, 2007 <https://www.americanmachinist.com/machining-cutting/article/21896290/adaptive-controls-save-tools-and-time>. 9. Gao Y BSc, MSc, Jones B. Discrete Control System Model for the Traverse Grinding Process. *Proceedings of the institution of Mechanical Engineers. Part 1: Journal of Systems and Control Engineering*. First Published February 1, 1992, pp. 19–27. 10. Zhan Qi Hu, Ming Li Xie, Yu Kun Li, Yi Tong Zhang. Research on Adaptive Control of Grinding Force of CNC Cams Grinder. *Key Engineering Materials* (Volume 416) September 2009. pp 360–364. <https://doi.org/10.4028/www.scientific.net/KEM.416.360>. 11. Mingli Xie; Zhanqi Hu; Yitong Zhang. Research on Adaptive Control of Grinding Force of CNC Cam Grinder. International Workshop on Intelligent Systems and Applications. Wuhan, China. 23–24 May 2009. (DOI: 10.1109/IWISA.2009.5073054). 12. Usov A., Tonkonogiy V., Dašić P., Rybak O. Modelling of Temperature Field and Stress–Strain State of the Workpiece with Plasma Coatings during Surface Grinding. *Machines*, Switzerland, 2019, 7(1), 20; (DOI: <https://doi.org/10.3390/machines7010020>).

Валентин Тихенко, Володимир Лебедев,  
Тетяна Чумаченко, Одеса, Україна

## АВТОМАТИЧНЕ КЕРУВАННЯ ТЕМПЕРАТУРНО-СИЛОВИМ РЕЖИМОМ ПРИ ОБДИРНОМУ ШЛІФУВАННІ СЛЯБІВ

**Анотація.** Для отримання високоякісного прокату поверхневий шар заготовок (слябів), що містить дрібні тріщини, раковини і окалину, повинен бути зачищений прямо в цехах металургійних підприємств. Існують різні способи зачистки слябів, проте пріоритет залишається за обробкою поверхневого шару абразивним кругом на копіювально-шліфувальних верстатах. Формування фізичних властивостей поверхневого шару сляба при обдирному шліфуванні залежить від температури в зоні контакту круга зі слябом, що забезпечує певний фазово - структурний склад і текстуру цього шару, його напружений стан. Температура, що виникає в зоні контакту шліфувального круга зі слябом, може становити 1200 - 1300<sup>o</sup>C. Вона є основною причиною утворення шліфувальних дефектів – глибоких змін фазово - структурного складу поверхневого шару, що створює сприятливі умови для утворення залишкових напружень і як наслідок – тріщин. При обробці, через геометричні похибки поверхні сляба, а також через місцеві зміни твердості, відбуваються періодичні коливання миттєвої глибини різання, що викликає періодичні зміни величини контактної температури шліфування в результаті чого можуть виникати теплові дефекти поверхневого шару. Інформацію про величину температури можна отримати непрямим шляхом, контролюючи один з технологічних параметрів, наприклад, потужність, затрачену на шліфування, з наступним перерахунком її в значення температури в режимі online. Температура шліфування описується як об'єкт управління у вигляді аперіодичної ланки. Комп'ютерне моделювання підтвердило працездатність системи підтримки заданої температури шліфування слябів при різних умовах функціонування, що імітують ситуації реального виробництва.

**Ключові слова:** обдирне шліфування; управління температурою шліфування слябу; аперіодична ланка.

V. Fedorovich, D. Fedorenko, I. Pyzhov, Y. Ostroverkh, Kharkiv, Ukraine

## **MODELING THE INFLUENCE OF METAL PHASE IN DIAMOND GRAINS ON SELF-SHARPENING OF GRINDING WHEELS ON CERAMIC BONDS**

**Abstract.** *The article presents the results of theoretical studies using finite element modeling, which made it possible to determine the rational characteristics of diamond wheels based on ceramic and polymer bonds. The effect of the parameters of the diamond-bearing layer on the change in its stress-strain state in the process of microcutting of hard alloys and superhard materials has been studied. It is established that the determining factor in the occurrence of critical stresses during grinding is the temperature in the cutting area, the increase of which in the presence of metal phase inclusions in diamond grains with high values of thermal expansion coefficient can lead to destructive stresses in grains and, consequently, their premature destruction. It is advisable to use diamond grains with a minimum content of metal phase and the use in the manufacture of synthetic diamonds solvent metals with a low value of this coefficient, which will significantly increase the use of potentially high resource diamond grains.*

**Keywords:** *diamond grinding wheel; processed material; diamond grain; superhard materials; wheel bond; stress-strain state; finite element method; equivalent stresses; self-sharpening; grinding modes.*

**Introduction.** The development of computer technology opens new perspectives for virtual integrated research of the processes of manufacture and operation of diamond abrasive tools (DAT). In recent years, based on the finite element method (FEM), a number of software packages with even more advanced capabilities have been developed. These primarily include *SIMULA Abaqus*, *SolidWorks Simulation*, *ANSYS* and *LS-Dyna*. Their use for simulation experiments on the developed models makes it possible to significantly reduce the volume of estimated machine research.

**1. Articulation of the problem.** As is well known, diamond wheels on organic and ceramic bonds are designed mainly for operation in self-sharpening mode. In world practice, one of the most promising approaches to improving the processing of diamond abrasive tools is based on the creation of prerequisites for the implementation of the necessary mechanisms for specific processing conditions (macro- or micro-destruction or a combination thereof) of self-sharpening of diamond grains and diamond layer as a whole. And for this you need to know the physics of the processes that occur both in diamond grains in particular and in the grinding system in general. Significant results in this direction can be obtained in the case of using the methodology of 3D modeling of the stress-strain state of tool systems and processing systems and refinement of the results by using machine experiments. This will allow to predict and implement in practice the optimal conditions for creating a controlled process of self-sharpening of

diamond grains in particular and the diamond-bearing layer in general, and, consequently, significantly increase the efficiency of the grinding process.

**2. Literature Review.** Along with the choice of the bond grade, grain and grinding modes, the choice of the quantitative and qualitative composition of the metal phase, which is part of the diamond grains (DG), is of paramount importance. A significant number of studies are devoted to the study of the influence of the metal phase on the specific consumption of diamonds, the productivity of grinding and the roughness of the processed surface, [1, 2, 3, 4]. Most of the recommendations for choosing a grade of diamond grains in wheels on ceramic bonds apply to the processing of carbide products, high-speed steels, titanium alloys. Model studies carried out by the authors [5, 6] indicate that a comprehensive selection of the grade of grains and their relative concentration can lead to a significant increase in the efficiency of the diamond grinding process. By the calculation method, it is possible to determine the stress-strain state (SSS) of the diamond-bearing layer not only during the manufacture of diamond-abrasive tools, but also at the stage of grinding various groups of processed materials (PM).

Modeling the limiting stress values by the finite element method [7] will allow avoiding expensive experimental studies and in the future create prerequisites for developing recommendations for grinding a wide range of grinded materials.

**3. Methodology of conducting model experiments.** *SIMULA Abaqus*, *SolidWorks Simulation*, *ANSYS* and *LS-Dyna* software packages were used for computer simulation of DAT operation processes.

Models of the "bond - DG – metal phase - PM" grinding system were developed for conducting simulation experiments (Fig. 1).

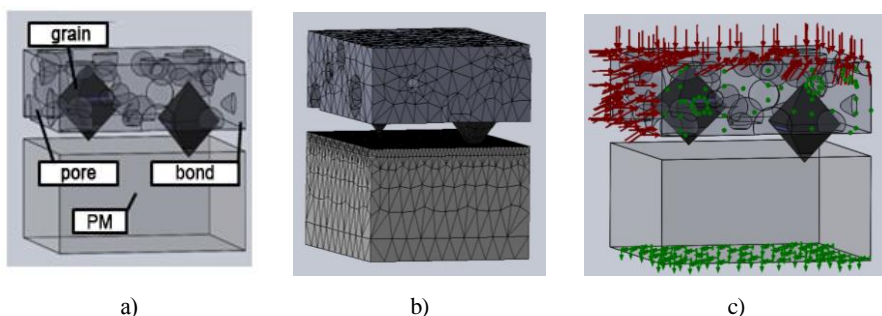


Figure 1 – 3D model (a), constructed finite element grid (b) and the stress scheme of the model (c) in the study of processes and grinding

When creating models, the shape, size and properties of its elements were taken into account, which were considered as elastic solids. Since the most common form of diamond crystals is considered to be an octahedron [8], DG was taken with its geometry. Grain sizes varied according to the grain size of diamonds (50/40, 100/80,  $125 \times 100$ ,  $200 \times 160$ ). Local inclusions of the metal phase in the DG were created in the form of arbitrarily oriented parallelepipeds, the volume content of which was set depending on the grain grade (AC-4 - 7.5%, AC6 - 6%, AC15 - 2.2%, AC32 - 0.6 %) [9–10]. The bonds were reproduced as prismatic fragments ranging in size from  $250 \times 250 \times 125 \mu\text{m}$  to  $1000 \times 1000 \times 500 \mu\text{m}$  depending on the size and concentration of grains in the diamond-bearing layer. In the volume of the bond the grain placing surfaces were put in a free order, the number of which varied depending on the concentration of diamonds (25%, 50%, 100%, 150%, 200%), which was set as a percentage ratio of the bond volume and the total volume of DG. The element of the system "PM" was modeled in the form of prismatic fragments with dimensions from  $250 \times 250 \times 125 \mu\text{m}$  to  $1000 \times 1000 \times 500 \mu\text{m}$ .

Finite element analysis was performed using octagonal *SOLID* elements. The ANSYS program selected the type of finite elements from the package library for each component of the system, the construction of a finite element grid and its selective thickening. Elements such as *Hex Dominant* and *Tetrahedron* were used to create the grid for metal phases. Grid thickening was performed in the areas of DG bonding, in the areas of their contact with the PM and the inclusion of metal phases, as well as on the contact surfaces of the system elements. This approach allowed to more accurately simulate the deformation of fragments of the model, taking into account the distance of the areas of ultimate effects.

Fixing of the model (setting of zero or other necessary displacements) was carried out using the attributes of the geometric model (points, lines, surfaces) [11]. The model was put under stress with static uniaxial evenly distributed load in the form of pressure and temperature values.

The choice of load limit parameters was made taking into account the temperature and force loads that accompany the grinding process.

When modeling the process of diamond abrasive grinding, the model was loaded with static uniaxial evenly distributed load  $P_y$  in the form of added values of normal force 0.5-4.0 N, which simulates the clamping force of the wheel in accordance with the technological parameters of diamond abrasive processing [12]. The feed motion of the  $S_{\text{feed}}$  and the rotation of the wheel were simulated by the longitudinal motion of the "bond - DG" element along the element of the "PM" system. Depending on the simulated cutting speed, different speeds of the "bond - DG" element were set. To increase the reliability of the simulation results, the value of the temperature load in the range of 400-800°C was chosen according to the data of works [13, 14], in which the values of temperatures in the grinding area during processing of materials of different hardness were experimentally established.

The following characteristics of system elements were included in the calculation

model: modulus of elasticity ( $E$ ), modulus of volumetric compression ( $G$ ), coefficient (CTE) of linear thermal expansion ( $\alpha$ ), Poisson's ratio ( $\mu$ ), yield strength ( $\sigma_0$ ), coefficient of thermal conductivity ( $\lambda$ ). Specifications of grain properties were performed according to reference data [15–17], taking into account information on temperature dependences of synthetic diamond properties (Fig. 2).

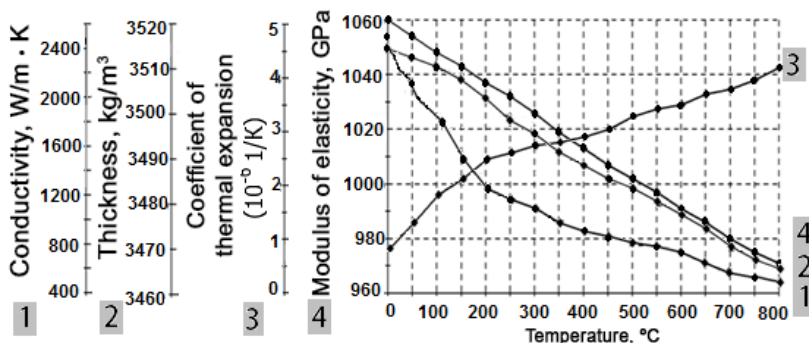


Figure 2 – Temperature dependences of synthetic diamonds properties

Since in the real grinding process the considered system is loaded with both force and temperature, in the course of researches depending on the total thermal and foreload the value of equivalent stresses  $\sigma_{eq}$  in elements of the system "metal phase - DG - bond - pore - PM" was determined. The bond was considered broken if the equivalent stresses ( $\sigma_{eq}$ ) exceeded the corresponding strength limits.

**4. The results of model experiments.** The decisive factor in increasing the stability of DAT, along with the rational choice of components of the diamond wheel is the use of scientifically sound grinding modes, which can significantly increase the service life of the tool.

To determine the rational parameters of grinding, a series of experiments was conducted to study the effect of normal pressure and temperature in the grinding area on the SSS of the microvolume of the diamond-bearing layer in the grinding area. The study was performed on a model that simulates grinding with a single grain.

Since the temperature in the grinding area dominates among the factors that determine the process of diamond abrasive processing, it is important to study the influence of this factor on the behavior of the "bond - DG – metal phase - PM" system. It is known that the temperature in the cutting area can rise significantly due to "salinization" of the working surface of the diamond wheel with sludge particles, while excessive heating of the bond and DG, which can lead to their destruction and premature failure of the tool. Therefore, a comparative analysis of the SSS system that imitates diamond grinding was performed at different temperature loads (400 °C, 600 °C and

800 °C).

It is established that with the increase of the clamping force of DG in the specified range of values, the level of maximum stresses  $\sigma_{eq}$  increases by 1.3%. More influential is the temperature factor that occurs in the cutting area during grinding: an increase in temperature from 400 °C to 800 °C causes an increase in the level of stresses in the grain more than twice. On the one hand, the information obtained indicates the feasibility of cooling the cutting area, and on the other hand, ceramic bonds are known to be heat-resistant, which allows their use in dry grinding. Processing of the simulation results showed that the dependence of equivalent stresses on the grinding temperature is linear and is satisfactorily described by the equation  $\sigma_{eq}=1.5265 \cdot T_{gr}+1.328$  (approximation reliability  $R^2 = 0.99$ ).

However, as shown in [18], the possibility of reducing the heat load during grinding by optimizing the cutting modes is much lower than, for example, determining the optimal characteristics of DAT, which reduces the friction of the wheel with PM. And this is an important condition for reducing the energy consumption of the grinding process.

During the research, a model was used that allows to observe the change of SSS of the system "metal phase - DG - bond - PM" depending on the qualitative and quantitative characteristics of the metal phase (Fig. 3).

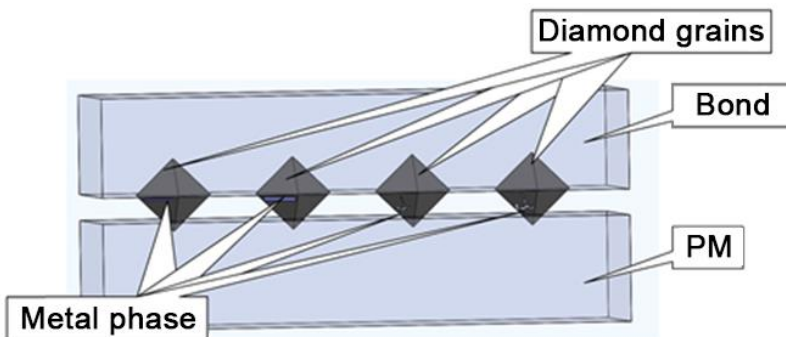


Figure 3 – 3D model for determining the influence of the metal phase on SSS of the system "metal phase - DG - bond - PM"

To identify the role of shape, size and composition of the metal phase, calculations were performed on models that imitate grains of grades AC6 and AC15 with a grain size of 125/100. According to the literature data [9, 19], the metal phase was modeled both in the form of rectangular parallelepipeds (simplified) and in the form of irregularly shaped elements, the volume of which was 2.2% and 6% of the grain volume, respectively, which corresponds to diamond powders of the AC15, AC6 grades. The level of maximum equivalent stresses ( $\sigma_{eq}$ ) and the volume of destructive stresses in the grain

( $V\sigma_{destr}$ ) were fixed as a criterion that determines the probability of self-sharpening of DG during grinding due to their micro-destruction under the action of stresses caused by temperature-force factors.

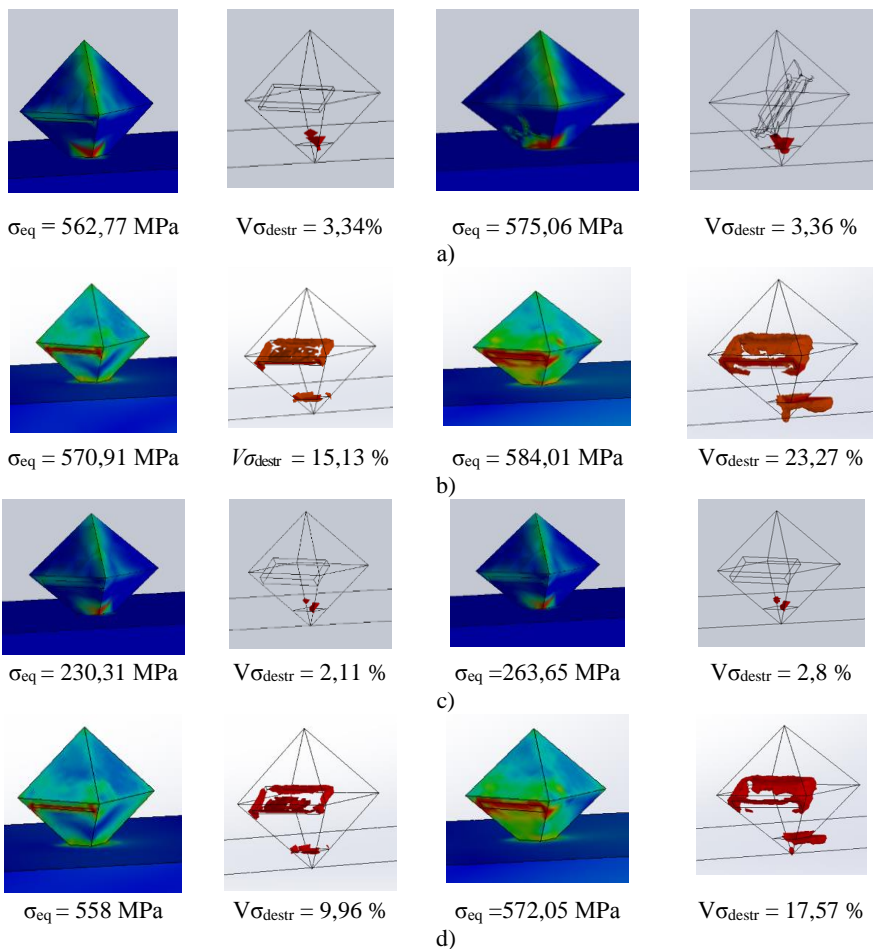


Figure 4 – Distribution of stresses in the grain in the contact area "grain - PM":  
 a) inclusion of metal phase  $Fe_{95}Si_5$  of simple and complex shape in AC15 grains (2%); bond K1-01; PM - VK8; T = 440 °C; b) metal phase  $Fe_{95}Si_5$  in grains AC15 (2%) and AC6 (6%); bond K1-01; PM – ASPK; T = 800 °C; c) metal phase  $Fe_{95}Si_5$  i  $Ni_{139,6}Mn_{59,6}(Cr_3C_2)_{0,8}$  in grains AC6 (6%) bond K1-01; PM – alloy VK8; T = 440 °C ; d) metal phase  $Fe_{95}Si_5$  in grains AC15 (2%) and AC6 (6%); bond K1-01; Sital AC-418; T = 760 °C

Examples of simulation results are given in Fig. 4, where it is seen that the areas where the maximum load level is recorded, are localized mainly in the area of inclusions of the metal phase, as well as in the area of contact of the DG with PM.

Calculation results showed that for cases of simple and complex shape of the metal phase with the same size of inclusions (Fig. 4 a), the stresses  $\sigma_{eq}$  practically do not change, and  $V\sigma_{destr}$  differs by only 0.7%. This indicates the feasibility of modeling the metal phase in the form of simple forms (plates), which reduces the calculation time. As the size of metal phase inclusions of the same composition increases, other conditions being same (Fig. 4 b), the stress level  $\sigma_{eq}$  increases by  $\sim 2 \div 2.5\%$ , while  $V\sigma_{destr}$  increases 2 times.

When grinding different PM in the case of identical in composition and size inclusions of the metal phase with increasing hardness of PM there is a tendency to increase the maximum stresses at the contact "DG - PM" and in adjacent areas (Fig. 4 c), while the value of  $V\sigma_{destr}$  increases from 2.1 % to 3.65%. With increasing the CTE of the metal phase for the considered solvent alloys while maintaining other equal conditions (Fig. 3 d) recorded an increase in the level of  $\sigma_{eq}$  by  $5 \div 10\%$  and almost twofold increase in  $V\sigma_{destr}$  (from 2.12% to 4.32%) in the row:  $Ni_{39,6}Mn_{59,6}(Cr_3C_2)_{0,8} > Fe_{95}Si_5 > Fe_{44}Co_{44}(Cr_3C_2)_{12}$ .

The influence of the composition and size of the metal phase on the level of  $\sigma_{eq}$  can be traced by the simulation results summarized in Table 1.

Table 1 – Maximum equivalent stresses (MPa) according to the results of modeling the process of grinding with a diamond wheel on the K1-01 bond

Metal phase composition	Processed material	Local temperature of the ground surface $T_{max}, ^\circ C$ [20, 21]	Volumes of destructive stresses in grain ( $V\sigma_{destr}, \%$ ) when using grains of different grades (grain size 125/100)		
			AC4 (7,5%)*	AC6 (6%)*	AC15 (2,2%)*
$Ni_{39,6}Mn_{59,6}(Cr_3C_2)_{0,8}$	ASPK	800	42.57	39.55	20.39
	Sital AC-418	760	26.37	23.35	13.24
	Alloy VK8	440	5.81	2.80	0.38
$Fe_{95}Si_5$	ASPK	800	26.29	23.27	15.13
	Sital AC-418	760	20.58	17.57	9.96
	Alloy VK8	440	5.13	2.11	0.29
$Fe_{44}Co_{44}(Cr_3C_2)_{12}$	ASPK	800	23.43	20.41	10.11
	Sital AC-418	760	14.73	11.71	6.64
	Alloy VK8	440	4.43	1.41	0.19

\* the relative volume of metal phase inclusions  $Fe_{95}Si_5, \%$

Therefore, the composition of the metal phase is of great importance, especially in the case when the CTE of the metal phase significantly exceeds the CTE of the diamond. The shape of the metal phase inclusions plays a secondary role, as does the modulus of elasticity. Based on the obtained data, it can be stated that according to the degree of influence on the level of stresses arising in the volume of DG during grinding, the specified parameters (shape, size, the CTE of metal phase, and hardness of PM) can be arranged in a row: metal phase composition > metal phase size > type of PM > metal phase shape.

The grinding temperature of the material has a decisive influence on the stresses arising at the contact of "DG - PM". According to [20, 21], the local temperature in the cutting area differs significantly from 440 °C for VK8 alloy to 800 °C for ASPK diamond. The results of the calculations showed that when grinding parts made of hard alloy VK8 in the self-sharpening mode, it is advisable to grind without cooling. In this case, the formation of wear areas on the grains will be accompanied by an increase in temperature in the cutting area, which will ensure rational self-sharpening of the grains.

Wheels with AC15 grains will also provide rational self-sharpening during dry grinding of the AC-418 sital under the condition of using diamond powders, mixing the metal phase based on alloys of the growth system with reduced CTE (for example,  $Fe_{95}Si_5$  а60  $Fe_{44}Co_{44}(Cr_3C_2)_{12}$ ). Instead, grinding of products from ASPK and sital AC-418 with wheels containing grains of grades AC2, AC4, AC6 should be carried out with cooling to prevent their thermal destruction.

It is established that the difference between the CTE of DG and metal phase determines the level of stresses at the contact of "DG – metal phase", which cause the appearance of microcracks in the grain during sintering of the diamond-bearing layer. Based on this, it is concluded that with increase of the CTE of solvent alloys used in the synthesis of diamonds, the effect of sintering temperature increases, which leads to the destruction of DG during grinding. This conclusion is generally consistent with the data of [22], where it is shown that with increasing grinding temperature above 650 °C, the loss of grain strength is greater, the greater the difference between the CTE of the metal phase and DG. This fact should be taken into account in the manufacture of diamond wheels and the development of grinding modes.

## **5. Conclusions**

The influence of qualitative and quantitative characteristics of diamond wheels on the SSS of the system "bond – metal phase - DG - PM" in the area of cutting diamond grains of brittle difficult-to-process materials has been calculated. The factors that determine the intensity of mutual destruction of the elements of the diamond-bearing layer of the wheel during grinding were identified. It is shown that in the considered range of force and temperature loads, that reproduce the real modes of diamond processing, the wear of diamond wheels is determined by the process of accumulation and development of microcracks in the bond and diamond grains.

It is established that the determining factor in the occurrence of critical stresses during grinding is the temperature in the cutting area, the increase of which in the presence of

inclusions in the DG metal phase with high CTE leads to destructive stresses in the grains and, consequently, their premature failure. It is advisable to use DG with a minimum content of metal phase and the use in the growth of synthetic diamonds of solvent metals with low CTE, which will significantly increase the utilization of DG. Otherwise, the grinding area must be forcibly cooled.

**References:** 1. *Semko M.F.* Basics of diamond grinding / M.F. Semko, A.I. Grabchenko, A.F. Rab and others - Kyiv: Tehnika, 1978 — 192 p. 2. *Grabchenko A.I.* Expansion of technological capabilities of diamond grinding / A.I. Grabchenko. - Kharkiv: Vishcha shkola, 1985 — 184 p. 3. *Bakul V.N.* Basics of design and manufacturing technology of abrasive and diamond tools: textbook for technical schools / V.N. Bakul, Y.I. Nikitin, E.B. Vernik and others – Moscow : Mashinostroenie, 1975 —296 p. 4. *Zakharenko I.P.* Superhard abrasive materials in tool manufacture / I.P. Zakharenko. – Kyiv : Vischa shkola, 1985 — 152 p. 5. *Mamalis, A.G., Grabchenko, A.I., Romashov, D.V., Fedorovich, V.A., Kundrak, J.* Determination of the diamond wheel structure in high-speed grinding using nanoindentation techniques: experimental and numerical simulation // Nanotechnology Perceptions Vol. 9, № 3 (2013), pp. 187–197. 6. *Janos Kundrák, Vladimir Fedorovich, Angelos P. Markopoulos, I. Pyzhov, Natalya Kryukova.* Improvements of the Dressing Process of Super Abrasive Diamond Grinding Wheels / Manufacturing Technology December 2014, Vol. 14, №. 4, pp. 545 – 554. 7. *Kundrák, J. Fedorenko, D.O. Fedorovich, V.O. Fedorenko, E.Y. Ostroverkh, E.V.* Porous diamond grinding wheels on ceramic binders: Design and manufacturing/ Manufacturing Technology 2019, Vol. 19, No. 3, pp. 446-454. 8. *Rakin V. I.* Morphology of artificial diamonds / V. I. Rakin, N. N. Piskunova // News of the Komi Scientific Center of the Ural Branch of the Russian Academy of Sciences (Syktyvkar). – 2012, Issue 3 (11), pp. 61–67. 9. *Bogatyрева G.P.* Impurities and inclusions in powders of synthetic diamonds of grades AC4 and AC6 / G.P. Bogatyreva, V.M. Maevsky, G. D. Ilitskaya et al. // Superhard materials. – 2006, №. 4, pp. 62–69. 10. To the question of the mechanism of softening of synthetic diamond crystals under high-temperature heating / A.L. Maistrenko, A.I. Borimsky, L.N. Devin et al. // Rock-cutting and metal-working tools - machines and technology of its manufacture and application: collection of scientific articles – Kyiv: ISM named by V.M. Bakul National Academy of Sciences of Ukraine, 2010, Issue. 13, pp. 272–279. 11. Principles of 3D modeling of the production and application of diamond composite materials / A. G. Mamalis, A. I. Grabchenko, V. I. Fedorovich et al. // Nanotechnology perception. – Basel: Institute of advanced study. – 2012, pp. 132–139. 12. *Reznikov A. N.* Abrasive and diamond processing of materials: Handbook / A. N. Reznikov, E. I. Aleksentsev, Y. I. Barats and others; ed. A.N. Reznikov, Moscow: Mashinostroenie, 1977 — 391 p. 13. *Yakimov A.V.* Thermophysics of mechanical processing / A.V. Yakimov, P.T. Slobodyanik, A.V. Usov, Kyiv–Odessa: Lybid, 1991 — 239 p. 14. *A.A. Burenin* Formation of the residual stress field under conditions of local thermal action / A. A. Burenin, E. P. Dats, E. V. Murashkin // Bulletin of the Russian Academy of Sciences. Rigid Body Mechanics, 2014, No. 2, pp. 124-131. 15. Physical properties of diamond: handbook / ed. N.V. Novikova, Kyiv: Naukova Dumka, 1987, 188 p. 16. Synthetic SVD diamond. [Electronic resource], Access: <http://www.efcvd.com/cvd/page.jsp?pageid=349#2>. 17. The Element Six CVD Diamond Handbook, Ascot (UK): Element Six, 2015 – 27 p. 18. Optimal solutions in metalworking: monograph / F. V. Novikov, V. A. Zhovtobryukh, G. V. Novikov. - Dnipro: LIRA, 2017 -- 476 p. 19. *Balykov A. V.* Modeling the work of a single diamond grain / A. V. Balykov, G. A. Mashkov, A. A. Korzakov // Bulletin of MSTU "Stankin". – 2009, No. 1, pp. 30–34. 20. *Kozakova N.V.* Quality management of diamond wheels at the stages of their manufacture and operation / N. V. Kozakova, V. V. Rusanov, I. A. Kalita // Visoki tehnologiji v mashinobuduvanni. Collection of scientific works. – 2009, No. 1, pp. 194–202. 21. *Kalafatova L.P.* The effect of cooling on the temperature and force parameters of the grinding process, as well as on the surface quality of sitals under various cutting conditions / L. P. Kalafatova, S. A. Poezd // Reliability of the tool and optimization of technological systems. 2008, Issue 23,

pp. 194–201. **22.** Babenko E.O. Improving the efficiency of diamond wheels on polymer and ceramic bonds: autoref. dis... Cand. Sc. 05.03.01 – "Processes of mechanical processing, machines and tools" / E. O. Babenko. —Kharkiv, 2014, 21 p.

Володимир Федорович, Дмитро Федоренко,  
Іван Пижов, Євгеній Островерх, Харків, Україна

## **МОДЕЛЮВАННЯ ВПЛИВУ МЕТАЛОФАЗИ В АЛМАЗНИХ ЗЕРНАХ НА САМОЗАТОЧУВАНІСТЬ ШЛІФУВАЛЬНИХ КРУГІВ НА КЕРАМІЧНИХ ЗВ'ЯЗКАХ**

**Анотація.** В останні роки на основі методу кінцевих елементів (МКЕ) розроблено ряд програмних пакетів зі ще більш розширеними можливостями. До них в першу чергу відносяться SIMULA Abaqus, SolidWorks Simulation, ANSYS та LS-Dyna. Їх використання для проведення імітаційних експериментів по розробленим моделям дає можливість значного скорочення об'єму коштовних верстатних досліджень. В світовій практиці одним з найперспективніших підходів до удосконалення процесів обробки алмазно-абразивним інструментом є такий, що базується на створенні передумов для реалізації потрібних, стосовно конкретних умов обробки, механізмів самозаточування алмазних зерен (АЗ) і алмазоносного шару в цілому. А для цього треба знати фізику процесів, які відбуваються як в алмазних зернах зокрема, так і в системі шліфування в цілому. При створенні моделей враховували форму, розміри і властивості її елементів, які розглядали пружними суцільними тілами. Оскільки найпоширенішою формою кристалів алмазу вважається октаєдр, АЗ приймали з його геометрією. Розміри зерен варіювали відповідно зернистості алмазів. Локальні включення металофази в АЗ створювали у вигляді довільно орієнтованих паралелепіпедів, об'ємний вміст яких задавався в залежності від марки зерна. Зв'язку відтворювали у вигляді призматичних фрагментів з розмірами, в залежності від розмірів і концентрації зерен в алмазоносному шарі. В об'ємі зв'язки в довільному порядку розміщували посадочні поверхні під зерна, кількість яких варіювали в залежності від концентрації алмазів, яку задавали як процентне відношення об'єму зв'язки і загального об'єму АЗ. Встановлено, що визначальним фактором появи критичних напружень при шліфуванні є температура в зоні різання, збільшення якої за наявності включень в АЗ металофази з високим КТР призводить до виникнення руйнуючих напружень в зернах і, як наслідок, їх передчасного руйнування. Доцільним є застосування АЗ з мінімальним вмістом металофази та використання при виробуванні синтетичних алмазів металів-розчинників з низьким КТР, що дозволить значно збільшити коефіцієнт використання АЗ. В іншому випадку слід здійснювати примусове охолодження зони шліфування.

**Ключові слова:** алмазний круг; оброблюваний матеріал; алмазне зерно; металофаза; зв'язка круга; напружено-деформований стан; метод кінцевих елементів; еквівалентні напруження; самозаточуваність; режими шліфування.

A. Chumak, S. Klimenko, S. Klimenko, A. Manokhin,  
A. Naydenko, M. Kopeikina, V. Burikin, Kyiv, Ukraine,  
M. Bondarenko, Cherkasy, Ukraine, V. Burlakov, Mariupol, Ukraine

## **FINISH MACHINING OF THE CUTTING INSERTS FROM CUBIC BORON NITRIDE BL GROUP COMPOSITE**

**Abstract.** *Finishing methods of machining of superhard composite's working elements based on cubic boron nitride BL group are considered. The results of the microgeometry formation research of the cutting inserts' surfaces during machining by free powders of synthetic diamond, grinding wheels and a method of vibro-magnetic-abrasive machining (VMAM) are presented. It is shown that during VMAM the friction between the inserts' surfaces and the abrasive particles result in microremoval of the material, which reduces the roughness of the cutting inserts' surfaces. It is established that additional fine grinding with 14/10 mkm synthetic diamond powder provides the absence of microgeometry defects of the cutting inserts' surfaces left by pre-machining. The result of high-quality rounding of cutting edges and the formation of surfaces of cutting inserts with less roughness is an increase in strength and wear resistance of metal-cutting tools in high-speed machining under conditions of significant loads.*

**Keywords:** *diamond machining; vibro-magnetic-abrasive machining; cutting inserts; CBN; surface roughness; friction forces.*

### **1. INTRODUCTION**

The development of modern mechanical engineering is associated with the creation and implementation of new materials and advanced technological processes of their machining. The unique properties of polycrystalline composites based on cubic boron nitride (CBN) allow their use in various fields of technology, including cutting tools, loaded parts of machines, devices, electronic equipment. Due to the high level of hardness of the products formation from such composites it is possible only with the use of technologies that use tools made of synthetic diamonds. Improving the superhard composites machining is associated with the study of the regularity of a complex multifactorial grinding process. At the same time, a significant limitation of machining efficiency is insufficient scientific substantiation of its finishing processes - grinding, finishing, polishing, conditions of lubricants and coolants application in conjunction with the strength and performance characteristics of the machined surface of the products [1].

One of the main reasons for failure of cutting CBN inserts is chipping of cutting edges, which is caused by exceeding the allowable values of stresses in the wedge of the tool [2, 3]. The studies show that rounding the cutting edges on tools of any material can significantly (from 2 to 8 times) increase the stability and

reliability of tools, improve the quality of products machined surfaces [4]. At present, diamond-abrasive machining technologies - grinding, finishing, vibro abrasive machining - are used to form replaceable multifaceted cutting inserts with given geometric parameters [5].

In vibro abrasive machining, the formation of the surfaces of the machined product is carried out by simultaneous chipping, abrasion and microcutting of the allowance fragments. The working tool in this process is an abrasive mix, which includes abrasive powder (with the addition of synthetic diamond powder) and abrasive granules. The components of the mix move under the influence of vibrations in the working chamber of the device. Chipping occurs when single peaks of grains from the abrasive mix collide with the product, abrasion occurs at relative mutual, almost parallel, movement of the product and elements of the abrasive mix, microcutting is accompanied by removal of the thinnest layers of material from the product surfaces. In addition, the vibro-abrasive machining is characterized by the impact stress on the workpiece, which can increase the defect of the machined surfaces.

To improve the productivity of the machining process and the quality of the machined surface is possible by using into the working area components that will add more elastic component to the working, such as replacing abrasive powder in the mix with ferromagnetic abrasive powder and applying a magnetic field to the machining area [6]. In this case, the magnetic field is used as a bond of the abrasive environment, and the vibration provides a gradual movement of the workpiece together with the abrasive granules through this environment, providing the forming process. Thus, the machining will take place with less intense chipping and the impact stress, but with more intensive abrasive machining and microcutting of the allowance. Machined surfaces of products, especially of brittle materials, such as CBN *BL* group, after such machining do not have microcracks and streaks which are characteristic to the conventional methods of abrasive machining.

Synthetic diamond particles will be contained in the irregularities of the abrasive granules and between the particles of ferromagnetic powder, and thus will be able to participate in the machining process, increasing its productivity.

Given the above, a new method of finishing abrasive machining-vibro-magnetic abrasive machining (VMAM), which involves abrasive removal of the allowance in the presence of a magnetic field with relative movement of abrasive grains and machined products due to forced vibrations in the machining area [7]. Machining is performed using various abrasive mixes, which include abrasive powders (synthetic diamond powders), alumina granules, ferromagnetic abrasive powders.

VMAM allows to form and control the surface roughness of composite products that have high mechanical properties and are non-magnetic, such as

cutting inserts with CBN, while increasing the productivity of finishing and the ability to form some special areas, such as rounding radii of cutting edges.

Magnetic abrasive powder is located between the poles of the electromagnet, forming an elastic environment. Thus, the magnetic field, creating elastic columns of single grains of ferromagnetic abrasive powder, acts as a bond of the tool. The elasticity degree of this bond is regulated by the change in magnetic field strength according to the different stages of machining. Thus, VMAM can approach grinding with free or bound abrasive, allowing you to take advantage of the first or second type of machining in one work cycle.

The movement of the workpieces relative to the columns of the magnetic abrasive tool is created by the vibration of the equipment working chamber, which houses the workpieces and the abrasive mix.

The goal of the presented work is to study the roughness of the surfaces of CBN *BL* group cutting inserts after additional machining by low-grain diamond powder based tools and vibro-magnetic-abrasive machining.

## 2. RESEARCH METHODS

The planes grinding of CBN cutting inserts was performed by powders of synthetic diamond «AC6» 160/125, 80/63, «ACM» 40/28, 28/20, 14/10 on cast iron grinders. The machining of inserts' back surfaces was performed by grinding wheels 1A1 300×126×40×5 AC6 80 / 63-4 B2-01 and 1A1 300×126×40×5 «ACM» 40 / 28-4 B2-01.

A special device [8] was made for performing experimental work with VMAM (Fig. 1).

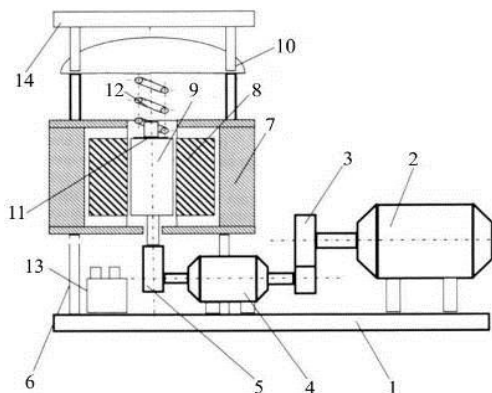


Figure 1 – The VMAM device scheme

The base of the device is the frame 1, on which the electric motor KD-50 is mounted ( $n = 2780$  rpm, 50 W) 2, lowering gear (oscillation frequency  $\sim 25$  Hz) 3, bearing unit 4, which is the support of the shaft of the eccentric vibratory drive (oscillations amplitude 4 mm) 5. On the racks 6 above the vibratory drive is a housing 7 with a stator 8 of a three-phase electric motor that creates a magnetic field. In the housing, in the inner space of the stator, there is a working chamber 9 for workpieces and abrasive mix. A cap 10 is fixed above the container and the stator. A spring 12 is inserted between the cap and the container cover 11, which provides the vibration of the working chamber. Power supply is carried out through the input circuit breakers 13. Above the cap is a fan 14 to cool the stator.

Given the high mechanical characteristics of CBN, the process of cutting inserts machining takes place in a container made of silicon carbide  $SiC$ , which provides its high wear resistance and eliminates the possibility of shielding the magnetic field. As the components of the abrasive mix ( $125 \text{ mm}^3$ ) were used electrocorundum granules  $Al_2O_3$ , «AC6» 28/20 synthetic diamond powder (in the amount of 15% of the total volume of the mix) and the «Feromap» ferromagnetic powder 200/100. 10 inserts were machined simultaneously. The processing time was 40; 120; 180; 360 min. The amount of removed material was estimated by weighing the inserts after the machining.

The CBN cutting inserts RNMN 070300 (CBN  $BL$  group 45–55%, TiC) were used as machined inserts.

The study of the microrelief of the CBN inserts surfaces was performed using the atomic-force microscope NT-206, which allowed to obtain microroughnesses profilograms, surfaces topograms and distribution of conditional (lateral) frictional forces (between the atomic-force microscope indenter and the studied surface) on the surface area  $S_{nom} = 169 \text{ mkm}^2$ . Analysis of microroughness profiles allowed to establish the arithmetic average ( $Ra$ ) and statistical average ( $Rq$ ) values of the of the microroughness profile ordinates deviation on the workpieces surface from the average line, as well as the maximum height of profile irregularities ( $Rmax$ ), total surface area ( $S_{fact}$ ) and surface evolution coefficient  $k = \pm S_{nom}/S_{fact}$ . The absolute estimates error was:  $\pm 0.002 \text{ mkm}$ .

Parameters of roughness and mechanical stresses of the machined surfaces measurement was performed at control points (area of  $13 \times 13 \text{ mkm}$ ) on the surface of the workpiece using also profilograph-profilometer *SurfTest SJ-201*. According to the distribution of lateral forces along the surface of the workpiece, which indirectly (in nominal units) allows to establish the distribution of friction forces  $\sigma$ .

Workpieces were pressed into plastic materials such as aluminum or copper wire and then the imprint was analyzed with an optical microscope to determine the cutting edge radius of the CBN inserts after VMAM.

### **3. RESEARCH RESULTS**

According to the technical conditions for CBN cutting tools, the working surface roughness parameter  $Ra$  should not exceed: front surface – 0.16 mkm, rear surface – 0.20 mkm, support surface – 0.40 mkm.

Based on the abovementioned, the processes of forming high-quality working surfaces of CBN cutting inserts should be given special attention to additional finishing.

Additional finishing of CBN  $BL$  group cutting inserts was performed by working surfaces grinding on front and back planes by powder of synthetic diamond «ACM» 14/10. The results of topographic studies and lateral friction forces for the CBN insert's unpolished surface are given in a Table 1. The scanning results, topographic studies and lateral friction forces for the CBN insert's polished surface are shown in Fig. 3, Table 2.

Table 1 – The topographic parameter values of the CBN insert's unpolished surface

A point number	$Ra$ , nm	$Rq$ , nm	$\sigma$ , c.u.
1	388	509	1200
2	275	336	5550
3	326	396	8800
4	393	460	9100

Table 2 – The topographic parameter values of the CBN insert's polished surface

A point number	$Ra$ , nm	$Rq$ , nm	$\sigma$ , c.u.
1	255	294	2000
2	232	257	2880
3	210	243	2000
4	209	254	5500
5	317	367	2160
6	264	367	4100

Table 3 – The topographic parameters values of the CBN insert's rear surface

A point number	$Ra$ , nm	$Rq$ , nm	$\sigma$ , c.u.
1	41	62	2100
2	141	162	9200
3	80	95	8500
4	75	94	2500

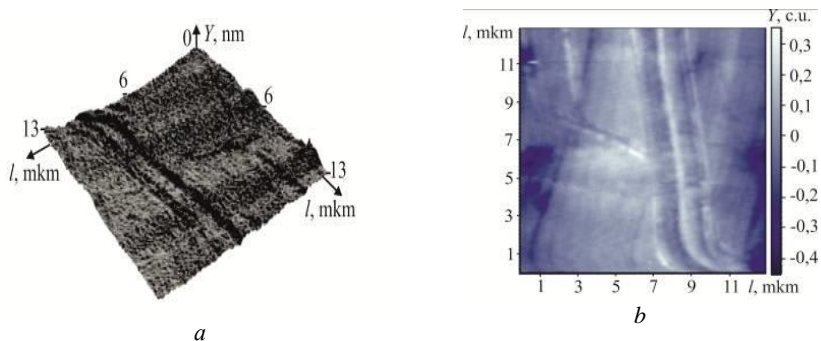


Figure 2 – The results of scanning the polished CBN insert’s profile:  
*a* – area’s surface 3D image; *b* – distribution of lateral friction forces

The study of topography on the rear surface and lateral friction forces at the control points of polished cutting inserts was also researched (Fig. 3, Table 3).

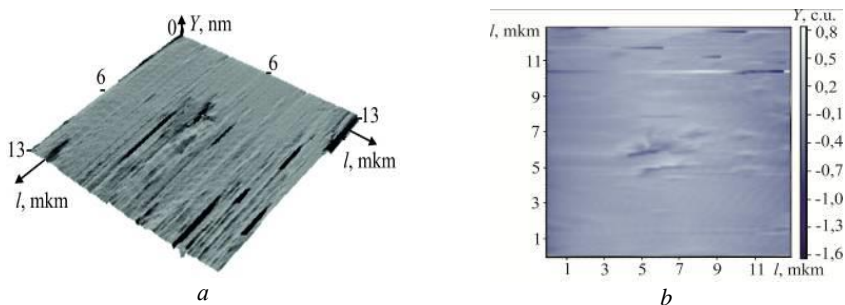


Figure 3 – The topographic research of the rear surface’s cutting insert:  
*a* – area’s surface 3D image; *b* – distribution of lateral friction forces

Analyzing the available data, it can be noted that for both unpolished and polished CBN *BL* group cutting inserts, areas with different roughness and appearance of micro-irregularities and, accordingly, with different degrees of friction force distribution are characteristic. It is determined that the value of microroughnesses for the polished surface is in the range  $Ra$  209–317 nm,  $Rq$  243–367 nm. The distribution of conditional friction forces on the inserts’ surface is in the range: 2000–5500 c.u. for polished base and 1200–9100 c.u. for unpolished base.

3D images of the cutting plate surface (Fig. 2, *a*) after grinding by synthetic diamond powder «AC6» 160/125 on the surface were analyzed. It is possible to note the presence of individual material breaks, grinding lines, dents and craters of different shapes and sizes. At the control points (Fig. 2, *a*) the topography of the surface is represented by sharp grinding lines, which indicates the instability of the machining process, which is due to the diamond powder particles heterogeneity in size and strength. The existence of such defects does not have a significant effect on the friction force distribution on the insert's surface (Fig. 2, *b*), which is due to the small size of the defects.

Surface defects have a slightly different appearance, namely the appearance of craters with a smooth surface and smooth transitions, which is due to the action of temperatures in the contact area of the machined surface and the grinding tool. Such defects have a significant area and affect the friction distribution on the insert's surface.

When using a tool with CBN cutting inserts, especially at high cutting speeds, the presence of such defects on working surfaces can significantly affect its stability, as in such areas the stresses can be localized, sufficient to generate microcracks and other microdefects that contribute to the cutting inserts' destruction.

The topography of the surface of the cutting inserts after additional grinding has a different look. It is mainly represented by the remnants of the grinding lines, the surface is devoid of sharp peaks, and the grinding lines themselves have the form of small depressions with smooth transitions. In some areas of the inserts it was possible to obtain surfaces on which defects in the form of craters are completely absent.

Additional grinding of cutting inserts' surfaces with «ACM» 14/10 synthetic diamond powder allows to improve the friction force distribution. Additional finishing of the inserts on the back surface with a diamond wheel with «ACM» 14/10 diamond powder allowed to significantly reduce the surface roughness but not its defectiveness (Fig. 4, *a*). The topography of the surface is mainly represented by craters of significant depth (Fig. 4, *b*). A possible explanation for this nature of the change in the rear surface topography is the imperfect technology of polishing, especially for the radial cutting inserts.

VMAM of cutting inserts was performed after their machining by diamond grinding. It should be noted that after diamond machining on the surface may appear some defects in the form of grooves, the removal of which with VMAM is impossible.

In the profilogram (Fig. 4, *a*) a roughness ( $Ra$  0.250) of the cutting inserts' surface after grinding was shown (Table 4). On the machined surface there are no sharp transitions between depressions and peaks, and last ones are dominated (Fig. 4, *b*). The machined surface is smooth and has no abnormal defects.

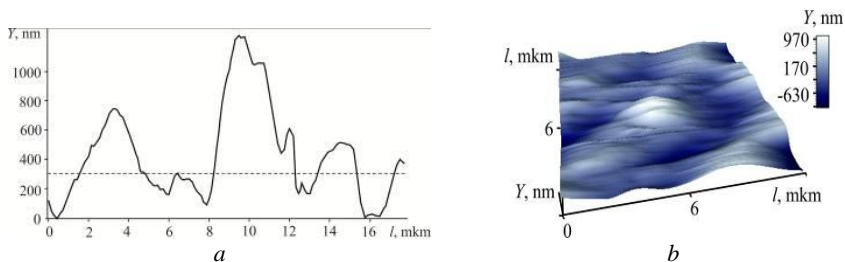


Figure 4 – The profilogram (a) and the surface area’s 3D image (b) of the cutting insert after diamond grinding

Table 4 – Parameters of roughness of the machined surfaces of the CBN’s cutting inserts

Method and time of machining	Values of surface parameters			
	$Ra$ , mkm	$Rq$ , mkm	$S$ , mkm <sup>2</sup>	$k$
Grinding	0.250	0.302	0.168	–
VMAM 40 min	0.225	0.303	0.181	0.933
VMAM 120 min	0.204	0.253	0.181	0.994
VMAM 180 min	0.197	0.253	0.170	0.994
VMAM 360 min	0.195	0.232	0.172	0.982

In Fig. 5 the relief of the surface and the distribution of the lateral friction forces’ average values (Fig. 5, b) were shown. Lighter fragments correspond to a greater value of the force.

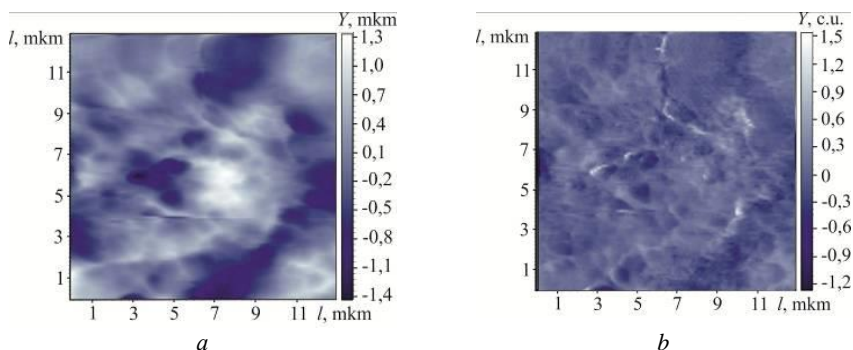


Figure 5 – The relief (a) and distribution of conditional friction forces on the insert’s surface (b) after diamond grinding

The distribution of the conditional friction forces’ values (Fig. 5, b) on the insert’s surface processed with diamond grinding indicates that there are some

defects with increased friction resistance compared to the average values on the surface (white dots and spots). These defects are caused by the presence on the surface of irregularities that exceed the average values or the adhesion of other materials that accidentally hit the surface of the plate. The presence of such defects allows us to conclude that the coefficient of friction at the micro level is not constant and in the process of using cutting inserts may vary depending on which part of its surface is in contact with chips at the moment.

In the first 40 minutes of VMAM is the most intensive removal of the allowance material from the cutting insert, accompanied by changing the roughness of the machined surface (Fig. 6, *a, b*, table. 4).

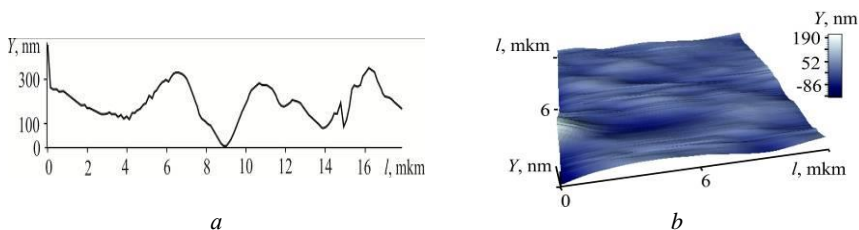


Figure 6 – The profilogram surface (*a*) and the area’s 3D image (*b*) of the cutting insert after 40 min of VMAM

The analysis of the obtained results shows that the VMAM process most intensively affects the vertices of microroughnesses, reducing their height parameters. It can be concluded that according to the decreasing of the surface evolution coefficient  $k$  depressions are predominant.

The distribution of the conditional friction forces’ values (Fig. 7, *b*) on the cutting insert’s surface after 40 min of VMAM indicates that there are almost no surface defects, as well as sharp transitions between depressions and peaks of microroughnesses. The peaks of the micro-irregularities are devoid of sharp peaks and have a flat character.

After 120 minutes of VMAM the machined surface is characterized by the roughness’ decreasing (Table 4). And there is a balance of values between the height of the peaks and the depth of the depressions of the microroughness on the machined surface, as evident by the value of the surface evolution coefficient  $k$ , which is close to one.

On the further evolution of the surface state after VMAM for 120 min can be judged by the image of the relief and the distribution of conditional friction forces on the machined surface (Fig. 8). As a result of machining the surface with smooth transitions between peaks and depressions and with the minimum number of defective zones with the increased degree of resistance to friction is formed.

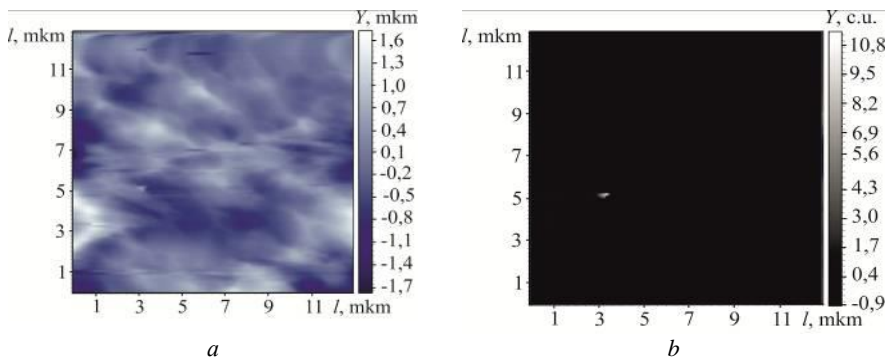


Figure 7 – Relief (a) and distribution of conditional friction forces on the insert's surface (b) after 40 min of VMAM

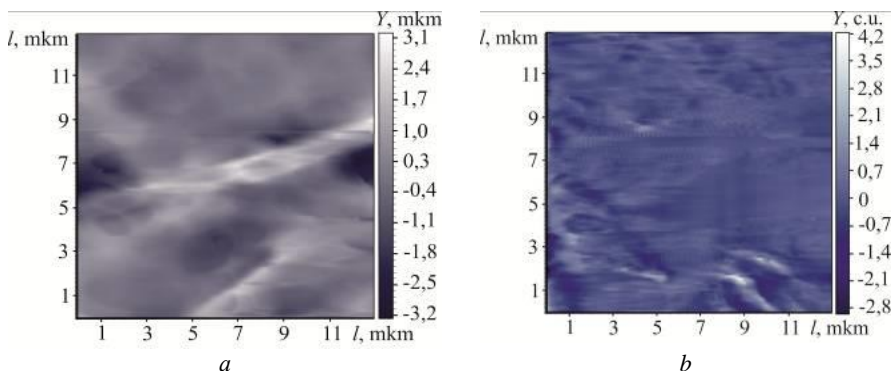


Figure 8 – Relief (a) and distribution of conditional friction forces on the insert's surface (b) after 120 min of VMAM

The further processing for 180 and 360 min. does not have a significant effect on the roughness of the machined surface (Table 4), which is associated with the destruction of the abrasive grains of the abrasive mix and reduce their cutting ability. It is advisable to renew the abrasive mix every 120 minutes to achieve a more intense change in the inserts' surface roughness.

The microroughnesses' height on the machined surface and the magnitude of the radius of the CBN insert's cutting edge curvature change asymptotically during machining (Fig. 9, a).

The roughness of the machined surface of the CBN cutting inserts was decreased as a result of VMAM. The shape of the relief corresponded to the relief

of the surface during the fatigue breaking, which leads to the removal of separate CBN's particles, as well as smoothing of separate grooves left during pre-machining. The fatigue breaking of the material in the machining area at VMAM occurs under the action of cyclic alternating loads, which are perceived by local areas of the machined surface when interacting with the components of the abrasive mix.

The fatigue mechanism of destruction at VMAM is realized in two stages: 1<sup>st</sup> – gradual accumulation of defects in a surface layer of the machined insert without visible destruction of the material; 2<sup>nd</sup> – after reaching a certain concentration of microdamages in the surface layer of the machined insert; there is a rapid destruction with the wear particles formation.

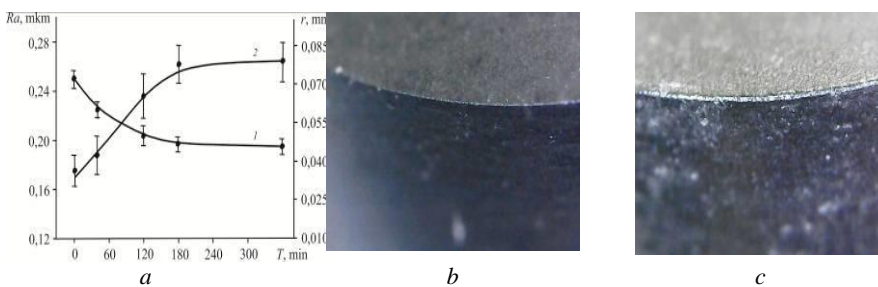


Figure 9 – The dependence of the microroughnesses' height of the machined surface (1) and the radius of the cutting edge (2) of the CBN cutting insert on the VMAM time (a), the cutting edge before finishing (b) and after 240 min of VMAM (c)

Rounding of edges ( $r$ ) for the CBN cutting inserts is one of the main factors for increase of durability of tools at high-speed machining, and also at impact machining. During VMAM, the cutting inserts are most intensively machined in the area where the surfaces of the inserts are connected, which is due to their lower geometric strength, as well as the higher frequency of micro-impacts of the abrasive particles of the mix on the edge rather than on flat surfaces. Machining time and components of an abrasive mix depend on surface's initial roughness during VMAM. It is possible to receive the cutting edges radius  $r$  from 10 to 50 microns. The cutting edge after VMAM has the correct geometric shape along the entire length with a smooth junction of front and rear surfaces (Fig. 9, b, c).

Based on the dependence presented in Fig. 10, a, the kinetics of rounding the edges of the CBN cutting inserts can be divided into three stages depending on the processing time: – 1<sup>st</sup> stage (0–40 min.) has a slight change in the cutting edge radius, as the fatigue breaking is the main mechanism, which is characterized by the presence of a certain time during which the surface layer of the cutting insert

increases the concentration of defects under the action of the abrasive environment to a certain critical level, after which the material is removed; – 2<sup>nd</sup> stage (40–180 min.) characterized by an intensive removal of the material and, as a consequence, an increase in the cutting edge radius due to the high concentration of surface defects; – at 3<sup>rd</sup> stage (180–360 min.) the radius of the edge almost does not change, which means that the process of material removal during VMAM at this time interval practically does not occur because the abrasive mix is no longer able to press a significant impact load on the machined surface due to great wear of abrasive particles, as well as the strengthening of the insert's surface layer as a result of machining.

Due to the cutting edges rounding, increased rounding of the tops of cutting inserts, reduced roughness of the insert's surfaces, the use of VMAM increases the strength and wear resistance of turning and milling tools which are operating in hard load conditions – discontinuous cutting, medium and large feeds, uneven allowance.

#### **4. SUMMARY**

The additional grinding of the surfaces of the CBN *BL* group cutting inserts by the powder of synthetic diamond “ACM” 14/10 provides the reduction of the lateral wear force on the insert's working surfaces (2000–5500 c.u. for grinding surfaces and 1200–9100 c.u. for a finished surface). Also a change in the topography of the surface occurs – there are no defects like the sharp peaks and craters, which appeared after previous machining in connection with which the wear force distribution has much more uniform character.

VMAM of the CBN *BL* group cutting inserts is an effective finishing operation. The abrasive environment is clinging to the insert's surfaces during the machining in the magnetic field, and due to the vibration effect, the process of friction between the inserts' surfaces and the abrasive environment, resulting in micro-removal of the material, which reduces the roughness of the machined surfaces of the cutting inserts. The cutting edges' radius size of the CBN inserts can be controlled by changing the parameters of VMAM in accordance with the conditions of further operation of tools with such cutting inserts.

The cutting edge after VMAM has the correct geometrical form along entire length with smooth junction of front and rear surfaces.

**References:** 1. *Instrumenty iz sverkhтверdykh materialov / pod red. N.V. Novikova, S. A. Klimenko.* – Moscow: Mashinostroyeniye, 2014. – 608 p. 2. *V.O. Trilisskiy, G.S. Bol'shakov, A.V. Lipov, Ye. N. Yarmolenko.* Finishnaya obrabotka smennykh mnogogrannykh plastin s tsentral'nymi otverstiyami. *Izvestiya VUZ. Povolzhskiy region. Tekhnicheskkiye nauki.* – 2010. – № 2 (14). – pp. 131–137. 3. *Burykin, V.V.* Obrabotka detaley tortsevoy frezoy, osnashchennoy polikristallicheskimi sverkhтвердыми materialami. *Inzheneriya poverkhnosti i renovatsiya izdeliy: mat. mezhdunarod. nauch.-tekhn. konf.,* 20–24.05.2019, g. Svalyava. – Kyiv: ATMU, 2019. – pp. 25–29.

4. A. S. Manokhin, S. A. Klimenko, S. An. Klimenko, V. M. Beresnev. Perspektivnyye tipy pokrytiy dlya instrumentov, osnashchennykh polikristallicheskim KNB. Nadtverdi materiali. – 2018. – № 6. – pp. 78–88. 5. V.M. Gakh. Vibrobrazivnaya obrabotka tverdosplavnogo instrumenta. Kramatorsk: DGMA, 2009. – 220 p. 6. L.M. Akulovich, L.Ye. Sergeyev. Tekhnologiya i oborudovaniye magnitno-abrazivnoy obrabotki metallicheskih poverkhnostey razlichnogo profilya. – Minsk: BGATU, 2013. – 372 p. 7. S.An. Klimenko, A.O. Chumak. Vibro-magnitna-abrazivna obrobka rízal'nikh plastin íz PKNB. Nadtverdi, kompozitsiyni materiali ta pokrityya: otrimannya, vlastivosti, zastosuvannya: tezi mizhnarod. nauk.-tekhn. konf., 28–29.05.2020, m. Kyiv: ÍNM NAN Ukraïni, 2020. – pp. 7–8. 8. S. A. Klimenko, V. Í. Burlakov, Yu. Ye. Rizhov ta ín. Patent Ukraïni na korisnu model' № 143357. Sposib obrobki bagatogrannikh plastin z nadtverdoï keramiki // Byul. «Promislova vlasnist'». – 2020. – № 14.

Анатолій Чумак, Сергій Клименко, Сергій Клименко, Андрій Манохін,  
Андрій Найдено, Марина Копейкіна, Віталій Бурикін, Київ, Україна,  
Максим Бондаренко, Черкаси, Україна,  
Віктор Бурлаков, Маріуполь, Україна

### **ФІНІШНА ОБРОБКА РІЗАЛЬНИХ ПЛАСТИН З КОМПЗИТУ НА ОСНОВІ КУБІЧНОГО НІТРИДУ БОРУ ГРУПИ BL**

**Анотація.** Розглянуті фінішні методи обробки робочих елементів з надтвердого композиту на основі кубічного нітриду бору групи BL (CBN(45–55 об.%)–TiC). Наведені результати досліджень формування мікрогеометрії поверхні різальних пластин при обробці вільними порошками синтетичного алмазу, шліфувальними кругами та методом вібро-магнітно-абразивної обробки (ВМАО). Розроблено схему та сконструйовано пристрій для практичної реалізації процесу ВМАО різальних пластин, що включає контейнер для оброблюваних пластин, вібраційну систему і пристрій для створення електромагнітного поля. Встановлено, що додаткове тонке шліфування поверхонь різальних пластин порошком синтетичного алмазу АСМ 14/10 дозволяє покращити розподіл латеральних сил тертя по робочих поверхнях пластин та при забезпечує відсутність дефектів у вигляді гострих вершин та кратерів, залишених попередньою обробкою. Показано, що в процесі обробки ВМАО різальних пластин, завдяки магнітному полю та вібраційному впливу здійснюється процес тертя між поверхнями пластин та абразивним середовищем, в наслідок чого відбувається мікровидалення матеріалу, що веде до зменшення шорсткості оброблених поверхонь пластин та забезпечує потрібне заокруглення різальної кромки, яка має правильну геометричну форму по всій довжині з плавним сполученням передньої та задньої поверхонь. Результатом якісного заокруглення різальних кромок та формування поверхонь різальних пластин з меншою шорсткістю є підвищення міцності та зносостійкості металорізального інструменту при високошвидкісній обробці деталей в умовах значних термобаричних навантажень.

**Ключові слова:** алмазна обробка; вібро-магнітно-абразивна обробка; різальні пластини; CBN; шорсткість поверхні; сили тертя.

A. Yakimov, L. Bovnegra, V. Tonkonogyi,  
V. Vaysman, V. Strelbitskiy, I. Sinko, Odessa, Ukraine

## **INFLUENCE OF THE GEOMETRIC CHARACTERISTICS OF THE DISCONTINUOUS PROFILE WORKING SURFACES OF ABRASIVE WHEELS FOR PRECISION AND TEMPERATURE WHEN GRINDING**

**Abstract.** *Grinding is the most common finishing method for hardened steel parts. Grinding is accompanied by a large heat release in the cutting area, under the influence of which structural changes appear in the thin surface of the processed parts, tensile stress and even microcracks, which significantly reduce the operational reliability of machines that include these parts. The use of abrasive wheels with an intermittent working surface makes it possible to reduce the temperature in the area of contact of abrasive grains with the material of the workpiece and, as a consequence, stabilize the quality of the surface layer of the workpieces. High-frequency vibrations in the elastic system of the machine, accompanying the work of an intermittent wheel, are a positive factor that reduces the energy consumption of the grinding process. However, under certain conditions of dynamic interaction of the tool with the workpiece, parametric resonance may occur, which worsens the geometric and physical-mechanical parameters of the quality of the surface layer of the processed part. The aim of the work is to realize the possibility of predicting the quality parameters of the surface layer of parts during intermittent grinding by studying the influence of the design features of the macrotopography of the working surface of abrasive wheels and processing modes on the nature of the dynamic interaction of the tool with the workpiece and the heat stress in the cutting area. It was found that the parametric vibrations of the elastic system of the machine tool can be shifted to a more stable area, due to an increase in the number of interruptions of the working surface of the abrasive wheel with a constant ratio of the length of the protrusions and depressions. The increase in the number of breaks on the wheel also contributes to a decrease in temperature in the cutting area. It was found that to maintain the stable operation of the elastic system of the machine, it is necessary to reduce the number of cavities on the grinding wheel with an increase in the cutting speed. However, both of these actions are accompanied by an increase in the heat stress of the grinding process. It has been experimentally established that for ordinary (pendulum) grinding, it is possible to achieve an increase in processing productivity by increasing the speed of the longitudinal movement of the table.*

**Keywords:** *macrotopography of the working surface; surface roughness; degree of tempering; dynamic interaction; processed material.*

Grinding is the final method of mechanical restoration. High speeds of rotation of grinding wheels make it possible to ensure, with this method of processing, a high accuracy of shape and roughness of surfaces of parts. One of the disadvantages of grinding is its high heat intensity, which can lead to a decrease in the specified physical and mechanical properties of the machined surfaces and, as a result, to a decrease in the durability of the mechanism. One of the reasons for the increase in the heat intensity of the grinding process is a decrease in the cutting

ability of the abrasive wheel due to the smoothing of the microrelief of its working surface and the seizure of the processed material with cutting grains. [1,2,3]. The studies [7,8,9] are devoted to the study of the influence of the shape of abrasive grains on the heat intensity of the grinding process. Despite the difficulties associated with ensuring the required physical and mechanical properties of the machined surfaces during grinding operations, this method of processing continues to be widely used in the industry. From works [10, 11] it is known that annually consumed 240,000 grinding wheels with a diameter of 200-500 tons, used only for flat grinding operations.

From works [12,13,14,15] it is known that the use of abrasive wheels with an intermittent profile can reduce the temperature in the area of their contact with the processed material by 30% or more. A decrease in temperature in the area of cuts of the processed material by abrasive grains occurs due to periodic interruption of the cutting process. [16,17] For the same reason, the cutting process is accompanied by high-frequency oscillations, which facilitate the formation of chips, promote periodic sharpening of cutting grains and, as a result, reduce the energy consumption of the grinding process [18, 19, 20]. However, the periodic interruption of the cutting process associated with the presence of cavities on the grinding wheel leads to inconsistency, rigidity of the technological system, which can lead to the appearance of parametric resonance [21, 22]. Parametric oscillations lead to a cyclic change in the cutting temperature (to cyclic burns on the processed surface) and a decrease in the accuracy of the shape of the ground surfaces [21, 22]. The aim of this work is to study the effect of macrotopography of the working surface of discontinuous-profile wheels and the parameters of processing modes on the dynamics and heat intensity of the grinding process.

Theoretical studies were carried out on the basis of thermal physics of cutting processes and theories of oscillations. Experimental studies were carried out on a 3G71M flat-grinding machine. As the test samples, we used flat rectangular tiles made of 18 khgt steel, 150 mm long, 20 mm wide, and 10 mm high. Grinding was carried out with three abrasive wheels PP 200 x 20 x 76 24A 40 CM2 7 K5, one of which had a continuous working surface. The working surface of the second wheel had 12 evenly distributed straight-profile depressions, the dimensions of which were half the size of the cutting protrusions. On the working surface of the third wheel, there were 30 depressions with the same ratio of the lengths of the projections and depressions. The study of the surface roughness was carried out using the "Profilometer 296" device.

Calculations were performed according to the following formulas:

$$|\Phi| \geq (1 + \Psi) / 2 \quad (1)$$

$$\Phi = \left[ \sin n_1 \cdot \tau_1 \cdot (n_1^2 \cdot \sin n_2 \cdot \tau_2 - n_2^2 \cdot \sin \eta) - 2 \cdot n_1 \cdot n_2 \cdot \cos n_2 \cdot \tau_1 \cdot \cos n_2 \cdot (\tau_1 + \tau_2) \right] \cdot \frac{1}{R + B} \quad (2)$$

$$\psi = n_1 \cdot n_2 \cdot \cos \eta \cdot \frac{1}{R^2 + B} \quad (3)$$

$$\eta = 2 \cdot n_2 \cdot (\tau_1 + \tau_2) \quad (4)$$

$$n_1 = \sqrt{\frac{2 \cdot c_0 + n_0}{2 \cdot m'} - h^2} \quad (5)$$

$$n_2 = \sqrt{\frac{2 \cdot c_0 - n_0}{2 \cdot m'} - h^2} \quad (6)$$

$$B = h \cdot (n_2 + h \cdot \sin 2n_2 \cdot \tau_1) \quad (7)$$

$$R = e^{(t_1 + t_2)} \quad (8)$$

$$n_0 = C_0 \cdot \left( \frac{t_1 - t_2}{t_f} \right) \quad (9)$$

$$\tau_1 = l_1 / W_{kr} \quad (10)$$

$$\tau_2 = l_2 / W_{kr} \quad (11)$$

$$l_1 = \frac{2 \cdot \pi \cdot R_{kr}}{n \cdot (1 + N)} \quad (12)$$

$$l_2 = \frac{2 \cdot \pi \cdot R_{kr}}{n \cdot (1 + N)} \quad (13)$$

$$N = l_2 / l_1 \quad (14)$$

Where:  $\tau_1$  – contact time of the abrasive tool with the processed material, s;  
 $\tau_2$  – time during which there is no interaction of the wheel with the workpiece, s;  
 $l_1$  – gap width of the working surface of the abrasive wheel, m;  
 $l_2$  – distance between two adjacent discontinuities, m;  
 $C_0$  – reduced stiffness of the elastic system of the grinding machine, kg / m;  
 $t_1, t_f$  – theoretical and actual thickness of the workpiece removal in one pass, mm;  
 $W_{kr}, R_{kr}$  – speed (m / s) and radius (m) of the grinding wheel, respectively;  
 $n$  – number of gaps of the same width evenly distributed over the working surface of the abrasive wheel;  
 $m^1$  – is the reduced mass of the wheel,  $(N * S2) / m$ ;  
 $n_0$  – cutting hardness kg / m;  
 $h$  – is the coefficient of damping of oscillations in time.

The results are shown in the figures 1-2.

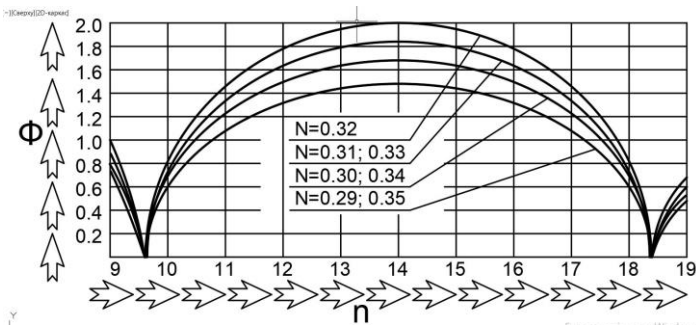


Figure 1 – Dependencies  $\Phi = f(n)$  plotted for different values of  $N$  taken from the interval  $0.29 \leq N \leq 0.35$

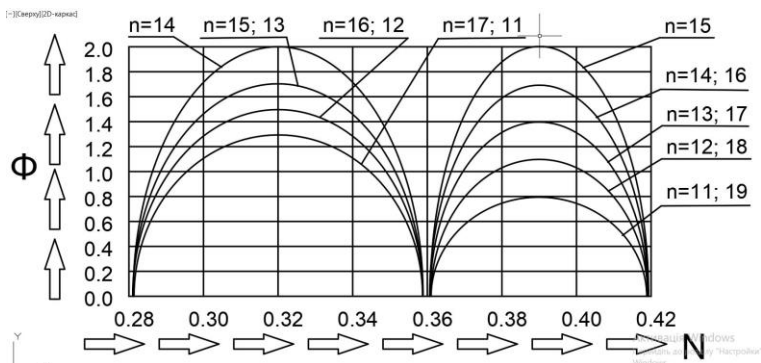


Figure 2 – Dependencies  $\Phi = f(N)$ , plotted for different values of  $n$ , taken from the interval  $11 \leq n \leq 19$

Fig. 1,2 shows the dependence of the left side of inequality (1) on the number of depressions on the working surface of the wheel  $n$  and on the coefficient  $N$ , which shows how many times the width of the depression differs from the length respectively. It can be seen from fig. 1,2 that the dependence  $\Phi = f(n, N)$  is a wavy surface. When this surface is cut by planes parallel to the coordinate plane  $(\Phi, n)$ , semi-ellipses are formed, the major axes of which have the same length, and the sizes of the minor axes depend on the numerical values of the coefficient  $N$ . When cutting the surface  $\Phi = f(n, N)$  by planes parallel to the coordinate plane  $(\Phi, N)$ , semi-ellipses are formed, the minor axes of which have equal dimensions, and the values of the major axes significantly depend on the number of depressions on the working surface of the discontinuous wheel.

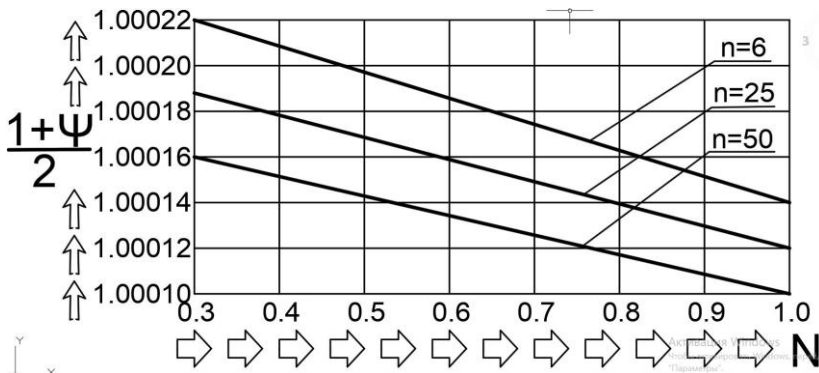


Figure 3 – Dependencies  $(1+\psi)/2=f(N)$  plotted for different values of  $n = 6, 25, 50$

Fig. 3 shows the effect of the geometric parameters of the working surface of the wheel N and n on the right-hand side of inequality (1).

Fig. 3 shows that the dependence  $(1+\psi)/2=f(n, N)$  looks like a plane that can be considered parallel to the coordinate plane  $(n, N)$ . It follows from inequality (1) that the parametric instability of the elastic system of the machine arises when the tops wavy surfaces, described by the graph  $\Phi = f(n, N)$ , protrude above the linear surface described by the graph  $(1+\psi)/2=f(n, N)$

Fig. 4 shows the cut line by the plane  $(1+\psi)/2=f(n, N)$  of one of the surface waves  $\Phi=f(n, N)$ .

The cut line looks like an ellipse, the major axis of which is parallel to the n axis, and the small one is parallel to the N axis.

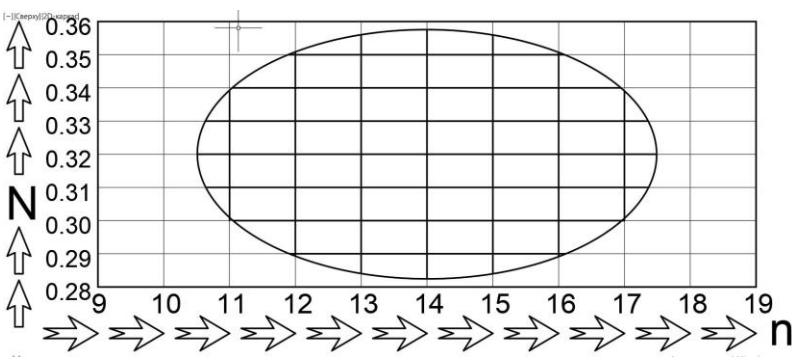


Figure 4 – Line of intersection of a ruled surface  $(1+\psi)/2=f(n, N)$  with a non-ruled surface  $\Phi = f(n, N)$

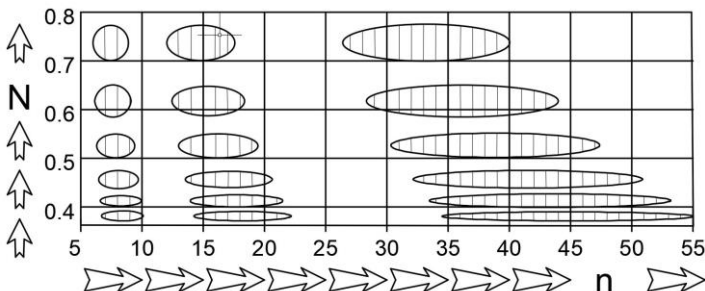


Figure 5 – Ellipse-like lines bounding the regions of parametric instability of the elastic system of the machine

Fig. 5 shows the ellipse-like boundaries of the regions of parametric non-stability of the elastic system of a grinding machine, which represent both lines of intersection of the surface described by the graphs  $(1+\psi \square /2=f(n, N))$  (linear flat surface) and  $\Phi=f(n, N)$  (undulating nonlinear surface).

From analysis of the shape and size of ellipses, built in the coordinate system  $(n, N)$ , limited by the intervals  $0,35 \leq N \leq 0,80; 5 \leq n \leq 55$  it is seen:

- with an increase in the number of ruptures ( $n$ ) of the working surface of an abrasive tool, the areas of unstable operation of the elastic system of the machine are lengthened (the sizes of large axes and ellipses increase; the distance between these areas (areas of stable operation) also increases;

- with an increase in the discontinuity coefficient  $N$ , the parametric non-stability area thickens (the size of the small axes of the ellipses increases). In this case, the distance between two adjacent ellipses also increases;

- a decrease in the discontinuity coefficient  $N$  shifts the area of parametric instability in the region of stable operation of the elastic system of the machine in the direction of large values of the breaking numbers of the working surface of the abrasive wheel.

It follows from everything that in order to ensure the stable operation of the elastic system of the machine, it is necessary to increase their number on the wheel when decreasing the size of the cavity in relation to the cutting protrusion.

For example, with  $N = 0.73$ , stable operation of the elastic system of the machine is provided by two intervals of the number of cutting protrusions:  $9 \leq n \leq 12$  and  $18 \leq n \leq 26$ , and with a decrease in the discontinuity coefficient to  $N = 0.375$ , the intervals of the number of cutting protrusions will change:  $10 \leq n \leq 14$  and  $22 \leq n \leq 34$ .

From fig. 6. it can be seen that an increase in the circumferential speed of the wheel  $W_{kr}$  leads to a shift in the regions of stable operation of the elastic system of

the machine (these areas are shaded) in the direction of a decrease in the number of slots on the working surface of the wheel  $n$ .

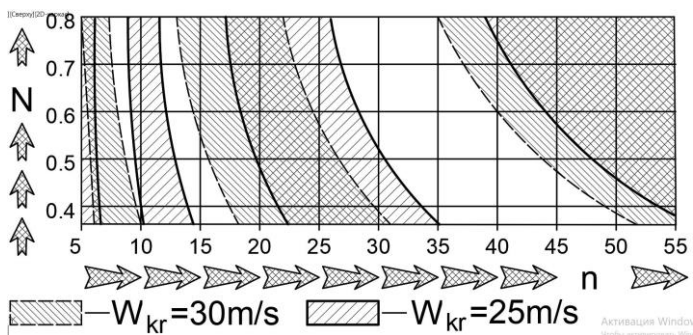


Figure 6 – Displacement of the areas of stable operation of the elastic system of the machine when changing the cutting speed

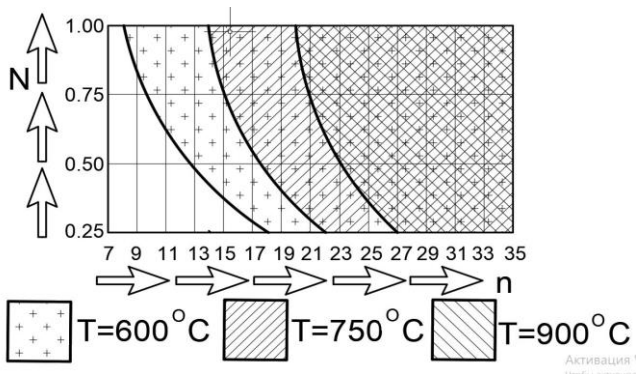


Figure 7 – Displacement of non-cut areas of intermittent grinding when the temperature of continuous grinding changes

Fig 7. three curved lines are shown, each point of which is a set of such geometric parameters of the working surfaces of the abrasive discontinuous wheel, at which the surface temperatures of continuous grinding  $T = 600^{\circ}\text{C}$ ,  $750^{\circ}\text{C}$ ,  $900^{\circ}\text{C}$  decrease to values that do not cause structural and phase transformations. From fig7. it can be seen that the areas of cut-free intermittent grinding with an increase in the temperature of continuous grinding are displaced in the direction of an increase in the number of depressions on the abrasive tool.

Fig. 8 shows the graphical dependence of the tempering degree of the workpiece surface layer on the longitudinal feed of the table of the surface grinding machine is presented. The degree of tempering was determined by the formula:  $N' = (H_m - H'_m) * 100 / H_m$ , where:  $H_m$  is the microhardness of the starting material before grinding, kg / mm<sup>2</sup>;  $H'_m$  - microhardness of the layer lying at a depth of 20-30 mkm after the grinding, kg / mm<sup>2</sup>. Samples of steel 12x2N4A were ground without cooling with a continuous wheel 24A 25 CM2 7 K5 in the following modes:  $W_{kr} = 22$  m / s;  $t = 0.03$  mm;  $W_d = 3$  m / min; 6m / min; 9m / min; 12 m / min ; 15m / min. From fig.8 it can be seen that the degree of tempering of the processed surface decreases with an increase in the longitudinal feed. After grinding flat parts made of 18 KhGT steel with an intermittent wheel, which has 30 cutting projections, and a solid wheel with same characteristics, the roughness heights of the machined surfaces have similar numerical values (fig.9). In other words, as the number of cuts on the discontinuous wheels increases, the surface roughness formed by these wheels approaches the surface roughness obtained by continuous grinding.

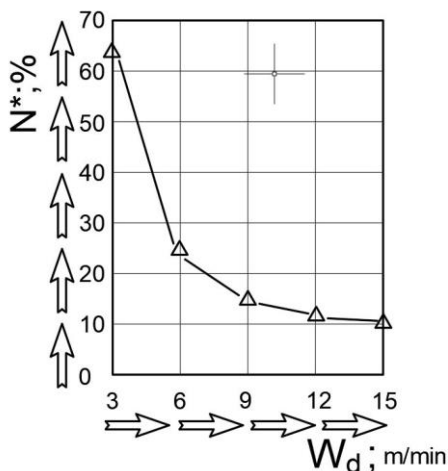


Figure 8 – Displacement of non-cut areas of intermittent grinding when the temperature of continuous grinding changes

Fig. 9 shows the experimental dependencies of the roughness parameter  $R_a$  on the longitudinal feed rate  $W_d$  when grinding flat samples of steel 18 KhGT with solid and two intermittent ( $N = 0.5$ ;  $n = 12$ ;  $n = 30$ ) wheels 24A40 CM 2 7 K 5 at modes:  $W_{kr} = 30$  m / st = 0.025 mm;  $W_d = 3$  m / min; 6 m / min; 9m / min; 12 m / min; 15m / min, without cooling.

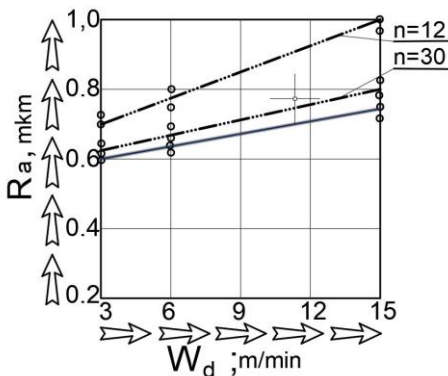


Figure 9 – Dependence of the roughness height of the processed surface on the longitudinal feed rate when grinding with a solid wheel (continuous line) and broken wheels (dash-dot lines)

From fig 9 it can be seen that an increase in the speed of the longitudinal movement of the table of the grinding machine surface leads to an increase in the roughness height of the machined surface. Moreover, the surface formed during grinding with a continuous wheel has a lower roughness in comparison with the surfaces processed by intermittent wheels. With an increase in the number of cutting protrusions on the wheel, the roughness parameter  $R_a$  decreases.

After grinding flat parts made of 18 KhGT steel, an intermittent wheel with 30 cutting projections and a continuous wheel of the same characteristics of the roughness heights of the machined surfaces have similar numerical values (Fig. 9). In other words, as the number of cuts on the discontinuous wheels increases, the surface roughness formed by these wheels approaches the surface roughness obtained by continuous grinding.

### Conclusions.

1. As a result of the research carried out, it became possible to predict the dynamic and thermal phenomena during intermittent grinding, when changing the operating parameters of the processing of the geometric parameters of the macrotopography of the working surface of abrasive wheels.

2. It was found that in order to maintain the stable operation of the elastic system of the machine, it is necessary, with an increase in the cutting speed, to reduce the number of depressions on the grinding wheel. However, both of these actions are accompanied by an increase in the heat stress of the grinding process. It has been experimentally established that for ordinary (pendulum) grinding, it is possible to achieve an increase in processing productivity by increasing the speed of the longitudinal movement of the table.

3. It was found that the parametric vibrations of the elastic system of the machine tool can be shifted to a more stable area by increasing the number of interruptions of the working surface of the abrasive wheel, with a constant ratio of the length of the protrusions and depressions. The increase in the number of breaks on the wheel also contributes to a decrease in temperature in the cutting area.

**References:** 1. *Anderson D., Warkentin A., Bauer R.* Comparison of spherical and truncated cone geometries for single abrasive-grain cutting. *Journal of Materials Processing Technology.* vol. 212, i. 9, pp.1946–1953 (2012). 2. *Aurich J.C., Kirsch B.* Kinematic simulation of high performance grinding for analysis of chip parameters of single grains. *CIRP Journal of Manufacturing Science and Technology.* vol. 5, pp. 164–174 (2012). 3. *Jiang J.L., Ge P.Q., Bi W.B., Zhang L., Wang D.X., Zhang Y.* 2D/3D Ground Surface Topography Modeling Considering Dressing and Wear Effects in Grinding Process. *International Journal of Machine Tools and Manufacture.* vol.74, pp. 29–40 (2013). 4. *Li Jia-Jie, Yan Ru-zhong.* Zuhe jichuang yu zidonghua jiagong jishu- Modul. *Mach. Tool and Autom. Manuf. Techn.* no. 6, pp. 92–95 (2012). 5. *Liu Yun-feng, Zhao Hong, Jing Jun-tao, Wei Shi-liang.* Jinganshi yu moliaomoju gongcheng – Diamond and abrasives eng..32, no. 4, pp. 55–59 (2012). 6. *Marinescu I.D., Rowe B., Dimitrov B., Ohmori H.* Tribology of abrasive machining process. William Andrew Publishing. 600 p (2012). 7. *Raphael Holtermann, Sebastian Schumann.* Modelling, Simulation and experimental investigation of chip formation in internal traverse grinding. *Production Engineering Research and Development.* vol. 7, i. 2, pp. 251–263 (2013). 8. *Xie J., Wei F., Zheng J. H., Tamaki J., Kubo A.* 3D laser investigation on micron – scale grain protrusion topography of truncated diamond grinding performance. *International Journal of Machine Tools and Manufacture.* vol. 51, i. 5, pp. 411–419 (2011). 9. *Yan Lan, Jiang Feng, Rong Yiming.* The research of grinding. *Jixie gongcheng xuebao – J. Mech. Eng.* 48, no. 11, pp. 172–182 (2012). 10. *Narasimha M.* Improving Cutting Tool Life a Review/M. Narasimha, K. Sridhar, et al.// *International Journal of Engineering Research and Development.* – vol. 7, Iss.1, pp. 67–75 (2013). 11. *Handbook of Machining with Grinding Wheels, Second Edition/ Ioan D. Marinescu, Mike P. Hitchiner.* CRC Press. – 750 p (2016). 12. *W. Brian Rowe.* Principles of modern grinding technology. Jordan Hill, Oxford OX2 8DP: UK. – 421 p. (2011). 13. *Bogutsky, V.* Calculating the profile of intermittent grinding wheel for the sharpening teeth of the broach/ Yu. Novoselov, L. Shron // *MATEC Web of Conferences* 224,01003 (2018) ICMTMTE 2018. DOI:<https://doi.org/10.1051/matec-conf/201822401003>. 14. *Yaroslavtsev V.M.* Otsenka effektivnosti preryivistogo rezaniya na osnove ispolzovaniya zakonomernostey izmeneniya teplonapryazhennosti protsessa/ V.M. Yaroslavtsev, N.G. Nazarov// *Nauka i obrazovanie: nauchnoe izdanie MGTU im. N.E. Bauman.* – 10 oktyabrya. - pp. 35–42 (2013). DOI:10.7463/1013.0623113. 15. *Lischenko N.V.* Opredelenie temperatury preryivistogo shlifovaniya /N.V. Lischenko, V.P. Larshin, A.V. Yakimov//Pratsi Odeskogo politehnichnogo unversitetu. – Vip.2 (39), pp. 80–85 (2012). 16. *Bogutskiy V.B.* O tselesoobraznosti primeneniya shlifovalnykh krugov s preryivistym profilem na operatsiyah ploskogo shlifovaniya/ V.B. Bogutskiy, Shron L.B.// *Progressivnyie tehnologii i sistemy mashinostroeniya.*– №2 (65), pp. 10–15 (2019). 17. *Bogutskiy V.B.* Analiz konstruktivnykh osobennostey shlifovalnykh krugov s preryivistoy poverhnostyu/ V.B.Bogutskiy, L.B. Shron, B.V. Bogutskiy, B.L. Shron//Uchenyie zapiski Krymskogo inzhenerno-pedagogicheskogo universiteta.- №35.-S.60-64 (2012). 18. *Rodriguez Rafael Lemes, Lopes Jose Claudio, Garcia Mateus Vinicius, Tarrento Gilson Eduardo, Rodriguec Alessandro Roger, Luiz Eduardo de Angelo Sanchez, Hamilton Jose de Mello, Paulo Roberto de Aguiar, Eduardo Carlos Bianchi.* Grinding process applied to workpieces with different geometries interrupted using CBN wheel. *The international Journal of Advanced Manufacturing Technology.*107, is. 3, pp. 1265–1275 (2020). DOI:10.1007/S 00170-020-05122-2. 19. *Tawakoli,T., Azarhoushang, B.* The oretical and experimental investigation of intermittent grinding of SiC with a segmented grinding wheel. *Int J Abras Technol.* 4 (1), pp. 90–99 (2011). <https://doi.org/10.1504/IJAT.2011.039005>. 20. *Fang C.,Xu,X.* Analysis of temperature distributions in surface grinding with intermittent wheels. *The International Journal of Advanced Manufacturing*

Technology. 71, pp. 23–31 (2014). [https://doi.org/10.1007/S\\_00170013-5472-1](https://doi.org/10.1007/S_00170013-5472-1). 21. Oborskiy G.A. Obobshchenie predstavleniy o dinamicheskoy karakteristike protsessa rezaniya /G.A. Oborskiy, P.A. Linchevskiy, A.A. Orgiyani, R.A. Maschey// Pratsi Odeskogo polltehn.univ-tu. - Vip.1 (38), pp. 66–70 (2012). URI: <http://pratsi.opu.ua/app/webroot/articles/1346754609.pdf>. 22. Orgiyani A.A. Intensivnost parametricheskikh rezonansov pri preryivistom rezanii/A.A.Orgiyani, I.M.Tvorischuk // Suchasni tehnologiyi v mshinobuduvanni – Modern technologies in mechanical engineering: 3b. nauk. Pr. - Kharkiv: NTU “KhPI”. - Vip.9, pp. 124–133 (2014). <http://repository.kpi.kharkov.ua/handle/KhPI-Press/16865>. 23. Nikitin S.P. Influence of technological parameters on the thermodynamic system of cutting equipment/S.P. Nikitin V.K.Zal'taberg//Russian Engineering Research. Vol. 32, №1, pp. 90–92 (2012). 24. Khanov A.M. Elastic and Thermal Dynamic Processes in the Grinding of Thermoprotective Coatings/ A.M Khanov, S.P. Nikitin, L.D Sirotenko. E.O. Trofimov,E.V.Matygullina// Russian Engineering Research. (2015). Vol. 35, №9, pp.708-710.

Олексій Якімов, Любов Бовнегра, Володимир Тонконогий,  
Владислав Вайсман, Віктор Стрельбіцький, Інна Сінько, Одеса, Україна

## **ВПЛИВ ГЕОМЕТРИЧНИХ ХАРАКТЕРИСТИК ПЕРЕРИВЧАСТОГО ПРОФІЛЮ РОБОЧИХ ПОВЕРХОНЬ АБРАЗИВНИХ КРУГІВ НА ТОЧНІСТЬ І ТЕМПЕРАТУРУ ПРИ ШЛІФУВАННІ**

**Анотація.** Шліфування є найбільш поширеним методом фінішної обробки деталей із заготованих сталей. Шліфування супроводжується виділенням великої кількості тепла в зоні різання, під дією якого в тонкому поверхневому шарі оброблених деталей виникають структурні зміни, напруження розтягу і навіть мікротріщини, що істотно знижують експлуатаційну надійність машин до складу яких входять ці деталі. Застосування абразивних кругів з переривчастою робочою поверхнею дозволяють знизити температуру в зоні контакту абразивних зерен з матеріалом деталі і, як наслідок стабілізувати якість поверхневого шару оброблюваних деталей. Високочастотні коливання в пружній системі верстата, які супроводжують роботу переривчастого круга, є позитивним чинником, що знижує енергоємність процесу шліфування. Однак, при певних умовах динамічної взаємодії інструменту із заготовкою може виникнути параметричний резонанс, який погіршує геометричні і фізико-механічні параметри якості поверхневого шару обробленої деталі. Метою роботи є реалізація можливості прогнозування параметрів якості поверхневого шару деталей при переривчастому шліфуванні за рахунок вивчення впливу конструктивних особливостей макротопографії робочої поверхні абразивних кругів та режимів обробки на характер динамічної взаємодії інструменту з заготовкою і теплонапруженість у зоні різання. Встановлено, що параметричні коливання пружної системи верстата можна зрушити в більш стійку область за рахунок збільшення кількості переривань робочої поверхні абразивного круга при незмінному співвідношенні протяжності виступів і западин. Збільшення числа розривів у крузі сприяє також зниженню температури в зоні різання. Встановлено, що для підтримки стійкої роботи пружної системи верстата необхідно при збільшенні швидкості різання зменшувати число западин на шліфувальному крузі. Однак, обидві ці дії супроводжуються збільшенням теплонапруженості процесу шліфування. Експериментальним шляхом встановлено, що для звичайного (маятникового) шліфування можна домогтися підвищення продуктивності обробки за рахунок збільшення швидкості та збільшення періодичності переміщення робочого столу.

**Ключові слова:** макротопографія робочої поверхні; шорсткість поверхні; ступінь відпущення; динамічна взаємодія; оброблювальний матеріал.

I. Yakovenko, Yu. Vasilevskiy, Y. Basova, Kharkiv, Ukraine,  
Milan Edl, Plzen, Czech Republic

## **TECHNOLOGICAL PROVISION OF THE ACCURACY FOR THE THREAD FORM OF ROD PUMPS**

**Abstract.** *Aspects of thread manufacturing used in downhole rod pumps are considered. Technological defects of distortion of lateral surfaces of a thread profile arising in the course of processing on CNC machines are described, and the factors which most influence formation of these defects are established. The influence of profile defects on the reliability of the threaded connection during the operation of rod pumps is analyzed, as well as the research on the dynamics and oscillations of machine systems is analyzed. With the performed analysis the mathematical model of real technological system in the course of machining process is created and investigated. The main technological factors that have the greatest influence on the occurrence of error in the shape of the thread surface are identified. With the help of software for analysis of dynamic systems, the necessarily calculations were performed and the behavior of the dynamic system in the process of forming the thread profile was considered. Based on the analysis of the obtained results, a system for managing the parameters of the technological process of threading and technological solutions formulated. The introduction of which had a positive impact on the stability of the machining process and reduce the frequency of the above defect.*

**Keywords:** *threaded connection; thread profile; technological system; cutting mode; oscillations; amplitude; mathematical modeling.*

**Introduction.** There are different types of rod pumps, which differ in the layout and design of the fastening system in the downhole, the design of certain components. The pump is a device with a length of more than ten diameters, the structure of which includes working, basing and connecting elements. Movable units are made with precise fits. The general design of the downhole pump consists of tubular parts connected by threads. That is, each pump part has at least two threaded surfaces. Rod pumps use different types of threaded connections, which differ in the type of profile, and generating, and technological requirements. The accuracy of the dimensions of the various threads is regulated by the relevant standards, which contain formulas for calculating the tolerance fields and/or a number of marginal deviations for individual dimensions and surface shapes [1,2].

**Formulation of the problem.** When machining threads with CNC lathes, a defect appears from time to time, which is a significant deterioration in the roughness of the side surfaces of the thread. The appearance of large notches, cyclically located along the turn of the thread is seen. Figures 1 and 2 show examples of parts with this defect on the internal thread. As can be seen in the figures, one part has more notches at the end of the threaded area (Fig. 1), and the other almost along its entire length (Fig. 2).



Figure 1 – Part with notches on the thread

All performed threads are machined on CNC lathes of different brands and year of manufacture, using turning cutters with replaceable plates. Plates with a full profile, which select the surface of the thread top on the last passes are also used, as well as general purpose ones, which are more universal.

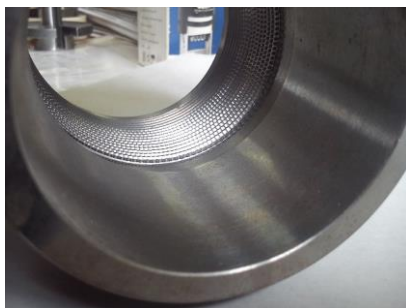


Figure 2 – Part with notches on the thread along its entire length

Cutting modes are selected according to the recommendations of the tool manufacturer, other standards and are adjusted depending on the conditions of the installment.

The appearance of the described defect is unsystematic. It takes place when making parts of different designs, the use of material from different batches, processing on different machines, different tools. But we can say that more often its appearance is observed while:

- processing of internal and conical threads,
- processing of large diameter threads,
- large departure of the processed surface.

Uncontrolled excessive reduction of surface roughness parameters and accuracy of the thread profile shape has significant negative effects in the process of further pumps functioning:

- stress concentration – areas with a small radius of curvature serve as a focus of local concentrations of mechanical stress and provoke the emergence and development of microcracks;
- violation of the tightness of the thread due to uneven load distribution on the side surfaces of the profile and, including at the macro level due to deviations in the contact density;
- undesirable deviation in geometry of the location of the connection parts;
- negative impact on the quality of galvanic coatings – insufficient uniformity and adhesion leads to local destruction of the protective layer, which contributes to unpredictable corrosion;
- provoking more intensive corrosion wear of products due to accumulation in the irregularities of aggressive substances.

The appearance probability of the abovementioned problems indicates that the considered production defect is unacceptable. In practice, in case the rejected parts cannot be corrected by elaborating the thread to a satisfactory quality, these parts are rejected and are not allowed to be used in the product. To minimize such cases, the technology of manufacturing parts must ensure the stable performance of threading operations on a given equipment with maintained quality.

**The purpose** of this article is to develop a mathematical model of the dynamics of forming the surface of thread profile on lathes based on the identification and study of factors that determine the errors of the shape of the threaded surface profile, as well as control the parameters of thread formation to ensure stable quality of the process.

The deviation of geometric shapes from the theoretically given ones is caused by the circumstances inherent in the method of threading and arises as a result of the manifestation of a number of technological reasons [3]. For the non-systemic nature of shape errors, the most important factors are: unsatisfying mechanical properties of the workpiece material; workpiece locating errors; inaccuracies in the adjustment of all technological equipment and, as a consequence, dynamic phenomena of the cutting process, such as vibrations. When considering the conditions of vibration, it is necessary to make allowance for the rigidity of the entire processing system. And this: the lathe machine itself, the foundation under the machine, the device for different turning conditions, the tool, the part itself and the processing modes (Machine-Tool-Workpiece system or MTW) [4]. The most common type of vibration when working on metal-cutting machines is self-oscillation [5,6]. Self-oscillating or «autoexcitation» is a process in which non-extinguishing oscillations can be excited due to an energy source that does not have oscillatory properties. Intense self-oscillations of the tool occur mainly in the

direction of the tangential component of the cutting force, where the rigidity of the cutter system is the lowest. They occur under the influence of friction forces on the back surfaces of the tool [7]. Prof. A. I. Kashirin and his followers consider this reason, along with the change of friction forces in the process of machining and wear of the tool, to be one of the main factors supporting self-oscillations [8]. Moreover, I. S. Amosov showed that the role of changes in the cross section of the cut during self-oscillations can be estimated at 85%, and the role of all other causes only in 15% [9]. These studies are mostly general in nature and do not take into account modern technological systems and their capabilities.

In [10] the issues of intensity of self-oscillations at change of effort due to intermittent cutting process and influence of oscillations on shape errors during processing by cutting tool are considered, and conditions of excitation of parametric resonances, and also their intensity at boring of intermittent surfaces are studied. The discontinuity of the bored surface is described by the piecewise constant functions  $\Phi(t)$ . The calculations according to the proposed model are in good agreement with the experimental data when varying the cutting modes. Studies of the Provincial Key Laboratory for Green Cutting Technology and Lanzhou Institute of Technology, Lanzhou, China [11] are devoted to the mutual influence of cutting process parameters and equipment condition on the occurrence of vibrations and their intensity during machining on CNC machines. In the research [12] the issues of damping of self-oscillations during machining with a cutting tool due to variation of the cutting depth parameter are considered.

However, all the considered works take into account the specific processing conditions and MTW system, which differ from the existing ones for the studied problem, and the use of these models requires reliable and complete information about the dynamic state of the mechanical cutting system. The analysis of the considered sources allows to use to some extent the techniques offered by authors for development of dynamic model of thread cutting process, its further research and development of recommendations for production.

The main elements of the MTW dynamic system, interacting with each other, in the study of its characteristics are hysteretic damping system (springing system) the working processes of friction, cutting and processes occurring in the engines.

Mathematical modeling is based on solving the Lagrange equation (1) for individual coordinate directions:

$$\frac{d}{dt} \left( \frac{dT}{d\dot{x}_i} \right) - \frac{dT}{dx_i} = - \frac{d\Pi}{dx_i} - \frac{dR}{d\dot{x}_i} + \Sigma Q_i, \quad (1)$$

where  $T$  – the kinetic energy,  
 $\Pi$  – potential energy,  
 $R$  – the dissipative function,  
 $Q_i$  – external forces,

$x_i$  – coordinates of displacements.

A dynamic machining system can be represented by a system with one degree of freedom. Figure 3 shows the surface of the part fixed in the chuck of the lathe, and the cutter in the carriage, which is set to turning with a depth of  $t$ , mm. The carriage is connected to the frame by stiffness  $j$ , N/m and damping coefficient  $b$ , Kg/s.

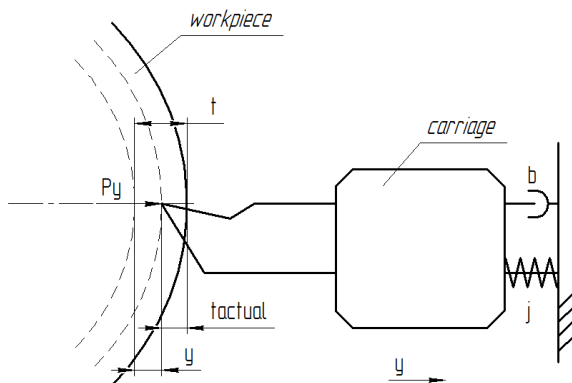


Figure 3 – Scheme of the process of longitudinal turning in the plane perpendicular to the axis of the part

When set to a given depth of cut ( $t$ ) turning process provides a cutting force ( $P$ ), which causes deformation of MTW system ( $y$ ), which in turn affects the actual position of the cutter edge. This closed-loop system can be described by the following block diagram (Fig. 4):

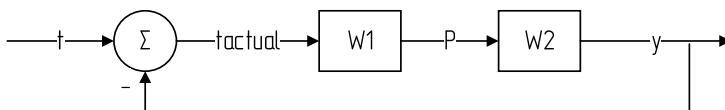


Figure 4 – Block diagram of the turning process with one degree of freedom

For a single coordinate it can be expressed by:

$$W1 = K = \frac{P}{t}$$

assuming that at the initial moment of time  $P$ ,  $t$ ,  $K$  are constants;

$$W2 = \frac{1}{m \cdot s^2 + b \cdot s + j},$$

based on the equation of forces (linearization of the Lagrange equation).

Then the total transfer function of this system will be:

$$W = \frac{W1 \cdot W2}{1 + W1 \cdot W2} = \frac{K}{m \cdot s^2 + b \cdot s + (j + K)},$$

where  $m$ ,  $b$ ,  $j$  – dynamic characteristics of the system, adopted on the basis of experimental studies for a specific MTW system,

$K$  – the coefficient of proportionality of the cutting force, which reflects the influence of the turning depth on the resulting force and is calculated by the cutting modes,

$s$  – the complex variable of Laplace transformation.

For the proposed dynamic system as controlled parameters, it is advisable to consider cutting modes (only depth and cutting speed, because it is not possible to vary the feed when cutting threads), as well as the length of tool and workpiece as elements that affect the rigidity of the system. The stiffness of other elements of the MTW system was established experimentally, and in the proposed model is taken into account as a constant. To control other characteristics related to the rigidity of the equipment (design of the device and the machine) is also impractical in this case, as it requires additional costs for equipment upgrades, in addition, the equipment is used not only for machining threaded surfaces.

Simulation of process dynamics is performed using special software. Figure 5 shows an example of a simulated system, which is given by the block method (top), as well as using a special block "transfer function" (bottom). The second option is more convenient, although it requires additional calculations to determine the coefficients of the transfer function, which can be performed automatically in Excel along with the variation of parameters.

Multiple simulations of the threaded surface forming with specific geometric parameters with a step of 2 mm and a length of 40 mm was carried out. In the simulation process, the following parameters were varied separately: cutting depth  $t$ , which depends on the number of passes of thread formation (and its dependent cutting force  $P$ ), cutting speed  $v$ , system rigidity  $j$ , which was set experimentally. The values of all other parameters were fixed as constants. All parameter values varied within the allowable ranges. The values of other parameters were constant and equal to the previously accepted.

The cut depth (number of passes) varied from 0.236 mm to 0.071 mm. The average of the values of the position deviation of the cutter from a set level was 0.0656 mm, and the average of the maximum position deviations of the cutter from the steady state was 0.121 mm.

When changing the cutting speed (turning speed) in the range from 25 m/min to 95 m/min, the average of the values of deviations of the cutter position from the set level was 0.0805 mm, and the average of the maximum deviations of the cutter position from the steady state was 0.1498 mm.

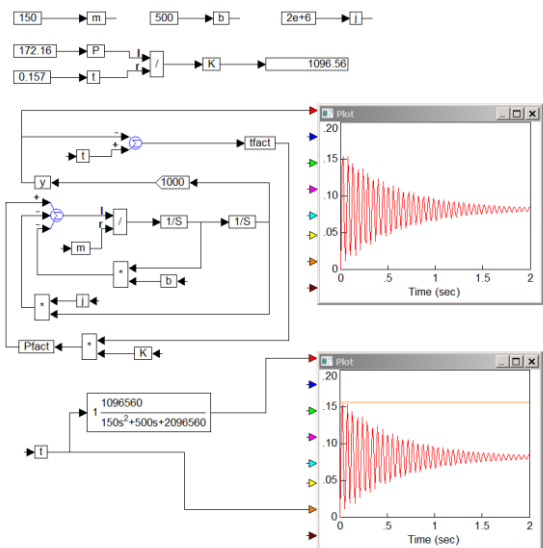


Figure 5 – Modeling of a dynamic system

The rigidity of the system varied from  $1 \cdot 10^6$  N/m to  $1.9 \cdot 10^6$  N/m. When changing this parameter, the average of the values of deviations of the cutter position from the set level was 0.0688 mm, and the average of the maximum deviations of the cutter position from the steady state was 0.1225 mm.

As shown by the results of the analysis of the proposed models, the position of the cutting surface of the tool has not just a fixed position error, but is in an oscillating state. Moreover, this condition has a significant amplitude during surface cutting, and also has a clear relationship with the varied parameters.

For a more detailed assessment of the impact of the considered parameters, the calculations were performed, which establish how the change of each parameter is reflected in the change of the initial value. The considered parameters have different degree of influence on the modeled system. For example, a small relative change in the cutting depth parameter causes a larger relative change in amplitude than the same or even a larger relative change in the cutting speed parameter.

This allowed to develop a software for managing technological parameters in the processing of threaded surfaces. These calculations are valid only for the considered specific processing system and the formed model of constant values of parameters which are established experimentally, and ranges of the varied parameters.

The calculation results, which were obtained on the basis of the proposed model, were checked during the processing of specific threaded surfaces of rod pump parts. The form errors in this case were avoided, which shows the adequacy of the model and the software.

Based on the evaluation of the obtained data and analysis of the simulation results, general technological measures are offered to improve the thread cutting process for specific geometrical parameters and shapes of threaded surfaces used in the manufacture of rod pumps (use of lubricants, timely control, sharpening and changing of cutting tools for ensuring the energy characteristics of the process in a given range, proper tightening of equipment connections, avoidance of imbalance of movable joints, etc.)

The proposed general measures are fully in line with the abovementioned recommendations.

### **Conclusions:**

1. Based on the analysis of the defect nature, the causes and factors that affect the appearance of defects in the side profile of the threaded surface of the rod pumps parts are identified. The quantitative nature of the occurrence of springing deformations in the MTW system during machining was also established, which allowed to create a dynamic model of the thread machining process.

2. The proposed model allows to determine the technological parameters of the operation (cutting speed and depth, tool departure parameters) for a specific thread profile with specific geometric parameters (diameter, pitch, length, profile), which will provide the required accuracy of the threaded surface shape. The software block of models allows to define processing parameters from the point of view of optimization of two factors: maintenance of stable process of cutting without return of self-oscillations and maintenance of the maximum productivity (minimum time of forming of a carving surface). The proposed model allows to use it to determine the parameters of operations of processing of threaded surfaces by cutters on similar equipment.

**References:** 1. TU U 29.1-14331730-001: 2007. Nasosy skvazhinnyye shtangovyie i opory zamkovyye k nim. Tekhnicheskkiye Usloviya - Vved. 25.03.2008. 2. *Yakovenko I.Ye., Vasilevskiy Yu.* Povysheniye tochnosti profilya rez'by pri obrabotke detaley shtangovykh nasosov // KHPI Mezhdunarodnaya nauchno-prakticheskaya konferentsiya magistrantov i aspirantov: materialy konf., 19–22 list. 2019 s. / pod red. E. I. Sokol; Nat. tech. un-t "Kharkiv. politekh. in-t" [to v.]. – Kharkiv: NTU «KhPI», 2019. - p. 548. 3. *Ananchenko V.N., Tsybriy I.K., Morgunov V.V.* - Osobennosti izgotovleniya i kontrolya rez'by na trubakh neftyanogo sortamenta - Vestnik DGTU, 2009. Spets. vypusk. "Tekhnicheskkiye nauki". Chast' I. pp. 48–55. 4. *Knight W.A., Tobias S.A.* Tensional vibrations and machine tool satability.

[Advances in machine tool decarage research / Proceedings of the 10th international NTDR conference]. Oxford, 1970. – pp. 299–323. **5.** *Astashev V.K., Korendyasev G. K.* V modelyakh vozbuzhdeniya avtokolebaniy pri rezanii metallov. Vestnik nauchno-tehnicheskogo razvitiya. Moscow. 2012. – № 5. – pp. 19–25. **6.** *Vasil'kov D.V., Aleksandrov A.S., Golikova V.V.* Sushchnost' avtokolebaniy v metallorezhushchihy stankakh. // Sistemnyy analiz i analitika, №1 (9) - St. Petersburg, 2019. 166 p., pp.16–22. **7.** *Novikov F.V., Kryuk A.G., Ryabenkov A.I., Ivanov I.Ye.* Analiticheskoye opredeleniye amplitudy avtokolebaniy pri tochenii. Vestnik Natsional'nogo tekhnicheskogo universiteta «KhPI» Sbornik nauchnykh trudov. Seriya: “Innovatsionnyye tekhnologii i oborudovaniye obrabotki materialov v mashinostroyenii i metallurgii”. - Kharkiv: NTU «KhPI». – 2014. – № 5 (1048), pp. 156–161. **8.** *Korendyasev K.* V fizicheskoy prirode effektov, lezhashchikh v osnove modeli vozbuzhdeniya avtokolebaniy pri rezanii Kashirina Vestnik nauchno-tehnicheskogo razvitiya. №12 (148), pp. 17–23. Moscow: 2019. ISSN: 2070-6847, DOI: <https://doi.org/10.18411/vntr2019-148-3>. **9.** *Amosov I.S.* Ostsillograficheskoye issledovaniye vibratsiy pri rezanii metallov. “Tochnost' mekhanicheskoy obrabotki i puti yeye povysheniya”: Sbornik nauchn. tr. – Moscow: Publ. Mashgiz, 1951. **10.** *Orgiyani A.A., Tvorishchuk I.M.* Intensivnost' parametricheskikh rezonansov pri preryvistom rezanii. ISSN 2078-7499. “Sovremennyye tekhnologii v mashinostroyenii”, 2014, vyp. №9, pp. 124–138. **11.** *Chuangwen X., Jianming D., Yuzhen C., Huaiyuan L., Zhicheng S., Jing X.* The relationships between cutting parameters, tool wear, cutting force and vibration. Advances in Mechanical Engineering. – 2018. – Vol. 10. – Iss. 1, pp. 1–14. **12.** *Shan'shin I.K., Shagniyev O.B., Burdakov S.F.* Adaptivnoye podavleniye neustoychivykh regenerativnykh avtokolebaniy vyborom glubiny rezaniya. “Nedelya nauki” St. Petersburg: “Materialy nauchnoy konferentsii s mezhdunarodnym uchastiyem, 19-24 noyabrya 2018 g. Institut prikladnoy matematiki i mekhaniki”. St. Petersburg. Publ: Politekh-PRESS, 2018. – pp. 338–341.

Ігор Яковенко, Юрій Василевський, Євгенія Басова, Харків, Україна,  
Мілан Едл, Пльзень, Чеська Республіка

## **ТЕХНОЛОГІЧНЕ ЗАБЕЗПЕЧЕННЯ ТОЧНОСТІ ФОРМИ ПРОФІЛЮ РІЗЬБИ ШТАНГОВИХ НАСОСІВ**

**Анотація.** Розглянуто аспекти виготовлення різьблень, які використовуються в свердловинних штангових насосах. Описано технологічні дефекти спотворення бокових поверхонь профілю різьблення, що виникають в процесі обробки на верстатах з ЧПК, та встановлено фактори, які найбільш впливають на утворення цих дефектів. Проаналізовано вплив дефектів профілю на надійність різьбового з'єднання в процесі експлуатації штангових насосів, а також проаналізовано дослідження з питань динаміки й коливань верстатних систем. Завдяки виконаного аналізу створено і досліджено математичну модель реальної технологічної системи, яка використовується в процесі обробки різьбової поверхні. Встановлено основні технологічні фактори, які мають найбільший вплив на виникнення похибки форми різьбової поверхні. За допомогою програмного забезпечення для дослідження динамічних систем виконано необхідні розрахунки та розглянуто поведінка системи Верстат-Приспосовання-Заготовка-Інструмент в процесі формування профілю різьби. На підставі аналізу отриманих результатів розроблена система керування параметрами технологічного процесу обробки різьбової поверхні та сформульовані технологічні рішення, впровадження яких мало позитивний вплив на стабільність якості процесу обробки та на зменшення частоти появи розглянутого вище дефекту точності форми профілю різьблення та підвищило ефективність виробництва.

**Ключові слова:** різьбове з'єднання; профіль різьблення; технологічна система; режим різання; коливання; амплітуда; математичне моделювання.

G. Klymenko, Y. Vasylychenko, Ye. Donchenko, Kramatorsk, Ukraine

## QUALITY MANAGEMENT OF CUTTING TOOLS ON HEAVY MACHINES

**Abstract.** *The work is devoted to improving the efficiency of cutting tools on heavy machines by developing a quality management system for its operation, determining rational operating regulations and developing general machine-building standards for cutting. The developed model of the tool operation control system for the first time allowed to systematically consider the structure and relationships of all components of the process. The qualimetric approach to the tool operation process made it possible to develop methods for quantitative assessment of the process quality and substantiate the structure of the preparatory information subsystem.*

**Keywords:** *quality management; cutting tool; machines; rational operation of the tool; system approach; quality system.*

Improving the efficiency of metalworking, introducing resource-saving technologies in mechanical engineering, improving the quality and competitiveness of products is possible without the development of scientifically grounded regulations for the operation of cutting tools, which significantly affect the working conditions and technical and economic indicators of mechanical engineering. Ukraine is implementing international standards ISO 9000 version 2000, which regulate the development of quality management systems for products and processes, the development of standards and regulatory materials [1–3]. In this regard, the issues of certification of production processes, in particular, the processes of operating the cutting tool, the determination of scientifically grounded cutting modes, consumption rates and other regulations for the operation of the tool, are of particular importance.

The solution of these issues is especially important when using cutting tools on heavy machines of high cost. This is what determines the need to reduce their downtime and organize the rational operation of the tool. The large dispersion of processing parameters on heavy machines, the variety of factors that affect the operation process, require an integrated approach to determining the control parameters of the tool operation process, the methodology of which requires development.

Purpose of the present work: increasing the efficiency of using cutting tools on heavy machines by developing a quality management system for the process of its operation, defining rational operating procedures and developing general machine-building standards for cutting.

The methodological basis of the work is a system approach to the study of the process of operating a tool, its conditions and features, the patterns of processes.

Theoretical research is based on the fundamentals of qualimetry, reliability theory, operations research, decision making, probability, and mathematical statistics.

Existing works considered certain aspects of the operation of tools, which concerned medium-sized machines and did not comprehensively investigate the whole process. As a result of the transition to market conditions for the operation of machine-building enterprises, the operating conditions for cutting tools on heavy machines have somewhat changed [4–7]. Foreign and domestic literature sources indicate the growing interest in assessing the quality of various production processes [8–10]. Nevertheless, there are no systematic studies of the quality of the tool operation process, which allow one to take into account all the variety of factors and their relationships that affect the control parameters, in the literature.

The current standards for cutting conditions in Ukraine give very contradictory recommendations, do not take into account modern processed and tool materials, do not take into account modern designs of cutting tools and their reliability, do not fully contain mathematical models that allow the use of computers to determine cutting conditions on heavy machines. The study of the reliability of the tool was limited to operational tests of their reliability. The use of tools for prefabricated structures requires the development of new mathematical models, taking into account complex reliability indicators. The costs of the cutting tool are calculated without taking into account the probabilistic nature of its operation, without taking into account the design of the tool and cutting conditions. Statistical studies of the processing parameters of parts on heavy machines allowed us to establish more common operating conditions for the tool. The work shows that 70% of the operations that are performed on rough heavy lathes are longitudinal turning of parts with a carbide tool. All parameters of tool operation on heavy machines have a large scatter, which confirms the need to consider the stochastic nature of the tool operation process. All these factors determined the main tasks of scientific research.

Based on the use of principles of the international standard ISO 9000: 2000, a quality system model of the process of operating tools on heavy machines has been developed. When building the structure of the system, the operation of the tool is for the first time considered as a set of processes: organizational, resource management, maintenance of the technological system, preparatory information, processing of parts and providing feedback (assessment, analysis, improvement).

The rational operation of the cutting tool is understood as such a process of its use, in which, along with high productivity and minimal costs, the lowest possible consumption of the tool is achieved with a given reliability and psychophysical load on the machine operator.

A qualimetric approach was used to quantitatively assess the quality of the operation process. The developed hierarchical structure of properties that make up

the quality of tool operation (Fig. 1) contains properties of purpose, which are characterized by target functions for multi-criteria optimization of the quality of the cutting tool operation process [1]. They represent a vector of process quality management criteria (the number indicates the level of consideration).

$$U^{-1} = (U_1^3, U_2^3, U_3^3, U_4^3, U_5^3).$$

Quality assessment is determined by:

$$K_I^j = f(P_I / P_I^{\partial T}),$$

where  $K_I^j$  - assessment of the complex  $i$ -property at the  $j$ -level of consideration;

$P_I$  u  $P_I^{\partial T}$  - production quality indicators and reference (basic).

The operational quality level (which is considered at level  $j+1$ ) is determined by:

$$V_{\mathcal{G}}^{j+1} = \sum_{i=1}^n K_i^j \cdot B_i^j,$$

where  $B_i^j$  - the weight of the  $i$ -property at the  $j$ -level of consideration.

Indicators of the levels of properties were determined on the basis of a questionnaire survey, instant observations, long-term statistical studies, laboratory experiments. The basic indicators adopted are the recommendations of norms, standards, and other regulatory documents [2]. An expert assessment of the properties that characterize the quality of operation made it possible to identify the most important of them, which were taken into account when developing an information and preparatory subsystem for the rational operation of the tool (Fig. 2).

Statistical studies of the quality of the operation of tools were used on the basis of an information databank, which calculates more than 5000 cases of machining parts on heavy machines, which are collected at factories in various fields of mechanical engineering.

For theoretical studies of the quality of operation, a methodology and software for a computer have been developed using the theory of qualimetry, as well as a methodology for expert assessment of the quality of tool operation.

To select a tool design from an information databank of designs, it is proposed to use the cluster analysis technique, which is developed on the basis of applied mathematical statistics using a computer (Statistica 5.5 software package).

When forming clusters, the used agglomerative hierarchical cluster-procedure. Instrument designs from the databank are combined into classes that are characterized by the area of regulations for their rational operation.

Operational and laboratory tests were carried out with VK8, T5K10, T15K6 carbide tools with wear-resistant coatings, vibration treatment and ion implantation. The acoustic emission method was used to control the quality of the coatings. To assess the mechanical properties of the studied steels (45, 40Kh, ShKh15SG, 12Kh18N9T, 9KhS), mechanical tests of the samples were carried out in accordance with the standards (DSTU 1497-73). The study of the operational strength of structures in order to determine the correction factors for the feed, which depend on the type of structure, were carried out in accordance with the method of stepwise increasing feed.

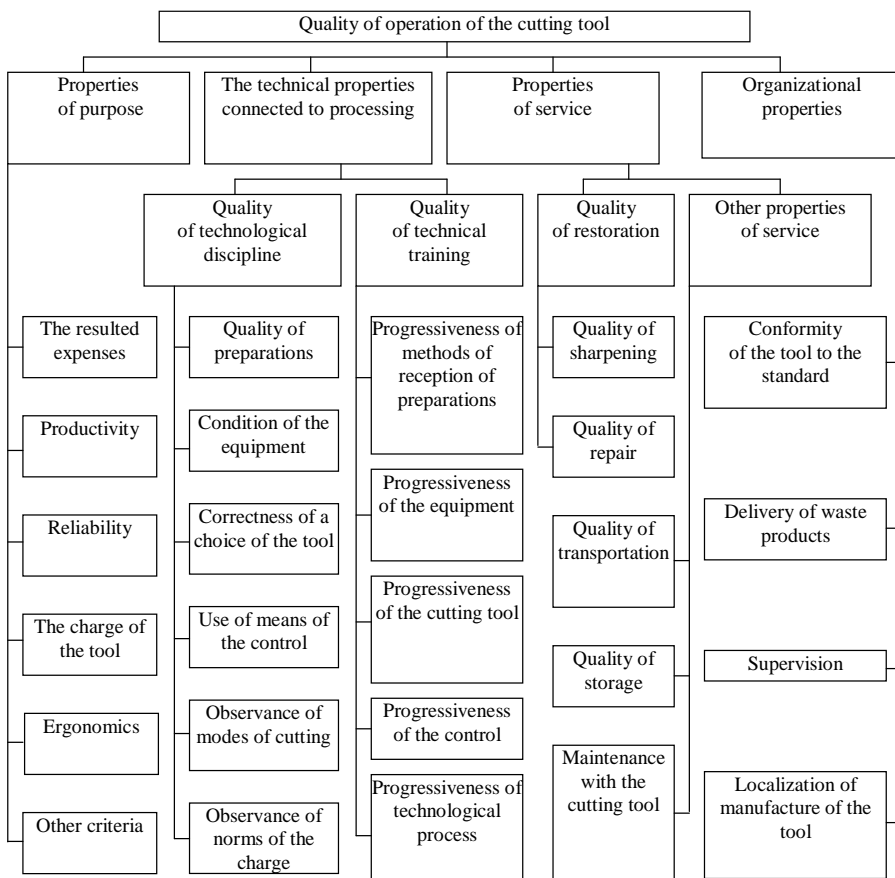


Figure 1 – The system of properties that make up the quality of the tool operation process

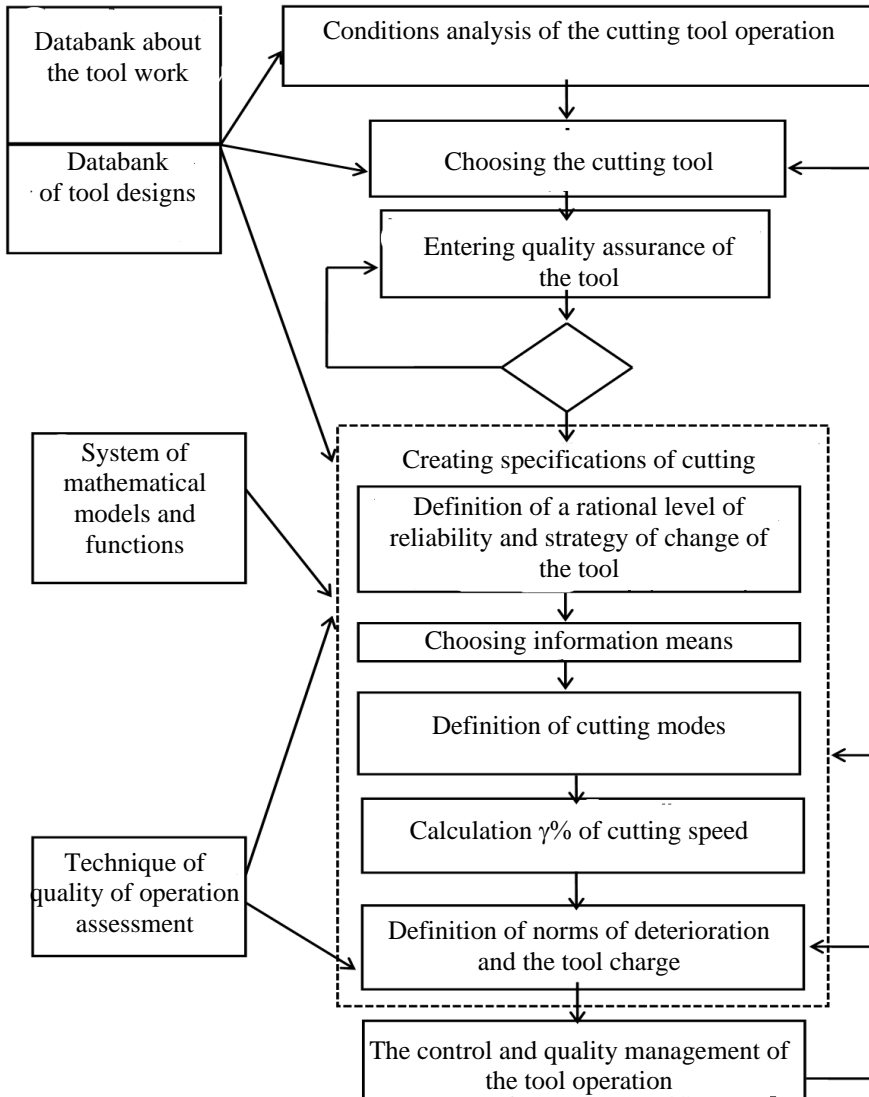


Figure 2 – Structure of the preparatory-information subsystem of cutting tools rational operation

## **Conclusions.**

1. For the first time, the new model of the operational process management system considered the structure and capabilities of all the constituent parts of the process.
2. The qualimetric approach to the process of the tool operating made it possible to develop methods for quantitatively assessing the quality of the process and to substantiate the structure of the preparatory information subsystem.
3. The research results were used in the development of general machine-building standards for cutting on heavy machines.

**References:** 1. *Klimenko G.P.* Definition of a degree of quality of operation of the cutting tool on heavy machine tools // the Bulletin of National technical university of Ukraine "KPII": Machine-building.- Kiev: NTUU "KPII", 2001.-№.40.- p.337-346. 2. *Klimenko G.P.* Management of quality of process of operation of the cutting tool on heavy machine tools // High technologies in mechanical engineering. The collection of scientific works NTU "XIII".- Kharkov, 2002.- № 1 (5).-p.157-160. 3. *Kovalov V., Vasilchenko Y., Dašić P.* Development of the integral complex of optimal control of heavy machine tools adaptive technological system for wind-power engineering parts // 8th International Conference Interdisciplinarity in Engineering, INTER-ENG 2014, 9-10 October 2014, Tirgu Mures, Romania Volume 9, 2015, pp. 145-152 <https://doi.org/10.1016/j.protcy.2015.02.022>. 4. *Jedrzejewski, J., Kwasny, W.* Development of machine tools design and operational properties. Int J Adv Manuf Technol 93, 1051–1068 (2017). <https://doi.org/10.1007/s00170-017-0560-2>. 5. *Jihong Chen, Jianzhong Yang, Huicheng Zhou, Hua Xiang, Zhihong Zhu, Yesong Li, Chen-Han Lee, Guangda Xu,* CPS Modeling of CNC Machine Tool Work Processes Using an Instruction-Domain Based Approach, Engineering, Volume 1, Issue 2, 2015, Pages 247-260, ISSN 2095-8099, <https://doi.org/10.15302/J-ENG-2015054>. 6. *Yanjun Han, Wu-Le Zhu, Lei Zhang, Anthony Beaucamp,* Region adaptive scheduling for time-dependent processes with optimal use of machine dynamics, International Journal of Machine Tools and Manufacture, Volume 156, 2020, 103589, ISSN 0890-6955, <https://doi.org/10.1016/j.ijmactools.2020.103589>. 7. *Koji Utsumi, Shoki Shichiri, Hiroyuki Sasahara,* Determining the effect of tool posture on cutting force in a turn milling process using an analytical prediction model, International Journal of Machine Tools and Manufacture, Volume 150, 2020, 103511, ISSN 0890-6955, <https://doi.org/10.1016/j.ijmactools.2019.103511>. 8. *Umut Karagüzel, Emre Uysal, Erhan Budak, Mustafa Bakkal,* Analytical modeling of turn-milling process geometry, kinematics and mechanics, International Journal of Machine Tools and Manufacture, Volume 91, 2015, Pages 24-33, ISSN 0890-6955, <https://doi.org/10.1016/j.ijmactools.2014.11.014>. 9. *Kovalov V., Vasilchenko Y., Turmanidze R., Dašić P., Sukova T., Shapovalov M.* The technique of designing high-power CNC lathes for enterprises of the heavy engineering industry. IOP Conference Series: Materials Science and Engineering, Vol. 568 (2019) (Special Volume with: Annual Session of Scientific Papers "IMT ORADEA 2019"; Oradea, Felix Spa; Romania; 30-31 May 2019), Article no. 012119; pp. 1-6. ISSN 1757-8981. <https://doi.org/10.1088/1757-899X/568/1/012119>. 10. *G. Klymenko, Y. Vasylichenko, V. Kvashnin* Modeling of cutting tools wear for lathes. Cutting & Tools in Technological System ISSN:

Галина Клименко, Яна Васильченко,  
Євгеній Донченко, Краматорськ, Україна

## **УПРАВЛІННЯ ЯКІСТЮ РІЗАЛЬНИХ ІНСТРУМЕНТІВ НА ВАЖКИХ ВЕРСТАТАХ**

**Анотація.** *Робота присвячена підвищенню ефективності використання різального інструменту на важких верстатах шляхом розробки системи управління якістю процесу його експлуатації, визначення раціональних регламентів експлуатації та розробки загально-машинобудівних нормативів різання. Методологічною основою роботи є системний підхід до вивчення процесу експлуатації інструменту, його умов та особливостей, закономірностей процесів. Статистичні дослідження параметрів обробки деталей на важких верстатах дозволили встановити найбільш поширені умови експлуатації інструменту. У роботі показано, що 70% операцій, що виконуються на чорнових важких токарних верстатах, складає повздовжнє обточування деталей твердосплавним інструментом. Всі параметри експлуатації інструменту на важких верстатах мають велике розсіювання, що підтверджує необхідність розгляду стохастичного характеру процесу експлуатації інструменту. На основі використання принципів міжнародного стандарту ISO 9000: 2000 створена модель системи якості процесу експлуатації інструментів на важких верстатах. Для кількісної оцінки якості процесу експлуатації використано кваліметричний підхід. Розроблена ієрархічна структура властивостей, що складають якість експлуатації інструменту, містить властивості призначення, що характеризуються цільовими функціями для багатокритеріальної оптимізації якості процесу експлуатації різального інструменту. Розроблена модель системи керування процесом експлуатації інструменту вперше дозволила системно розглянути структуру та взаємозв'язки усіх складових частин процесу. Кваліметричний підхід до процесу експлуатації інструменту дав змогу розробити методи кількісної оцінки якості процесу та обґрунтувати структуру підготовчо-інформаційної підсистеми. Результати досліджень використані при розробці загально-машинобудівних нормативів різання на важких верстатах.*

**Ключові слова:** *управління якістю; різальний інструмент; верстати; раціональна робота інструменту; системний підхід; система якості.*

Ya. Garashchenko, N. Zubkova, Kharkiv, Ukraine

## **EVALUATION OF THE FORECASTED EFFICIENCY OF PERFORMANCE OF RATIONAL ORIENTATION OF THE PRODUCT IN THE WORKSPACE OF ADDITIVE INSTALLATIONS**

**Abstract.** *Preliminary evaluation of the predicted efficiency of the optimization problem of the rational orientation of the product in the working space of layered construction of additive units is proposed to perform based on the analysis of the original triangulation 3D-model of a complex product by its spherical mapping. The condition of reflection on the sphere is that the values of angles in the spherical coordinate system for the faces normal of the triangulated model of product fall into the range of values of a certain triangular face of the sphere model. Examples of evaluation based on the analysis of spherical mapping of the original 3D model of products are considered. Industrial products with different surface complexity were selected as test 3D models. This approach allowed to perform a comparative analysis of the results depending on the design features of the products. The practical implementation was performed in the subsystem of visual assessment of geometric characteristics of triangulated 3D-models, which is part of the technological preparation system for the complex product manufacture by additive methods. This system was developed in NTU "KhPI" Department of Integrated Technologies of Mechanical Engineering named after M.F. Semko.*

**Keywords:** *technology planning; additive manufacturing; triangulated model; assessment of manufacturability, product orientation in the workspace.*

**Introduction.** The current direction of research aimed at improving the efficiency of the assessment of manufacturability, design improvement and reasonable choice of manufacturing strategy by additive technologies is the development of DfAM (Design for Additive Manufacturing) approaches [1].

When it comes to additive technologies, the source geometric information for manufacturing is a triangulated 3D-model of an industrial product, usually in STL format [2]. The triangulated model unifies the representation of the product surface, which creates the preconditions for the analysis of the system of triangular faces without restrictions concerning the structural complexity.

One of the main optimization problems of the technological preparation of additive processes is to determine the rational orientation of the product in the workspace of the layered build of the installation [3, 4]. The possibility of solving this optimization problem significantly depends on the geometric complexity of the product surfaces. Preliminary assessment of the design (component surfaces) of the product in the technological preparation for adaptation to the definition of rational orientation is of interest to ensure the required level of efficiency of the processes of the layered build.

**Literature analysis.** As a rule, the choice of the rational orientation of the product is performed by solving the optimization problem using a set of criteria

[3, 5]. The orientation option is chosen to take into account the most important factors. Since the orientation affects many factors, its choice during construction is based on the following:

- surface quality characteristics, building time, complexity, and volume of auxiliary support structures [6];
- the number of construction layers [7];
- the height of the product on the coordinate axis Z [8, 9];
- the area of the surfaces in contact with support structures (the area of the faces of the triangulated model with the coefficient of the normal on Z-axis in a given range of values) [8];
- surface error (the area of the faces with normal that are not perpendicular or parallel to the Z-axis, ie  $|N_z| \neq 1$  and  $N_z \neq 0$  [7], the area of the faces with normal  $|N_z| = 1$  and  $N_z = 0$  [10], the difference between the volumes of the original 3D-model and the ready-made product [8]);
- physical and mechanical properties of the product [8].

Despite a large number of works [3-13] to solve this problem, there is still no scientifically based quantitative assessment of the manufacturability of the product to the definition of rational orientation. Therefore, to test the design for adaptability to determine the rational orientation of the product in the working space, it is necessary to develop a special assessment that takes into account the features of layered manufacturing.

Taking into account the works [6, 14], to determine the rational orientation the angle between the normal of the triangular faces and the vector of the build direction (Z coordinate axis) is chosen as the studied feature of the triangulated 3D-model of the product. This investigated feature is the most significant of the geometric properties of the triangulated 3D-model, because it determines the roughness and errors in shaping the surfaces of the product, and therefore, the building step. Surfaces with a negative angle of inclination of the normal towards the Z-axis determine the design of support structures and, therefore, the complexity of post-processing processes for their removal.

**The purpose of the article** is to substantiate the possibility of a quantitative assessment of the manufacturability of the structure as for the task of determining the rational orientation of the product in the working area of layered building based on the analysis of the spherical reflection of the triangulated 3D-model.

**Research methodology.** The research was performed using the subsystem of visual analysis of the triangulation 3D-model of the product (screen form is presented in Fig. 1), designed to test its design in solving problems of technological preparation. The subsystem is a part of the system of technological preparation for the materialization of complex products by additive technologies, developed at the Department of Integrated Technologies of Mechanical Engineering named after M.F. Semko in NTU "KhPI". This system allows to

assess the manufacturability of the product design and analyze the effectiveness of additive technologies in its manufacture.

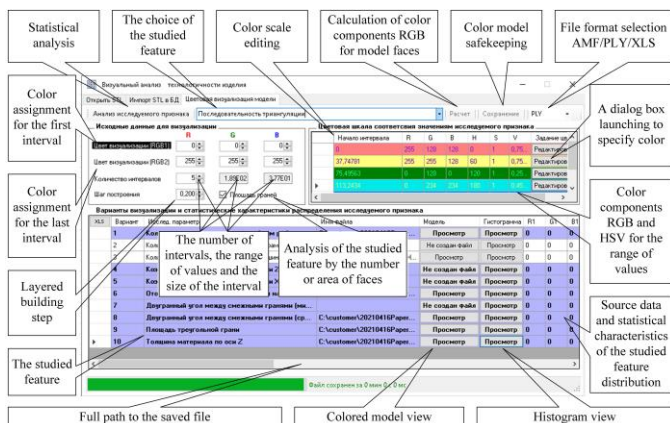


Figure 1 – Screen form of the subsystem of visual analysis of the product 3D-model

When developing the subsystem of visual analysis (color visualization) of the triangulated product model, the following main tasks were solved:

- assessment of correctness and rationality of triangulation of CAD-model;
- testing the subsystem manufacturability;
- visual assessment of the possibility of determining the rational orientation of the product in the working area of construction (examples are presented in Fig. 2).

The subsystem allows to perform color visualization on the surface of the model and statistical analysis of the distribution of values according to the selected feature of the 14 proposed characteristics [15, 16];

For additive technologies with layered building, the greatest roughness and deviations from the correct shape of surfaces are observed for faces that have an angle between their normal and the vector of the building direction (coordinate axis Z)  $\alpha_{NZ}$  in a certain range of values. The following intervals of values are conditionally distinguished:  $\alpha_{NZ}$  ( $0^\circ$ ,  $\alpha_{NZlimit}$ ) and  $\alpha_{NZ}$  ( $180-\alpha_{NZlimit}$ ,  $180^\circ$ ) [17]. The threshold value of the angle  $\alpha_{NZlimit}$  ( $30^\circ$ ,  $50^\circ$ ) depends on the chosen AM-method, technological characteristics of the equipment, source material and for some AM-methods (SLA, SLM, FDM, etc.) on the requirements of support structures [18]. Surfaces with the smallest deviations of the form have an angle  $\alpha_{NZ}$  ( $\alpha_{NZlimit}$ ,  $180-\alpha_{NZlimit}$ ). The minimum value of deviations is a characteristic for surfaces with angles  $\alpha_{NZ} = \{0^\circ; 90^\circ\}$ , i.e., for horizontal (directly formed without contact with the support structure or with the medium from the source material)

and vertical surfaces. For horizontal hanging surfaces, i.e., those which are with an angle  $\alpha_{NZ} = 180$ , for example, for FDM such surfaces are ideal only if they are adjacent to the table.

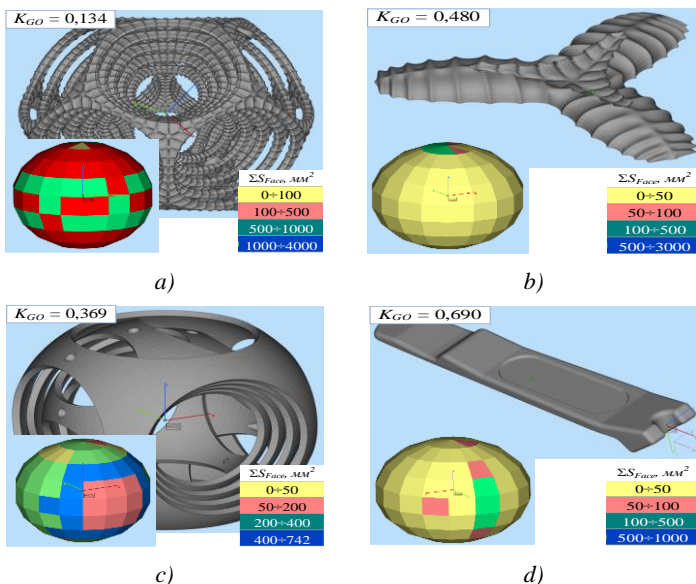


Figure 2 – Examples of color visualization by mapping to a triangulated sphere the total area of the faces of triangulated models of products at intervals of angles  $\theta$  and  $\varphi$  for vectors of normal faces in a spherical coordinate system (the obtained calculation data and their statistical analysis for the presented test 3D-models *a-d* are shown in Fig. 3 and in Table 1)

In technological preparation, the visualization of a product 3D-model by adding color to the surface areas depending on the value of the coefficient  $N_Z$ , offers information for decision-making on creating support structures and subsequent processing. But such visualization has obvious limitations for products that have internal surfaces (cavities) and a large number of complex-shaped surfaces. Therefore, to remove the restrictions imposed by the features of the studied design, it is proposed to perform the mapping of the product model to the sphere (color scale of the studied feature - the total area of the faces). The condition for mapping to the sphere is that the angles in the spherical coordinate system for the normal faces of the 3D-model of the product fall into the range of values of a certain face of the triangulation sphere model [19, 20]. The angles in

the spherical coordinate system for the normal faces of the 3D-model are calculated using the coefficients of the unit vector of the normal  $N_x, N_y, N_z$  [20].

The examples of spherical display of test 3D-models of products, presented in Fig. 2, show a high enough level of informativeness to determine the rational orientation. The problem of determining the rational orientation of the product in the workspace using a spherical map is to orient the surface with a larger area so that the normals of their faces are in a given range of values of their angles in the spherical coordinate system. In this case, the minimum error of layered shaping of the product surfaces is provided [3-13].

The proposed approach (visualization) also demonstrates the possibility of working out the design (assessment of the suitability of the 3D-model) for the rational orientation of the product in the working area of construction [19]. This creates the conditions for quantitative assessment of the manufacturability of the product based on the data of the distribution of the area of the 3D-model faces taking into account the intervals of reflection on the sphere.

It seems most appropriate to assess the suitability of the structure to the orientation by determining the deviations from the uniform distribution of the areas of the faces reflected on the sphere. The sphere model, as a product, is the least suitable for solving this problem. Therefore, the hypothesis is proposed that the efficiency of the rational product orientation can be a coefficient of concentration of the density of the surface area distribution along the triangular faces of the sphere reflection (by the angles of inclination of the normals of the triangular faces of the 3D-model  $\theta$  and  $\varphi$  in the spherical coordinate system) [21]:

$$K_{GO} = \frac{1}{2} \sum_{i,j}^{n,m} |D_{ij} - d_{ij}|, \quad (1)$$

where  $n, m$  is the number of intervals for angles  $\theta \in [0, 180)$  i  $\varphi \in [0, 360)$  in the spherical coordinate system for the normals of the triangular faces of the 3D-model, respectively (recommended value  $n = 4 \div 6, m = 2n; D_{ij}, d_{ij}$  - the relative area of the faces of 3D-models of the product and the sphere, respectively, that fall into the  $ij$ -th region of the values of angles  $\theta$  and  $\varphi$  for the normals,  $d_{ij} = 1/nm$  ;

In case of uniform distribution of the investigated feature (product surface area) when mapping to the sphere  $d_{ij} = 1/n_{tr\_sphere}$  , where  $n_{tr\_sphere}$  is the number of triangular polygons of the sphere.

Spherical display of the sphere 3D-model as a function (1) will have a coefficient  $K_{GO} = 0$ . Such value of the coefficient demonstrates the lack of a rational solution for the orientation of the sphere. Obtaining a larger coefficient of  $K_{GO}$  will indicate the possibility of determining the smaller area of values of the product rotation angles for its rational orientation. That is, a smaller relative

number of variants of the rational orientation of the product model, and accordingly a simpler solution of the optimization problem.

**Results of the research.** The hypothesis was tested by calculating  $K_{GO}$  coefficient using dependence (1) for test 3D-models of complex products mapped to the triangulation model of the sphere ( $n = 6$ ,  $m = 12$ , respectively  $\Delta\theta = \Delta\varphi = 20^\circ$ ). The chart of the distribution density of the number of 3D-models by  $K_{GO}$  coefficient is presented in Fig. 3.

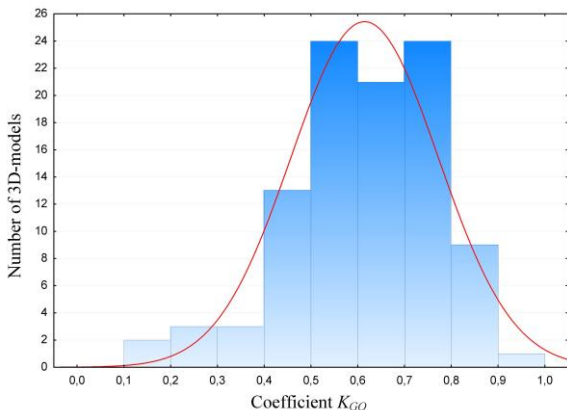


Figure 3 – Chart of the distribution density of the number of 3D-models by the value of coefficient  $K_{GO}$

The set of test 3D-models is a sample of a sufficiently large group of products that were manufactured on SLA (laser stereolithography), SLS (selective laser sintering), and FDM (fused deposition modeling). The sample size was 100 products.

Statistical analysis of  $K_{GO}$  coefficients allowed to determine the following characteristics:

- minimum, maximum and arithmetic mean  $\{K_{GO}\}_{min} = 0.107$ ,  $\{K_{GO}\}_{max} = 0.909$ ,  $\overline{K_{GO}} = 0.611$ , respectively;

- lower and upper quartiles  $Q_1\{K_{GO}\} = 0.519$  and  $Q_3\{K_{GO}\} = 0.733$ , respectively;

- standard deviations  $\{K_{GO}\} = 0.016$ .

Comparative analysis of  $K_{GO}$  coefficients (Fig. 2, 3) on the example of a sample of 3D-models of products also confirmed the hypothesis. As the value of  $K_{GO}$  coefficient decreases, the predicted efficiency of the problem of determining the rational orientation of the product in the construction workspace reduces. The evaluation of the product design by  $K_{GO}$  coefficient is justified for the cases of

solving this optimization problem according to the criteria that depend on the location of the surfaces, i.e. the area of the 3D-model faces and their orientation. Such optimization criteria include statistical characteristics of surface roughness and deviation from the correct shape of surfaces.

Based on the analysis of the results of calculations and manufacturing practices of the considered products for models with coefficient  $K_{GO} < 0.4 \div 0.5$  (for 15÷25% 3D-models of products) the surface quality and accuracy of shaping should be neglected and the following optimization criteria should be chosen for rational orientation of the product: the height of the product gravity center, construction height, number of layers or construction time. For  $K_{GO} > 0.5 \div 0.6$  (for most product 3D-models), multicriteria optimization should be considered.

It is important to determine the rational degree of detail (the number of intervals of values of the angles of inclination of the normals) reflection on the sphere. Therefore,  $K_{GO}$  coefficients were additionally determined for a small group of 3D-models of products (Fig. 2) for several intervals of values of angles  $\theta, \varphi = \{5^\circ; 10^\circ; 20^\circ; 30^\circ\}$ . The values of  $K_{GO}$  coefficients are given in table 1.

Analysis of the values of  $K_{GO}$  coefficient presented in table 2 shows their growth as the sphere detail increases, and therefore, the number of intervals of values of angles  $\theta, \varphi$  rises. This increase in  $K_{GO}$  demonstrates the increase in the manufacturability of the structure as the accuracy of determining the rational orientation of the product in the construction working space rises. To ensure a comparative assessment of manufacturability of products, it is proposed to use a sphere to display 3D-models with the interval of values of angles  $\theta, \varphi = \{20^\circ; 30^\circ\}$ .

In the case of mass customized additive production to ensure automated technological preparation, it is of interest to group products according to  $K_{GO}$  coefficient. This approach will allow using uniform technological techniques for a group of products with similar  $K_{GO}$ s to solve the problems of orientation and their placement in the working space of layered construction. This approach creates opportunities to minimize the cost of technological preparation and increase the efficiency of the subsequent problem of forming a set of layers according to the adaptive strategy with a variable construction step.

Table 1 – Coefficients of the suitability of test 3D-models of industrial products to determine the rational orientation of  $K_{GO}$

Test model	The intervals of values of angles $\theta, \varphi$ in the spherical coordinate system			
	30°	20°	10°	5°
1 (Fig. 2a)	0.109	0.134	0.173	0.202
2 (Fig. 2b)	0.429	0.480	0.500	0.572
3 (Fig. 2c)	0.323	0.369	0.437	0.496
4 (Fig. 2d)	0.581	0.690	0.778	0.802

**Conclusions.** The proposed relative indicator  $K_{GO}$  to assess the effectiveness of determining the rational orientation of the product according to the quality criteria of the obtained surfaces allows with high informativeness to assess manufacturability (design suitability) for its manufacture by additive technologies.  $K_{GO}$  coefficient determines the relative number of rational options from the set regarding the orientation of the product in the workspace of the layered building.

Manufacturability assessment to determine the rational orientation in the workspace allows to group products with similar indicators. This approach will allow ensuring the greatest efficiency of manufacturing technology in terms of roughness and accuracy of the resulting surfaces by defining a unified manufacturing strategy for a group of products with similar design features.

**References:** 1. *Diegel O., Nordin A., Motte D.* A Practical Guide to Design for Additive Manufacturing. Springer Series in Advanced Manufacturing, 2019, doi: 10.1007/978-981-13-8281-9. 2. *Gibson I., Rosen D., Stucker B., Khorasani M.* Additive manufacturing technologies. 3rd Edition. Cham (Switzerland): Springer Nature Switzerland AG, 2021, 675 pp., doi: 10.1007/978-3-030-56127-7. 3. *Eranpurwala A., Ghiasian S.E., Lewis K.* Predicting Build Orientation of Additively Manufactured Parts With Mechanical Machining Features Using Deep Learning. Proceedings of the ASME 2020 International Design Engineering Technical Conferences and Computers and Information in Engineering Conference. Volume 11A: 46th Design Automation Conference (DAC). Virtual, Online. August 17–19, 2020, V11AT11A023. ASME., doi: 10.1115/DETC2020-22043. 4. *Hong S., Byun K., Lee H.* Determination of optimal build direction in rapid prototyping with variable slicing. Int. J. Adv. Manuf. Technol. 2006, No. 28. P. 307-313, doi: 10.1007/s00170-004-2355-5. 5. *Canellidis V., Giannatsis J., Dedoussis V.* Genetic-algorithm-based multi-objective optimization of the build orientation in stereolithography. Int J Adv Manuf Technol, 2009, 45: 714–730. doi: 10.1007/s00170-009-2006-y. 6. *Singhal S.K., Pandey A.P., Pandey P.M., Nagpal A.K.* Optimum part deposition orientation in stereolithography. Computer-Aided Design & Applications. 2005, Vol. 2, Nos. 1-4, pp. 319-328. 7. *Bablani M., Bagchi A.* Quantification of errors in rapid prototyping processes, and determination of preferred orientation of parts, Transactions of the North American Manufacturing Research Institution of the SME, Vol. XXIII, SME, Houghton, MI, May 1995, pp. 319-324. 8. *Thompson D.C., Crawford R.H.* Optimizing part quality with orientation, in Marcus, H.L. et al. (Eds), Solid Freeform Fabrication Symposium 1995, University of Texas, Austin, August 1995. 9. *Vitjazev Ju.B.* Rasshirenie tehnologicheskikh vozmozhnostej uskorenno go formoobrazovanija sposobom stereolitografii: Dis... kand. tehn. nauk: 05.02.08, Kharkiv, 2004, 228 p. 10. Pat. 54398U UKRAYINA, MPK B29C 35/08, B29C 41/02, G06F 17/50, G06F 19/00. Sposib posharovoyi pobudovy vyrobiv na bazi vykhidnoyi trianhulyatsiynoyi 3D modeli / *Abdurajimov L.N., Chernyshov S.I., Dobroskok V.L., Vityazhev Yu.B.*; zayavnyk i patentovlasnyk Nats. tekhn. un-t "Kharkiv's'kyy politekhn. in-t". – № u201004548; Zayavl. 19.04.2010; Opubl. 10.11.2010, Byul. № 21. 11. *Moroni G., Syam W. P., Petrò S.*, Functionality-based Part Orientation for Additive Manufacturing, Procedia CIRP, 2015, 36, pp. 217-222. 12. *Zhang Y., Bernard A., Gupta R. K., Harik R.* Feature Based Building Orientation Optimization for Additive Manufacturing, Rapid Prototyping Journal, 2016, 22(2), pp. 358-376. 13. *Rocha A. M. A., Pereira A. I., Vaz, A. I. F.* Build Orientation Optimization Problem in Additive Manufacturing, Proc. International Conference on Computational Science and Its Applications, Springer, 2018, pp. 669-682. 14. *Abdurajimov L.N.* Povyshenie jeffektivnosti integrirovannyh tehnologij poslojnego vyrashhivaniya izdelij putem morfologicheskogo analiza ih 3D obraza na jetape podgotovki k materializaciji: Dis. kand... tehn. nauk: 05.02.08. Kharkiv: NTU "Khark. pol. in-t.", 2012, 264 p. 15. *Ranjan Rajit, Samant Rutuja, Anand Sam.* Design for manufacturability in additive manufacturing using a graph based approach. In: ASME 2015 International Manufacturing Science and Engineering

Conference. American Society of Mech. Engineers, 2015, pp. 1-10. doi: 10.1115/MSEC2015-9448. 16. *Shwe P. Soe.* Quantitative analysis on SLS part curling using EOS P700 machine, Journal of Materials Processing Technology, 212 (2012), pp. 2433–2442. doi: 10.1016/j.jmatprotec.2012.06.012. 17. *Daekeon A., Hochan K., Seokhee L.* Fabrication direction optimization to minimize post-machining in layered manufacturing, International Journal of Machine Tools and Manufacture, Volume 47, Issues 3–4, March 2007, pp. 593-606. doi: 10.1016/j.ijmachtools.2006.05.004. 18. *Kumke M., Watschke H., Vietor T.* A new methodological framework for design for additive manufacturing. Virtual And Physical Prototyping Vol.11, Iss. 1, 2016, pp. 3-19. doi:10.1080/17452759.2016.1139377. 19. *Garashchenko Ya.* Vizualna otsinka mozhlyvosti ratsionalnoi oriantatsii vyrobu pry posharovii pobudovi na ustanovkakh adytyvnykh tekhnolohii. Visnyk ZhDTU. Seriya: Tekhnichni nauky. Zhytomyr: ZhDTU, T. 1, № 2(80), 2017, pp. 3-10. doi: 10.26642/tn-2017-2(80)-3-10. 20. *Garashchenko Ya.* Otsenka yskhodnoi 3D-modely na prysposoblenost k opredeleniyu ratsyonalnoi oryentatsyy yzdelyia pry posloinom postroyeny. Rezanye y ynstrument v tekhnolohycheskykh systemakh, 2017, Vip. 87, pp. 28-40. 21. *Podgornyy A.Z., Mylashko O.G., Kirsho S.M., SHilofost N.M.* Statistika: Uchebnoe posobie dlya inostrannykh studentov, Odessa: Atlant, 2012, 195 p.

Ярослав Гаращенко, Ніна Зубкова, Харків, Україна

## **ОЦІНКА ПРОГНОЗОВАНОЇ ЕФЕКТИВНОСТІ ВИКОНАННЯ ЗАДАЧІ РАЦІОНАЛЬНОЇ ОРІЄНТАЦІЇ ВИРОБУ У РОБОЧОМУ ПРОСТОРІ АДИТИВНИХ УСТАНОВОК**

**Анотація.** *Запропоновано виконувати попередню оцінку прогнозованої ефективності оптимізаційної задачі раціональної орієнтації виробу у робочому просторі поширеної побудови адитивних установок на основі аналізу вихідної триангуляційної 3D-моделі складного виробу шляхом її сферичного відображення. Умовою відображення на сферу є потрапляння значень кутів в сферичній системі координат для нормалей граней триангуляційної моделі виробу в область значень певної трикутної грані моделі сфери. Розглянуто приклади оцінки на основі аналізу сферичного відображення вихідної 3D-моделі виробу. В якості тестових 3D-моделей обрані промислові вироби з різною складністю поверхонь. Такий підхід дозволить виконати порівняльний аналіз результатів в залежності від конструктивних особливостей виробів. Найбільш доцільним видається оцінка пристосованості конструкції виробу до виконання оптимізаційної задачі раціональної орієнтації шляхом визначення відхилень від рівномірного розподілу площ граней відображених на сферу. Запропонований відносний показник для оцінки ефективності визначення раціональної орієнтації виробу за критеріями якості отриманих поверхонь дозволяє з досить високою інформативністю оцінювати технологічність (пристосованість конструкції) для його виготовлення адитивними технологіями. Такий показник визначає відносну кількість раціональних варіантів з множини можливих щодо орієнтації виробу у робочому просторі адитивної установки. Практична реалізація виконувалась у підсистемі візуальної оцінки геометричних характеристик триангуляційних 3D-моделей, що входить до системи технологічної підготовки виготовлення складних виробів адитивними методами. Дану систему розроблено на кафедрі «Інтегровані технології машинобудування» НТУ «ХП».*

**Ключові слова:** *технологічна підготовка; адитивні технології; триангуляційна модель; оцінка технологічності, орієнтація виробу у робочому просторі.*

**CONTENT**

<b>Balanou M., Papazoglou E.I., Markopoulos A.P., Karmiris-Obratański P.</b> Experimental investigation of surface topography of AL7075-T6 alloy machined by EDM .....	3
<b>Veres P.</b> The importants of clustering in logistic systems.....	11
<b>Dyadya S., Kozlova Ye., Germashev A., Logominov V.</b> Simulation of the machined surface after end milling with self-oscillations .....	19
<b>Oliinyk S., Kalafatova L.</b> Technological fixtures for machining large-sized thin-walled shells of complex profile .....	28
<b>Mitsyk A., Fedorovich V., Grabchenko A.</b> Interaction of the abrasive medium with the treated surface and the process of metal removal during vibration treatment in the presence of a chemically active solution.....	42
<b>Molnár V.</b> Tribology and topography of hard machined surfaces .....	49
<b>Nagy A.</b> Investigation of the effect of areal roughness measurement length on face milled surface topographies .....	60
<b>Sztankovics I.</b> The effect of the circular feed on the surface roughness and the machining time .....	70
<b>Strelchuk R.</b> Surface roughness modeling during electric discharge grinding with variable polarity of electrodes.....	77
<b>Tihenko V., Lebedev V., Chumachenko T.</b> Automatic control of temperature and power conditions during rough grinding of slabs .....	85
<b>Fedorovich V., Fedorenko D., Pyzhov I., Ostroverkh Y.</b> Modeling the influence of metal phase in diamond grains on self-sharpening of grinding wheels on ceramic bonds .....	92
<b>Chumak A., Klimenko S., Klimenko S., Manokhin A., Naydenko A., Kopeikina M., Burikin V., Bondarenko M., Burlakov V.</b> Finish machining of the cutting inserts rom cubic borine nitride BL group composite .....	102
<b>Yakimov A., Bovnegra L., Tonkonogyi V., Vaysman V., Strelbitskiy V., Sinko I.</b> Influence of the geometric characteristics	

of the discontinuous profile working surfaces of abrasive wheels for precision and temperature when grinding .....	115
<b><i>Yakovenko I., Vasilevskiy Yu., Basova Y., Milan Edl.</i></b> Technological provision of the accuracy for the thread form of rod pumps .....	126
<b><i>Klymenko G., Vasylchenko Y., Donchenko Ye.</i></b> Quality management of cutting tools on heavy machines .....	135
<b><i>Garashchenko Ya., Zubkova N.</i></b> Evaluation of the forecasted efficiency of performance of rational orientation of the product in the workspace of additive installations .....	142

Наукове видання

**РІЗАННЯ ТА ІНСТРУМЕНТИ**  
**в технологічних системах**

Міжнародний науково-технічний збірник

**Випуск № 94**

Укладач *д.т.н., проф. О.М. Шелковий*

Оригінал-макет *А.М. Борзенко*

Відп. за випуск *к.т.н., проф. С.В. Острроверх*

В авторській редакції

Матеріали відтворено з авторських оригіналів

Підп. до друку 12.02.2019. Формат 60x84 1/16. Папір СоруРарег.  
Друк - ризографія. Гарнітура Таймс. Умов. друк. арк. 10,93. Облік. вид. арк. 11,0. Наклад 300 прим.  
1-й завод 1-100. Зам. № 1149. Ціна договірна.

---

Видавничий центр НТУ «ХП»  
Свідоцтво про державну реєстрацію ДК № 116 від 10.07.2000 р.  
61002, Харків, вул. Кирпичова, 2